

T-2253

THE INFLUENCE OF THE SURROUNDING MEDIUM
IN ELECTROMAGNETIC PROSPECTING FOR
AN ELONGATED CONDUCTOR

by
Doo-Sung Lee

ARTHUR LAKES LIBRARY
COLORADO SCHOOL of MINES
GOLDEN, COLORADO 80401
CLOSED RESERVE

ProQuest Number: 11016698

All rights reserved

INFORMATION TO ALL USERS

The quality of this reproduction is dependent upon the quality of the copy submitted.

In the unlikely event that the author did not send a complete manuscript and there are missing pages, these will be noted. Also, if material had to be removed, a note will indicate the deletion.



ProQuest 11016698

Published by ProQuest LLC (2019). Copyright of the Dissertation is held by the Author.

All rights reserved.

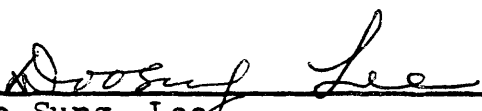
This work is protected against unauthorized copying under Title 17, United States Code
Microform Edition © ProQuest LLC.

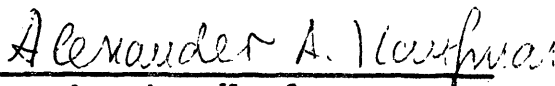
ProQuest LLC.
789 East Eisenhower Parkway
P.O. Box 1346
Ann Arbor, MI 48106 – 1346

A thesis submitted to the Faculty and Board of Trustees of the Colorado School of Mines in partial fulfillment of the requirements for the degree of Doctor of Philosophy in Geophysics.

Golden, Colorado


Date Oct. 30, 1979

Signed: 
Doo Sung Lee

Approved: 
Alexander A. Kaufman
Thesis Advisor

Golden, Colorado

Date Nov 5, 1979


Phillip R. Romig
Head of Department

ABSTRACT

The electromagnetic field about a conducting cylinder in uniform space is investigated for the case of an infinitely long linear current source and for magnetic dipole sources. The asymptotic behavior of the fields is discussed in both the frequency domain and in the time domain.

By comparing the secondary and the normal fields, the optimum ranges of frequency and time are obtained. From the results of the numerical evaluation, it is found that the resolving capability of the methods in the frequency and the time domains are very much different. The time domain method possesses a much higher resolving capability than the conventional frequency domain methods. Even in the frequency domain there is a big difference between measuring the in-phase and the quadrature component. Measuring the inphase component provides higher resolving capability than measuring the quadrature component. However, the resolving capability of the methods in the frequency domain can be increased significantly by measuring the quadrature component at two different frequencies. The calculation results show that the maximum ratio of the secondary to the normal field of this method can be comparable to that of the time domain method.

<u>CONTENTS</u>	<u>Page</u>
ABSTRACT	iii
ILLUSTRATIONS	Vii
ACKNOWLEDGEMENTS	Xi
INTRODUCTION	1
CHAPTER I.	
INFLUENCE OF THE SURROUNDING MEDIUM IN CASE OF TWO DIMENSIONAL MODEL	6
Frequency responses of the normal field	6
Current density	11
Behavior of the frequency responses of the normal field	11
Transient responses of the normal field	16
Current density	19
Behavior of the transient responses ...	19
Frequency and the transient responses of the secondary field	20
Fundamental part of the secondary field	24
Frequency responses	24
Transient responses	27
Linear harmonic part of the secondary field	34
Frequency responses	35
Transient responses	38
Discussion about the secondary field ...	40
Influence of the surrounding medium	42

	<u>Page</u>
CHAPTER II.	
THE ELECTROMAGNETIC FIELDS OF A CONDUCTING CYLINDER WHEN THE SOURCE IS A MAGNETIC DIPOLE(SURROUNDING MEDIUM IS AN INSULATOR)	47
Derivation of formulae	47
Electromagnetic field due to a magnetic dipole	56
Axial magnetic dipole	56
Transverse magnetic dipole	57
Vertical magnetic dipole	59
Analysis of function $A_n(m)$	61
Small value of m	61
Low frequency approximation	64
Frequency responses of the magnetic field . . .	64
Axial magnetic dipole	64
Transverse magnetic dipole	67
Discussion about the magnetic field in the frequency domain	67
Transient responses of the magnetic field . . .	74
Asymptotic behavior of the magnetic field at the late stage	75
Horizontal profiling	77
CHAPTER III.	
INFLUENCE OF THE SURROUNDING MEDIUM ON THE FREQUENCY AND THE TRANSIENT RESPONSES IN THE PRESENCE OF A CONDUCTING CYLINDER(AXIAL MAGNETIC DIPOLE)	85
Derivation of field equations	85

	<u>Page</u>
Boundary condition	87
Normal field	90
Secondary magnetic field	90
Secondary electric field	92
Examination of the results	92
Magnetic field	92
Electric field	94
Analysis of the magnetic field in the frequency domain	98
Z component of the magnetic field	98
Vertical component of the magnetic field	102
Transient responses of the magnetic field	105
CONCLUSION	108
APPENDICES	111
Fourier transform	111
Calculation of the Bessel function	113
List of symbols	115
REFERENCES	117

ILLUSTRATIONS

Figures		Pages
1-1.	Linear current source in uniform space	7
1-2.	Configuration of line source O and observer P in equatorial plane of cylinder	7
1-3.	Frequency response of the normal magnetic field	12
1-4.	Frequency response of the normal electric field	12
1-5.	Transient response of the normal electric field	18
1-6.	Transient response of the normal electro- motive force	18
1-7.	Frequency response of the fundamental part of the secondary electric field	26
1-8.	Frequency response of the fundamental part of the secondary magnetic field	26
1-9.	Transient response of the fundamental part of the secondary electric field	31
1-10.	Transient response of the electromotive force for the fundamental part	31
1-11,12	Frequency response of the fundamental part of the magnetic field for several different ratios of conductivities	41
1-13,14	Frequency response of the magnetic field for several different ratios of conductiv- ities	43
1-15,16	The ratios of the total magnetic field to the normal magnetic field in the frequency domain	44
1-17	The ratios of the total electromotive force to the normal electromotive force in the time domain	45

Figures	Pages
2-1.	The cylindrical body and source R and observer P with the cylindrical coordinate system 48
2-2,3	Frequency response of the magnetic field for several different geometries of the system(Source is an axial magnetic dipole).. 65
2-4.	Frequency response of the quadrature component of the magnetic field with the leading term of the low frequency asymptote removed (Source is an axial magnetic dipole) ... 68
2-5,6	Frequency response of the magnetic field for several different geometries of the system(Source is a transverse magnetic dipole) 69
2-7.	Frequency response of the quadrature component of the magnetic field with the leading term of the low frequency asymptote removed (Source is a transverse magnetic dipole).... 70
2-8.	Configuration of the observer P and cylinder when the primary field, in the vicinity of the cylinder, is uniform 72
2-9.	Transient response of the magnetic field (Source is an axial magnetic dipole)..... 76
2-10.	Transient response of the magnetic field (Source is a transverse magnetic dipole).... 76
2-11,12	Horizontal profiling with fixed frequency, $a/\delta_i=0.6$, and separation(Transmitter is an axial magnetic dipole) 78
2-13,14	Horizontal profiling with fixed frequency, $a/\delta_i=1.5$, and separation(Transmitter is an axial magnetic dipole) 79
2-15,16	Horizontal profiling with fixed frequency, $a/\delta_i=0.6$, and separation (Transmitter is a transverse magnetic dipole) 81
2-17,18	Horizontal profiling with fixed frequency, $a/\delta_i=1.8$, and separation(Transmitter is a transverse magnetic dipole) 82

Figures	pages
2-19,20	Horizontal profiling with fixed frequency, $a/\delta = 0.6$ and separation (Transmitter is a transverse magnetic dipole. The vertical component of the magnetic field is calculated, assuming primary field is uniform in the vicinity of the cylinder) 83
2-21,22	Horizontal profiling with fixed frequency, $a/\delta = 0.6$, and separation (Transmitter is a transverse magnetic dipole. The horizontal component of the magnetic field is calculated, assuming the primary field is uniform in the vicinity of the cylinder)..... 84
3-1,2	Frequency response of the magnetic field in the presence of a conducting cylinder in uniform space (Transmitter is an axial magnetic dipole) 99
3-3,4	Ratio of the total to normal magnetic field in the frequency domain (Transmitter is an axial magnetic dipole) 101
3-5.	Frequency response of the quadrature component of magnetic field with the leading term of the low frequency asymptote removed (Source is an axial magnetic dipole) 103
3-6,7	Frequency responses of the vertical component of magnetic field (Source is an axial magnetic dipole) 104
3-8.	Transient response of the magnetic field (Source is an axial magnetic dipole) 106
3-9	Ratio of the total to the normal magnetic field in the time domain (Source is an axial magnetic dipole) 106
 Tables	
1-1.	Comparison of the normalized electric field in the frequency domain computed from exact formula and asymptotic expression..... 28

Tables	Pages
1-2. Comparison of the normalized magnetic field in the frequency domain computed from exact formula and asymptotic expression	28
1-3. Comparison of the normalized electric field in the time domain computed from exact formula and asymptotic expression	33
1-4. Comparison of the normalized magnetic field in the time domain computed from exact formula and asymptotic expression	33
3-1. The inphase component of the electric field with $\alpha=40$, $\beta=2$, $u=39.04$ and $\hat{z}=0.5$	96
3-2. The normalized electric field when a source is located very far from the cylinder ($\alpha=40$, $\beta=2$, $z=0.2$ and $\phi-\phi_0=\pi/3$)	96

ACKNOWLEDGEMENTS

I wish to express my appreciation to my advisor, Dr. Alexander A. Kaufman for his kind help and guidance during the course of this research.

A special word of thanks goes to Drs. F. A. Hadsell, G. R. Edwards, G. V. Keller and R. S. Fisk for their suggestions and corrections during the preparation for the report.

I also thank the Colorado School of Mines for financial aid in the form of research assistantship.

Finally I would like to thank my wife, Yeong Ae, for her assistance and encouragement during my studying at Colorado School of Mines.

INTRODUCTION

The electromagnetic methods are the most successful tools in mining geophysics (Parasnis, 1966). These methods were first used more than 50 years ago in Sweden (Parasnis, 1966). Since then many different inductive methods have been developed. Conventionally, these methods can be classified into the following three groups.

Group 1. Frequency methods in the near zone.

The transmitter is a loop carrying a harmonically time-varying current. Measurements are performed in the near zone; that is, the ratio of the separation to the skin depth of the medium is less than one. The following methods are included in this group:

a. Two coil system: Slingram and tilt angle methods (Keller, et al, 1966). Some of these methods are based on determining the azimuth and the dip of the ellipse of the polarization. Other methods measure only the amplitude and the phase of the magnetic field at different frequencies.

b. Airborne systems.

Group 2. Frequency methods in the wave zone; that is, the ratio of the separation to the skin depth is large. The methods in which measurements are carried in the wave zone are as follow:

a. VLF

The antenna of a VLF transmitter constitutes a vertical electric dipole. Measurements are carried out by using a coil tuned to the frequency of the selected VLF station.

b. AFMAG

This method uses the natural magnetic fields at audio frequencies. The space between the ionosphere and the earth's surface acts as a wave guide for these fields with the result that their vertical components are normally very small. A receiver coil at any point will show that the plane of polarization tilts out of the horizontal (Ward, 1969).

c. Turam Method (wave zone)

The primary field of this method is produced by a long cable or a large loop and the receiver consists of two coils. For each measurement the ratio of the intensities at two points is measured (Parasnis, 1966).

Group 3. Transient methods

a. Ground systems:

There are several kinds of transient methods, including those of Sirotek (1977), Crone (1977), Newmont (1955). These systems are used in the ground surveys. Usually the energy of these methods is supplied inductively by pulses in an insulated cable loop and a receiver coil measures the signal when the current is turned off. The advantage of these methods is that only the secondary field needs to be measured.

b. Airborne system:

The induced pulse transient (INPUT) system has been employed for aerial electromagnetic survey. In this system, pulses are sent through a horizontal loop at a repetition rate of several hundred times a second, using a small 'bird' towed on a cable about 150 m behind aircraft. This bird houses a coil which detects the secondary decaying signal from the ground. Measurements are made at times from about $100 \mu\text{s}$ after the current is turned off to about $2000 \mu\text{s}$ (Parasnis, 1966).

The interpretation of all the above mentioned methods is mainly based on the frequency and transient responses which are obtained through calculation or physical modeling for the case of an ore body surrounded by an insulator. It is usually assumed that the influence of the surrounding medium is negligible.

An extensive amount of theoretical work has been done on the induced electromagnetic fields of conducting bodies. The analytical model of a conducting sphere has been investigated by Wait (1951, 1953 and 1960), Ward (1959 and 1967), and Fuller (1971), and others. The above literature mainly discusses the derivation of secondary fields in the frequency domain and their behavior in a conducting medium. Negi (1969), Nabighian (1970 and 1971), and Verma (1972), investigated the conducting sphere in the time domain.

Most previous investigators studied the behavior of the secondary field, which is primarily due to the induced currents in the conductor, without considering the influence of the surrounding medium. The influence of the surrounding medium is defined as geological noise which comes from the induced currents in the surrounding medium and sometimes from the galvanic part of the secondary field. Neglecting the influence of surrounding medium, the depth of investigation is controlled by the ratio of the useful signal to the ambient noise. Ambient noise consists of telluric noise, industrial noise, and measuring error due to unstable orientation of a transmitter and a receiver. This problem can be solved by developing better instruments. However, the maximum depth of investigation of the orebody is restricted by the ratio of the useful signal to the geological noise. If the geological noise is greater than the useful signal, it is impossible to get reliable information about the orebody. Thus the main concern in EM prospecting is to find the optimum conditions which allow one to get the maximum ratio of the useful signal to the geological noise (Kaufman, 1961). Kaufman (1961) investigated the galvanic and the inductive part of the secondary field of a conducting sphere in the frequency domain.

In this dissertation the influence of the surrounding medium is investigated for the quadrature and the inphase components, in the frequency domain, and the time domain due to an infinitely long cylindrical conducting body excited by; (i) an

infinitely long line source, and (ii) a magnetic dipole source. Comparing the normal and secondary fields, the optimum ranges of time and frequency are obtained for the model being considered. The influence of electrical charges on the secondary field is also considered.

CHAPTER 1. INFLUENCE OF THE SURROUNDING
MEDIUM IN CASE OF TWO DIMENSIONAL MODEL

Introduction

A horizontally elongated body is here modeled as a cylinder. This cylinder is excited by an infinitely long line source, which is parallel to the axis of the cylinder (Fig. 1-2).

The line source carries harmonically time-varying current $I = I_0 e^{-i\omega t}$ (1-1) where ω is frequency, in radians per second, I_0 is the amplitude of the sinusoidal current, and t is time.

In this case the changing source current generates an inductive current in the surrounding medium and in the conducting body. The field due to the current in the surrounding medium is called the normal field and the field due to the current in the conducting body is called the secondary field. Thus, the resulting electromagnetic field is the sum of the normal and the secondary field.

Frequency Response of Normal Field

The system of field equations can be constructed from Maxwell equations.

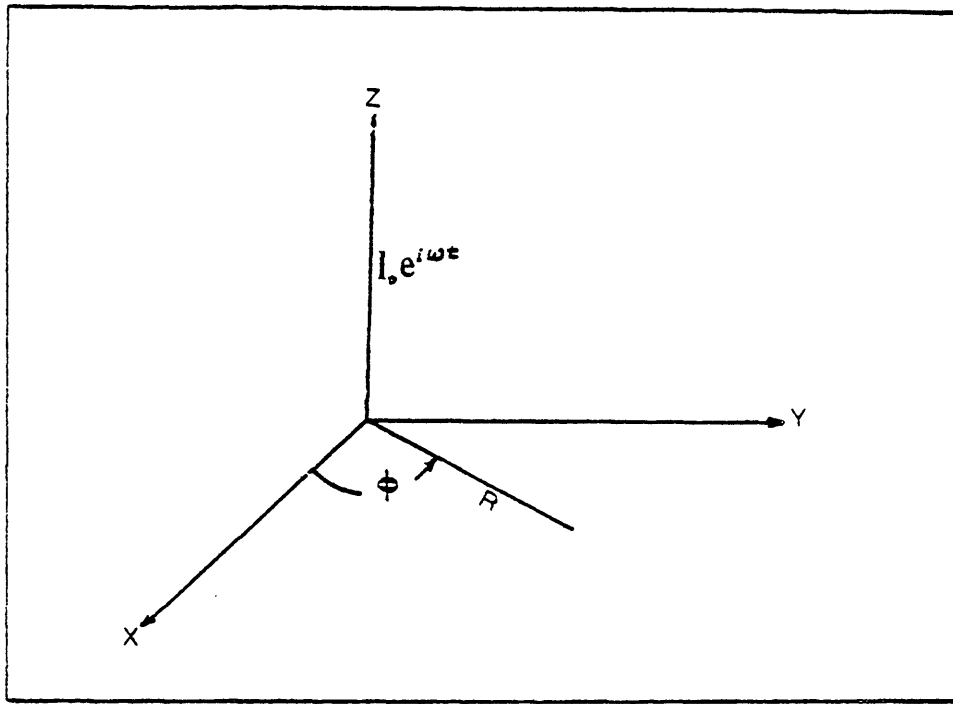


Figure 1-1. Linear current source in uniform space

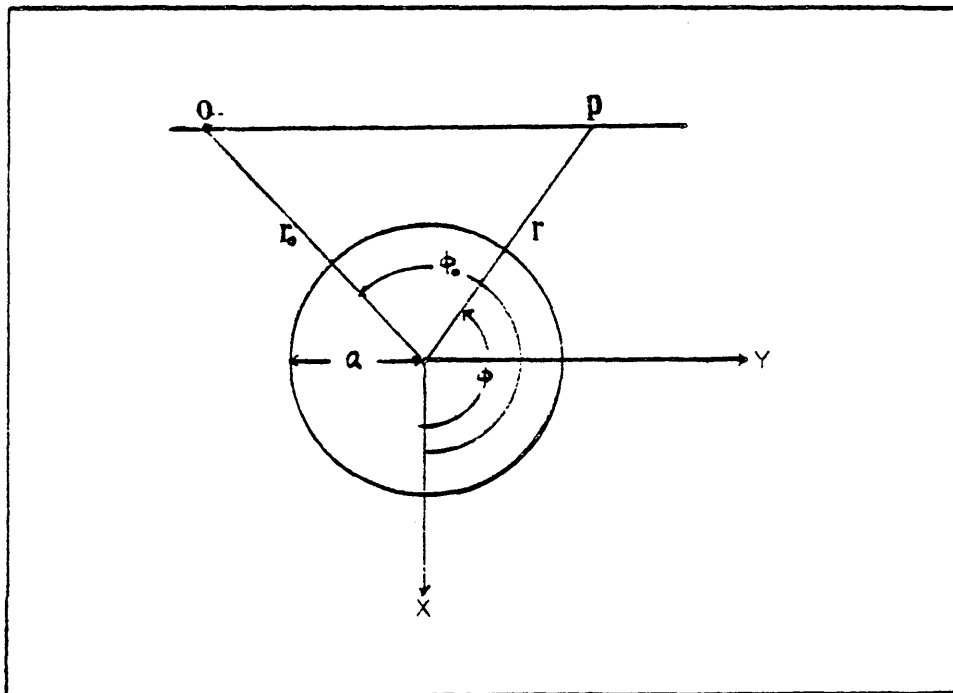


Figure 1-2. Configuration of line source O and observer P in equatorial plane of cylinder.

For the case of a harmonically varying source and quasistationary field behavior, Maxwell's equations can be written as:

$$\begin{aligned} \text{curl } \vec{E} &= iw \mu \vec{H}, & \text{Div } \vec{E} &= 0. \\ \text{curl } \vec{H} &= \gamma \vec{E}, & \text{Div } \vec{H} &= 0. \end{aligned} \quad (1-2)$$

where γ is the conductivity of the medium and μ is magnetic permeability.

From equation (1-2)

$$\text{curl curl } \vec{E} = iw \mu \text{ curl } \vec{H}$$

$$\text{or } \nabla^2 \vec{E} + k^2 \vec{E} = 0. \quad (1-3)$$

By analogy

$$\nabla^2 \vec{H} + k^2 \vec{H} = 0 \quad (1-4)$$

where k is the wave number of the medium:

$$k = \sqrt{iw \mu \gamma}$$

(Note that displacement currents are neglected).

If the source current is directed along the Z-axis (Figure 1-1), it can be shown using the Helmholtz theorem that the resultant electric field has only a Z-component. Therefore, equation(1-3) can be written as:

$$\frac{d^2 E_Z}{dR^2} + \frac{1}{R} \frac{dE_Z}{dR} + K^2 E_Z = 0$$

where R, ϕ, Z are a cylindrical coordinate system.

The solutions of the above equation are linear combination of modified Bessel functions $K_0(kR)$ and $I_0(kR)$ (Wait, 1960). Considering the fact that the electric field should go to zero as R approaches infinity and the behavior of the functions $K_0(kR)$ and $I_0(kR)$,

$$\lim_{R \rightarrow \infty} K_0(KR) = 0$$

$$\lim_{R \rightarrow \infty} I_0(KR) = \infty,$$

the proper solution of the above wave equation is

$$E_Z = M K_0(KR). \quad (1-5)$$

To determine the constant M , the field in the vicinity of the source is considered. At a point which is very close to the source, the magnetic field is defined mainly by the source

current. From equation (1-2)

$$\lim_{R \rightarrow 0} \oint \vec{H} \cdot d\vec{l} = I_0$$

or

$$\lim_{R \rightarrow 0} H_\phi = \frac{I_0}{2\pi R} \quad (1-6)$$

The relation between H_ϕ and E_z is

$$H_\phi = \frac{1}{iw\mu} \cdot \frac{\partial E_z}{\partial R} \quad (1-7)$$

From the above equations,

$$\lim_{R \rightarrow 0} \left[\frac{M}{iw\mu} \frac{d}{dR} K_0(KR) \right] = \frac{I_0}{2\pi R}$$

or

$$M = - \frac{iw\mu I_0}{2\pi} \quad (1-8)$$

Thus, the corresponding electric and magnetic fields are

$$E_z = - \frac{iw\mu I_0}{2\pi} K_0(KR) \quad (1-9)$$

$$H_\phi = \frac{I_0}{2\pi} \cdot K \cdot K_1(KR) \quad (1-10)$$

Defining e_z and h_ϕ by

$$E_z \triangleq - \frac{\rho I_0}{2\pi R^2} e_z$$

and

$$H_{\phi} \cong \frac{I_0}{2\pi R} h_{\phi}$$

where ρ is the resistivity of the medium one obtains

$$e_z = K^2 R^2 \cdot K_0 \quad (KR) \quad (1-11)$$

and

$$h_{\phi} = K R \cdot K_{\phi} \quad (KR) \quad (1-12)$$

In the above equation KR can be written as:

$$KR = \frac{(1+i)R}{\delta}$$

where δ is the skin depth of the medium,

$$\delta = \sqrt{\frac{2}{\gamma \mu \omega}}$$

Frequency responses are calculated using equations (1-11) and (1-12). These results are shown in Figures(1-3) and (1-4) as a function of R/δ .

Current Density

According to Equation (1-9) the current density, j_z , in the medium is

$$j_z = - \frac{I_0 K^2}{2\pi} K_0 \quad (KR)$$

or

$$j_z = \frac{I_0}{2\pi R} e_z \quad (1-13)$$

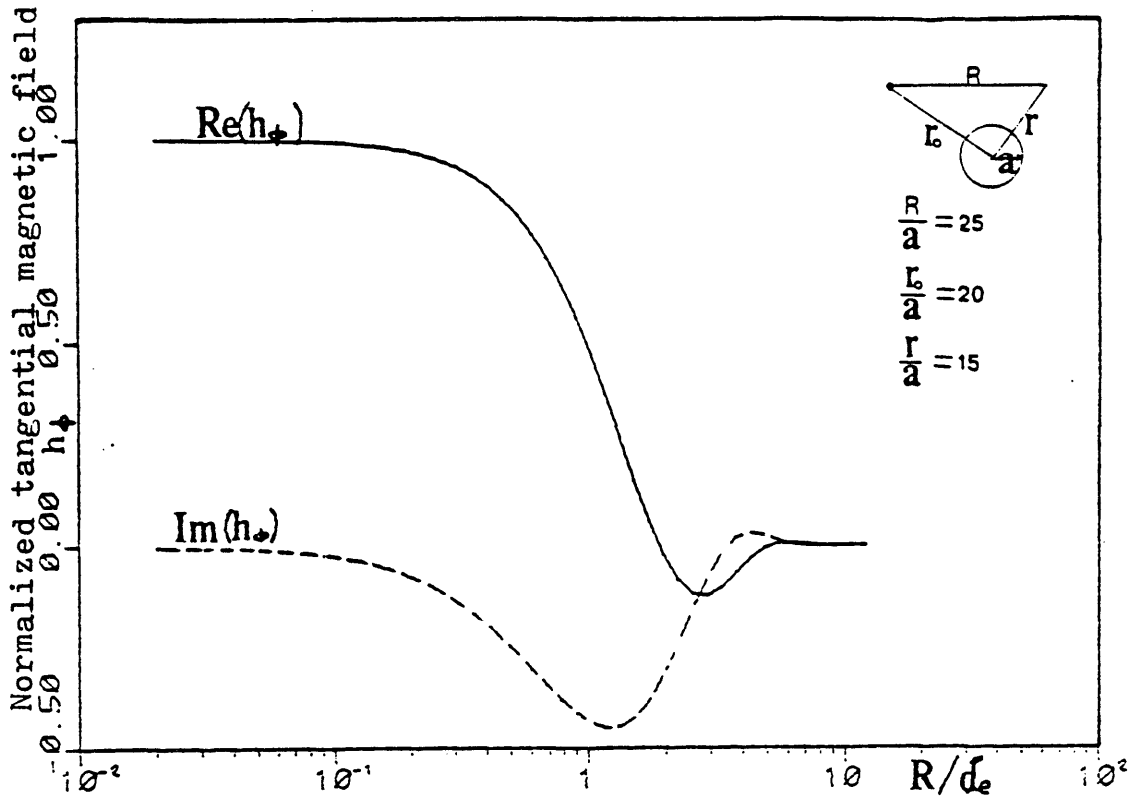


Figure 1-3. Frequency response of the normal magnetic field.

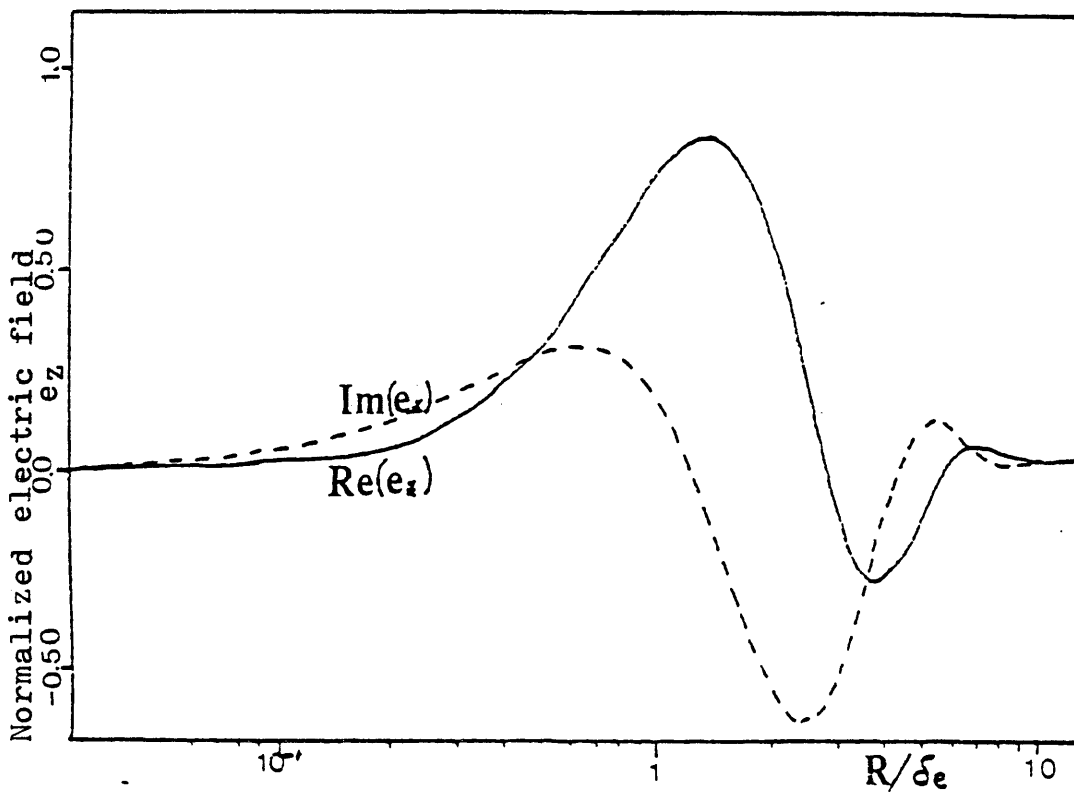


Figure 1-4. Frequency response of the normal electric field.

Thus the current density has the same behavior as the frequency response of electric field. From Figure (1-4), it can be noticed that the location of maximum current density is shifted farther from the source as the frequency decreases.

The total current in the medium is

$$J = \int_{w.s} j_z \cdot dS$$

where w.s represents "whole space". Hence

$$J = 2\pi \int_0^{\infty} j_z R dR$$

or

$$J = - I_0 K^2 \int_0^{\infty} K_0(KR) \cdot R dR$$

Substituting $x = KR$

$$J = - I_0 \int_0^{\infty} x K_0(x) dx$$

$$= - I_0 .$$

(1-14)

This result can be interpreted as follows: The terminal of the linear source is located very far from the observation point and the current I_0 flows through the closed path in the surrounding medium.

Behavior of the Frequency Responses of the Normal Field

At the low frequency, $R/\delta < 1$ or $KR < 1$, the Bessel function in equations (1-11) and (1-12) can be approximated by:

$$K_0(KR) \cong \ln \frac{2}{\gamma_0 KR} \quad (1-15)$$

where $\gamma_0 = 1.781072$ (Euler's Constant)

If $|KR| \ll 1$,

$$K_0(KR) \cong -\ln KR$$

and

$$K_1(KR) \cong \frac{1}{KR} + \frac{KR}{2} \ln KR \quad (1-16)$$

Substituting the above expressions into equation (1-11)

$$\begin{aligned} e_z &= -\frac{1}{2} K^2 R^2 \ln(K^2 R^2) \\ &= -\frac{i}{2} w \mu \gamma R^2 \ln(w \mu \gamma R^2) + \frac{\pi}{4} w \mu \gamma R^2 \end{aligned} \quad (1-17)$$

Thus, the inphase component of the electric field is

$$R_e[E_z] = -\frac{I_0 \mu w}{8} \quad (1-18)$$

and the quadrature component is

$$I_m[E_z] = \frac{I_0 \mu w}{4\pi} \ln \frac{\gamma \mu w R^2}{2} \quad (1-19)$$

Similarly, the magnetic field becomes

$$R_e [H_\phi] = \frac{I_0}{2\pi R} \left(1 - \frac{\pi}{8} \gamma \mu w R^2\right) \quad (1-20)$$

$$I_m [H_\phi] = \frac{I_0 \gamma \mu w R^2}{8\pi} \ln \gamma \mu w R^2 \quad (1-21)$$

Thus at the low frequencies, the inphase component of the electric field does not depend on the conductivity of the medium. As usual, the quadrature component of electric field is bigger than the inphase component at the low frequencies. In a real case, the quadrature component is proportional to w at the low frequencies. However, in this case, due to the infinitely long line source the quadrature component of the magnetic field is proportional to $w \ln w$.

Now, let us investigate the high frequency part of the spectrum. If the magnitude of KR is bigger than unity,

$$K_0(KR) \cong \sqrt{\frac{\pi}{KR}} e^{-KR},$$

and
$$K_1(KR) \cong \sqrt{\frac{\pi}{KR}} e^{-KR}.$$

Thus e_z and h_ϕ in equations (1-11) and (1-12) become

$$e_z \cong K^2 R^2 \sqrt{\frac{\pi}{2KR}} e^{-KR},$$

and

$$h_{\phi} \cong KR \sqrt{\frac{\pi}{2KR}} e^{-KR},$$

or

$$E_z \cong -\frac{i\omega \mu I_0}{2\pi} \sqrt{\frac{\pi}{2KR}} e^{-KR}, \quad (1-22)$$

$$H_{\phi} \cong \frac{I_0}{2\pi} \sqrt{\frac{\pi KR}{2}} e^{-KR} \quad (1-23)$$

Thus, by increasing the frequency the fields decay very rapidly.

The following facts can be recognized:

- i) Due to the skin effect, at the high frequencies most of the current is concentrated near the source. Thus, the field does not depend on the conductivity of the medium.
- ii) Decreasing the frequency, the skin depth increases. In other words, the location of maximum current density moves farther from the source, and the fields start to feel this current in the medium.

Transient Responses of Normal Field

Transient response of the field due to step on current source is discussed.

$$\begin{aligned} I(t) &= 0 & t &\leq 0 \\ &= I_0 & t &> 0. \end{aligned}$$

In equations (1-9) and (1-10), transformation of variable as

$$K_e R = a \sqrt{S} \quad \text{with } a = \sqrt{\mu\gamma} R, \text{ we get}$$

$$e_z = a^2 s K_0(a \sqrt{S}).$$

For the response to the step function

$$e_z(t) = \mathcal{L}^{-1} \left\{ e_z(s)/s \right\}$$

or

$$e_z(\tau) = \frac{1}{2\tau} e^{-\frac{1}{4\tau}}$$

$$E_z(\tau) = -\frac{\rho I_0}{2\pi R^2} \frac{1}{2\tau} e^{-\frac{1}{4\tau}}, \quad (1-24)$$

where

$$\tau = \frac{t}{\mu\gamma R^2}.$$

By analogy

$$H(\tau) = \frac{I_0}{2\pi R} e^{-\frac{1}{4\tau}} \quad (1-25)$$

or

$$h(\tau) = e^{-\frac{1}{4\tau}}.$$

Fig. (1-5) shows the transient response of the normal electric field and Fig. (1-6) shows the transient response of the normal electromotive force.

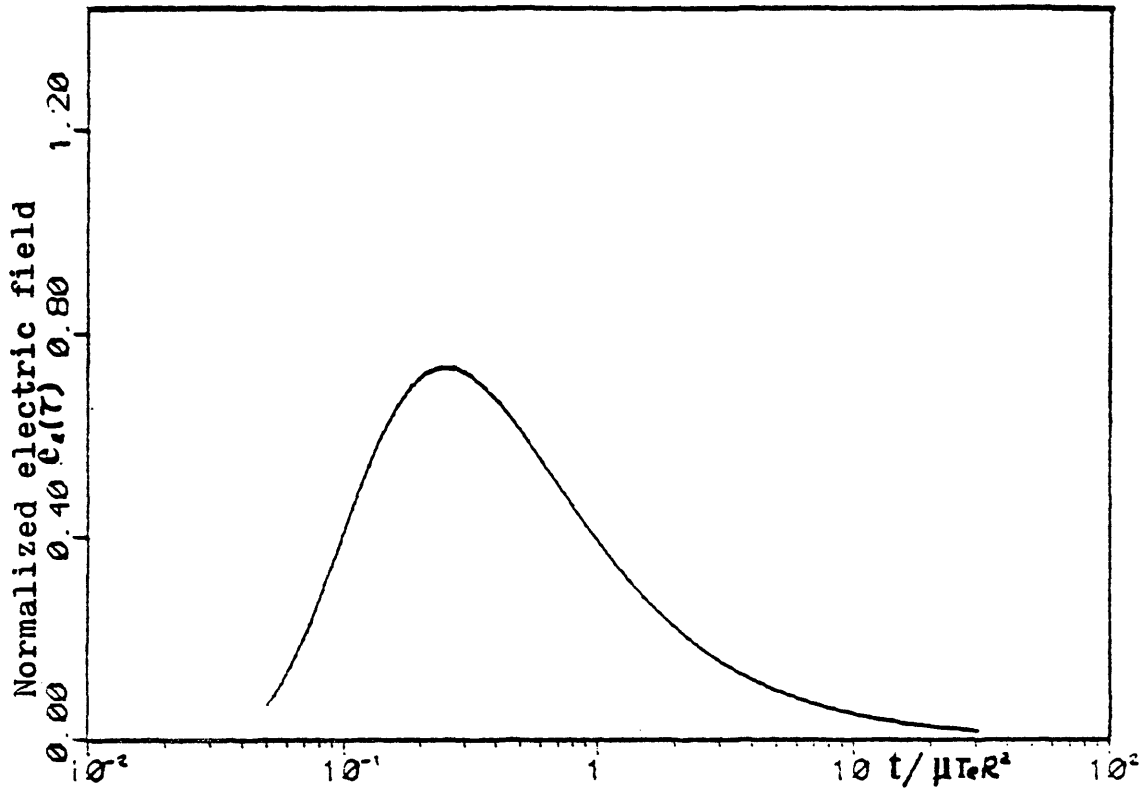


Figure 1-5. Transient response of the normal electric field.

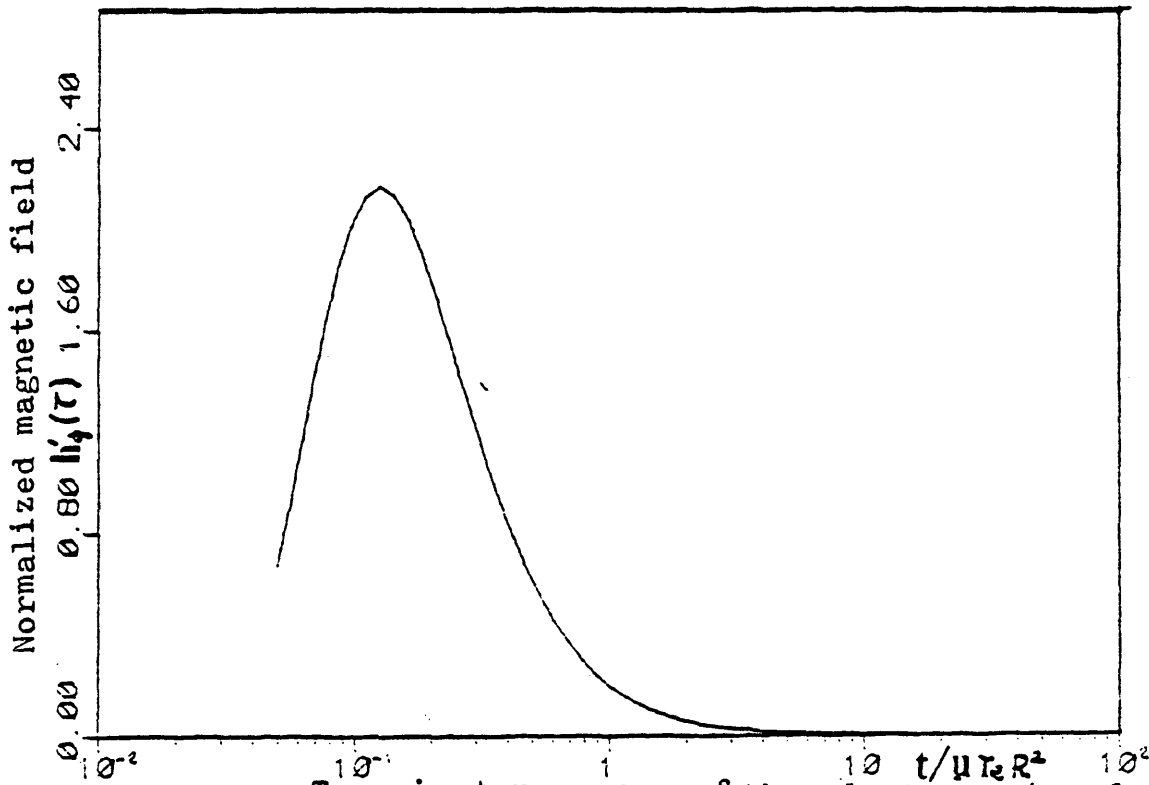


Figure 1-6. Transient response of the electromotive force.

Current Density

From equation (1-13) and figure (1-5), it can be seen that the location of the maximum current density is shifted farther from the source as time increases. This phenomenon can be explained by the skin effect in the time domain. At the early stage, induced current mainly concentrates near the source, and, as the time increases, the current diffuses farther from the source in the medium.

Behavior of the Transient Responses

At the large stage, $\tau \gg 1$, equations (1-24) and (1-25) can be written as

$$E(\tau) \cong \frac{\rho I_0}{4\pi R^2} \frac{1}{\tau} \left(1 - \frac{1}{4\tau}\right), \text{ and} \quad (1-26)$$

$$H(\tau) \cong \frac{I_0}{2\pi R} \left(1 - \frac{1}{4\tau}\right).$$

or

$$H(t) \cong \frac{I_0}{2\pi R} \left(1 - \frac{\mu\gamma R^2}{4t}\right), \quad (1-27)$$

Usually the measurement is carried out after the source current is turned off. From equation (1-25)

$$H_-(\tau) = \frac{I_0}{2\pi R} \left(1 - e^{-\frac{1}{4\tau}}\right), \quad (1-28)$$

where $H_-(\tau)$ denotes the field after the source current is turned off. From equation (1-28), the following facts are found:

i) The field approaches the primary field as the time decreases.

ii) For the case of $\tau \gg 1$.

$$H_-(\tau) \cong \frac{I_0}{2\pi R} \frac{1}{4\tau}$$

or

$$H_-(t) \cong \frac{I_0 R \mu}{8\pi t} \gamma .$$

Thus at the late stage the magnetic field is proportional to the conductivity of the medium. The above mentioned phenomenon also can be recognized by considering the behavior of the current density.

From the above discussion, it should be noted that (i) the quadrature component of the magnetic field is proportional to $\gamma \ln \gamma$ at low frequencies. (ii) At the late stage the magnetic field is proportional to γ .

The Frequency and the Transient Responses of the Secondary Field

To find the secondary fields, it is required to establish a set of boundary conditions which can determine the proper solution from the general solution of the wave equation (1-3). These conditions are continuity of tangential components of the electric and the magnetic field.

To facilitate applying boundary conditions and to find the form of the secondary field, the normal field is expressed in cylindrical coordinates (r, ϕ, z) , of which the Z-axis is along the axis of the cylinder (Fig. 1-2).

In equation (1-9)

$$R = [r^2 + r_0^2 - 2rr_0 \cos(\phi - \phi_0)]^{1/2}$$

Applying the addition theorem (G.N. Watson), we get

$$K_0(K_e R) = \sum_{n=0}^{\infty} \sigma_n K_n(K_e r_0) I_n(K_e r) \cos n(\phi - \phi_0) \quad (1-29)$$

where $\sigma_0 = 1$

$\sigma_n = 2$ for $n = 2, 3, 4, \dots$ and

$K_n(K_e r)$, $I_n(K_e r)$ are Bessel functions.

Now the normal field can be written as

$$E_N = - \frac{i\omega\mu I_0}{2\pi} \sum_{n=0}^{\infty} \sigma_n K_n(K_e r_0) I_n(K_e r) \cos n(\phi - \phi_0) \quad (1-30)$$

The above equation suggests the secondary field has the following form

$$E_S = - \frac{i\omega\mu I_0}{2\pi} \sum_{n=0}^{\infty} A_n K_n(K_e r) \cos n(\phi - \phi_0) \quad (1-31)$$

Taking into account the fact that the field has a finite value at the position $r = 0$, the field inside the conductor should have the following form as

$$E_i = - \frac{i\omega \mu I_0}{2\pi} \sum_{n=0}^{\infty} B_n I_n(K_i r) \cos n(\phi - \phi_0) \quad (1-32)$$

In the above equations, K_e is the wave number of the surrounding medium and K_i is that of the cylinder. A_n and B_n are the coefficients which are determined through applying boundary conditions.

$$E_z^e = E_z^i \text{ at } r = a$$

or

$$\begin{aligned} & \sum_{n=0}^{\infty} [\sigma_n K_n (\lambda_e r_0) I_n(K_e a) + A_n K_n (K_e a)] \cos n(\phi - \phi_0) \\ &= \sum_{n=0}^{\infty} B_n I_n(K_i a) \cos n(\phi - \phi_0) \end{aligned} \quad (1-33)$$

$$H_\phi^e = H_\phi^i$$

or

$$\begin{aligned} & \sum_{n=0}^{\infty} K_e [\sigma_n K_n (K_e r_0) I'_n(K_e a) + A_n K'_n (K_e a)] \cos n(\phi - \phi_0) \\ &= \sum_{n=0}^{\infty} K_i B_n I'_n(K_i a) \cos n(\phi - \phi_0) \end{aligned} \quad (1-34)$$

Taking into account the orthogonality of the trigonometric functions, equations (1-33) and (1-34) become

$$\sigma_n K_n (K_e r_o) I'_n (K_e a) + A_n K'_n (K_e a) = B_n I_n (K_i a)$$

$$K_e \sigma_n K_n (K_e r_o) I'_n (K_e a) + A_n K'_n (K_e a) = K_i B_n I'_n (K_i a)$$

From the above two equations A_n is defined as

$$A_n = - \frac{I'_n (\rho) I_n (m\rho) - m I_n (\rho) I'_n (m\rho)}{K'_n (\rho) I_n (m\rho) - m K_n (\rho) I'_n (m\rho)} \sigma_n K_n (\alpha\rho)$$

where

$$m = \sqrt{\gamma_i/\gamma_e}, \quad \rho = K_e a, \quad \alpha = r_o/a.$$

Thus, the secondary fields are

$$E_s = - \frac{\rho_e I_o}{2\pi R^2} K_e^2 R^2 \sum_{n=0}^{\infty} \sigma_n A_n K_n (\alpha\rho) K_n (K_e r) \cos n (\phi - \phi_o) \quad (1-35)$$

$$H_s = \frac{I_o}{2\pi R} K_e R \sum_{n=0}^{\infty} \sigma_n A_n K_n (\alpha\rho) K'_n (K_e r) \cos n (\phi - \phi_o) \quad (1-36)$$

where ρ_e is the resistivity of surrounding medium

$$A_n = A_n^o \sigma_n K_n (\alpha\rho)$$

The secondary fields consist of the fundamental and harmonics. From equation(1-35), the fundamental part of the field is

$$E_o^S = - \frac{\rho_e I_o}{2\pi R^2} K_e^2 R^2 A_o^o K_o(\alpha\rho) K_o(K_e r) \quad (1-37)$$

Comparing equation (1-37) with (1-11), it can be recognized that this part of the field is caused by the linear source with current, $I_o A_o^o(\alpha\rho)$, which is distributed parallel to the axis of the cylinder. It also can be imagined that this current flows throughout the surrounding medium. Correspondingly this part of the field must depend on the electrical properties of the surrounding medium.

Fundamental Part of the Secondary Field

As is shown in equation (1-37), this part of the field does not depend on ϕ . In other words, this part of the field is caused by the linear current. Thus, the magnetic field has only ϕ -component and the electric field has only a Z-component.

Frequency Responses.

From equation (1-36) the magnetic field of this part becomes

$$H_o^S = \frac{I_o}{2\pi R} K_e R A_o^o K_o(\alpha\rho) K_1(K_e r) \quad (1-38)$$

where

$$A_o^o = \frac{I_1(\rho) I_o(m\rho) - m I_1(m\rho) I_o(\rho)}{K_1(\rho) I_o(m\rho) + m K_o(\rho) I_1(m\rho)} \quad (1-39)$$

Substituting $r = \beta a$, $R = ua$ and

Writing

$$E_o^S = - \frac{\rho_e I_o}{2\pi R^2} e_o^S$$

$$H_o^S = \frac{I_o}{2\pi R} h_o^S$$

Then

$$e_o^S = u^2 \rho^2 A_o^\circ K_o(\alpha\rho) K_o(\beta\rho) \quad (1-40)$$

and

$$h_o^S = u\rho A_o^\circ K_o(\alpha\rho) K_1(\beta\rho) \quad (1-41)$$

Using equations (1-40) and (1-41), the frequency responses of electric and magnetic fields are calculated. These results are shown in Fig. (1-7) and (1-8).

The low frequency part of the spectrum is considered. If the magnitude of the argument of the Bessel function in equation (1-40) and (1-41) is less than one, $|m\rho| < 1$, $|\alpha\rho| < 1$ and $|\beta\rho| < 1$, the function A_o° becomes

$$A_o^\circ \cong \frac{\rho^2 (1-m^2)}{2} \quad (1-42)$$

Thus the e_o^S and h_o^S are

$$e_o^S \cong \frac{u^2 (1-m^2)}{2} \rho^4 (\ln \alpha \ln \beta + \ln \alpha\beta \ln \rho + \ln^2 \rho) \quad (1-43)$$

or

$$E_o^S \cong \frac{I_o w \mu \gamma_i a^2}{4\pi} [\ln \alpha \ln \beta + 1/2 \ln \alpha\beta \ln (i w \mu \gamma_e a^2) + 1/4 \ln^2 (i w \mu \gamma_e a^2)]$$

$$h_o^S = \frac{u(m^2-1)}{2\beta} \rho^2 (\ln \alpha + \ln \rho) \quad (1-44)$$

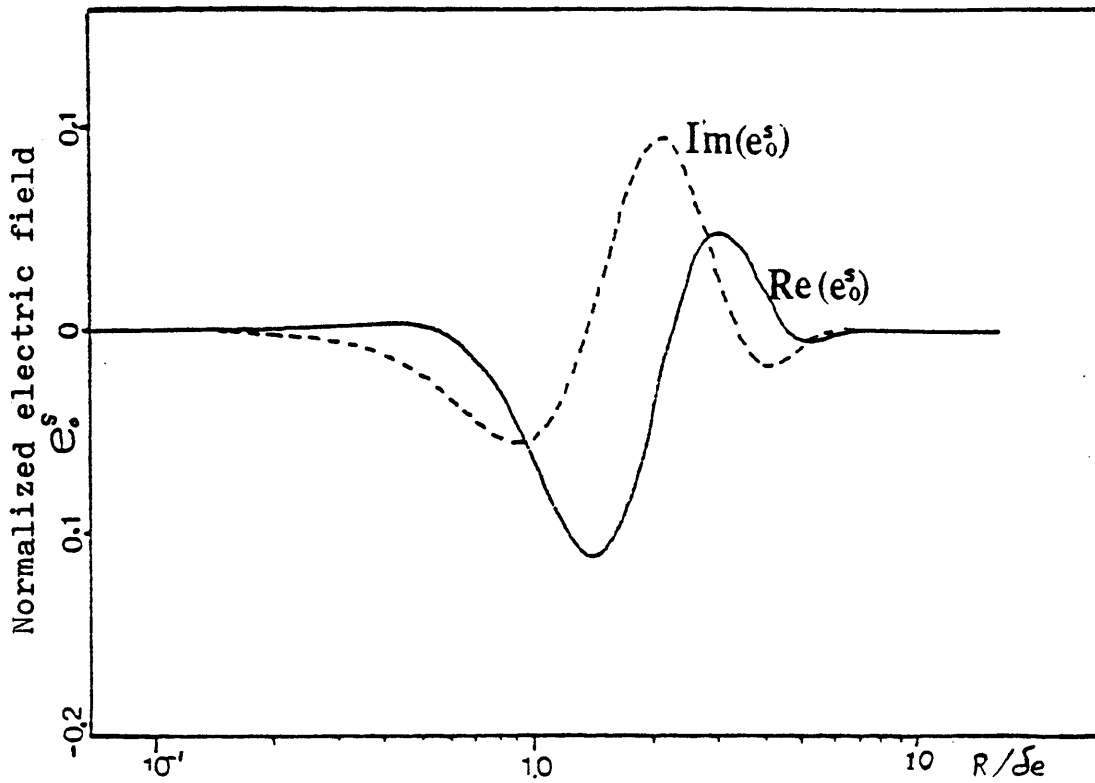


Figure 1-7. frequency response of the fundamental part of the secondary electric field.

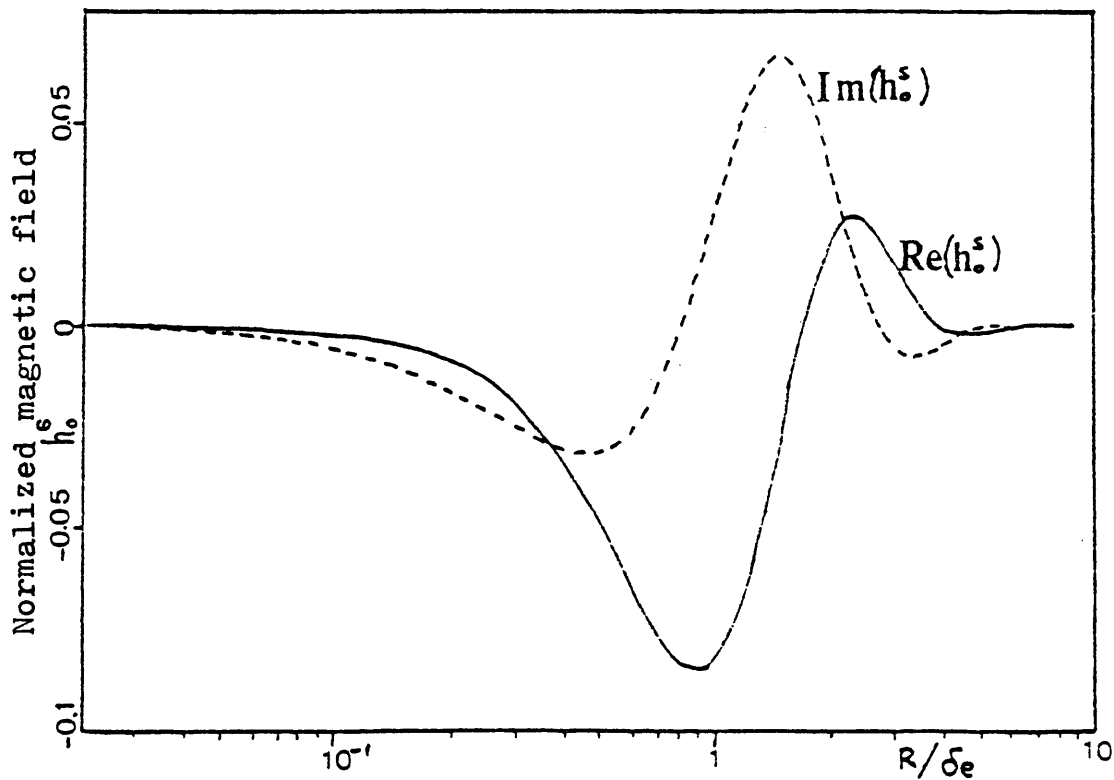


Figure 1-8. Frequency response of the fundamental part of the secondary magnetic field.

For the case of $m^2 \gg 1$ and $\rho \ll 1$

$$h_o^S \approx \frac{um^2}{2\beta} \rho^2 \ln \rho$$

or

$$h_o^S \approx \frac{u}{4\beta} (i\omega\mu \gamma_i a^2) \ln (i\omega\mu\gamma_e a^2) \quad (1-45)$$

At the low frequencies, from equations (1-43) and (1-45), it can be noticed that the fundamental part of the field depends on the conductivities of the cylinder and the surrounding medium.

Table (1-1) and (1-2) give results of calculations of the electric and magnetic field by using the full expressions and the asymptotic expressions for cases $\alpha=20$, $\beta=15$, $u=25$, and $m=10$.

From these two tables, it can be recognized that at the low frequencies, $R/\delta_e < 0.16$, the asymptotic expressions (1-43) and (1-44) give very similar values for the fields.

Transient Response

The transient response due to step function can be obtained through Fourier transform. From equation (1-40) and (1-41).

$$e_o(t) = \frac{2}{\pi} \int_0^{\infty} \frac{\text{Im}[e_o^S]}{w} \cos wt \, dw$$

$$\text{or } e_o(t) = \frac{2}{\pi} \int_0^{\infty} \mu\gamma_e R^2 R_e [A_o^\circ K_o(\alpha\rho) K_o(\beta\rho)] \cos wt \, dw$$

Table 1-1. Comparison of the normalized electric field in the frequency domain computed from exact formula and asymptotic expression.

R/δ _e	Inphase component of \bar{e}_z		Quadrature component of \bar{e}_z	
	Full expression	Asymptote	Full expression	Asymptote
0.01	0.692×10^{-7}	0.692×10^{-7}	-0.236×10^{-7}	-0.236×10^{-7}
0.02	0.798×10^{-6}	0.798×10^{-6}	-0.322×10^{-6}	-0.322×10^{-6}
0.04	0.860×10^{-5}	0.860×10^{-5}	-0.428×10^{-5}	-0.428×10^{-5}
0.08	0.835×10^{-4}	0.834×10^{-4}	-0.543×10^{-4}	-0.547×10^{-4}
0.16	0.667×10^{-3}	0.661×10^{-3}	-0.640×10^{-3}	-0.657×10^{-3}
0.32	0.325×10^{-2}	0.285×10^{-2}	-0.640×10^{-2}	-0.694×10^{-2}

Table 1-2. Comparison of the normalized magnetic field in the frequency domain computed from exact formula and asymptotic expression.

R/δ _e	Inphase component of h_ϕ		Quadrature component of h_ϕ	
	Full expression	Asymptote	Full expression	Asymptote
0.01	-0.207×10^{-4}	-0.207×10^{-4}	-0.121×10^{-3}	-0.121×10^{-3}
0.02	-0.833×10^{-4}	-0.831×10^{-4}	-0.421×10^{-2}	-0.421×10^{-2}
0.04	-0.335×10^{-2}	-0.334×10^{-2}	-0.135×10^{-2}	-0.136×10^{-2}
0.08	-0.137×10^{-2}	-0.135×10^{-2}	-0.423×10^{-2}	-0.425×10^{-2}
0.16	-0.564×10^{-2}	-0.557×10^{-2}	-0.120×10^{-1}	-0.123×10^{-2}
0.32	-0.226×10^{-1}	-0.235×10^{-1}	-0.271×10^{-1}	-0.294×10^{-1}

Through transformation of variables as

$$X = \mu \gamma_e R^2 w \text{ and } \tau = \frac{t}{\mu \gamma_e R^2} \quad (1-46)$$

$$e_o(\tau) = \frac{2}{\pi} \int_0^{\infty} \text{Re} [A_o^\circ K_o(\alpha\rho) K_o(\beta\rho)] \cos \tau X dX \quad (1-47)$$

where Im and Re mean the imaginary and the real part respectively. In the same way, the magnetic field becomes

$$h_o(t) = \frac{2}{\pi} \int_0^{\infty} \frac{\text{Im} [h_o^S]}{w} \cos wt dw.$$

In a real case usually the electromotive force is measured. The electromotive force and the magnetic field have the relation,

$$\oint \vec{E} \cdot d\vec{l} = - \frac{\partial}{\partial t} \int \vec{B} \cdot d\vec{s}.$$

Thus the derivative of the magnetic field with respect to time is considered.

$$h'_o(t) = - \frac{2}{\pi} \int_0^{\infty} \text{Im} [h_o^S] \sin wt dw$$

or

$$h'_o(\tau) = - \frac{2}{\pi} \frac{1}{\mu \gamma_e R^2} \int_0^{\infty} \text{Im} [h_o^S] \sin \tau x dx$$

$$\text{writing } h'_o(\tau) = \frac{1}{4\mu\gamma_e R^2} \cdot F_o(\tau)$$

Then

$$F_o(\tau) = -\frac{\delta}{\pi} \int_0^{\infty} \text{Im}[h_o^S] \sin \tau X \, dX \quad (1-48)$$

Using equations (1-47) and (1-48), the transient responses are calculated numerically (see appendix). These results are shown in Fig. (1-9) and (1-10).

Behavior of the transient field at the late stage is discussed. Asymptotic expressions for the transient field are obtained from the asymptotic expression at low frequencies.

Substituting $\rho^2 = k^2 S$, $k^2 = \mu\gamma_e a^2$ in equations (1-43) and (1-44)

$$e_o^S = \frac{u^2 (1-m^2)}{2} k^4 S^2 (\ln \alpha \ln \beta + 1/2 \ln \alpha \beta \ln k^2 S \\ + 1/4 \ln^2 k^2 S)$$

Using the following relations in the Laplace transform,

$$L^{-1} \{ \ln S \} = -1/t$$

$$L^{-1} \{ \ln^2 S \} = 2/t \ln(\gamma_o t)$$

or

$$L^{-1} \{ k^2 S \ln k^2 S \} = 1/k^2 \cdot 1/\tau_o^2$$

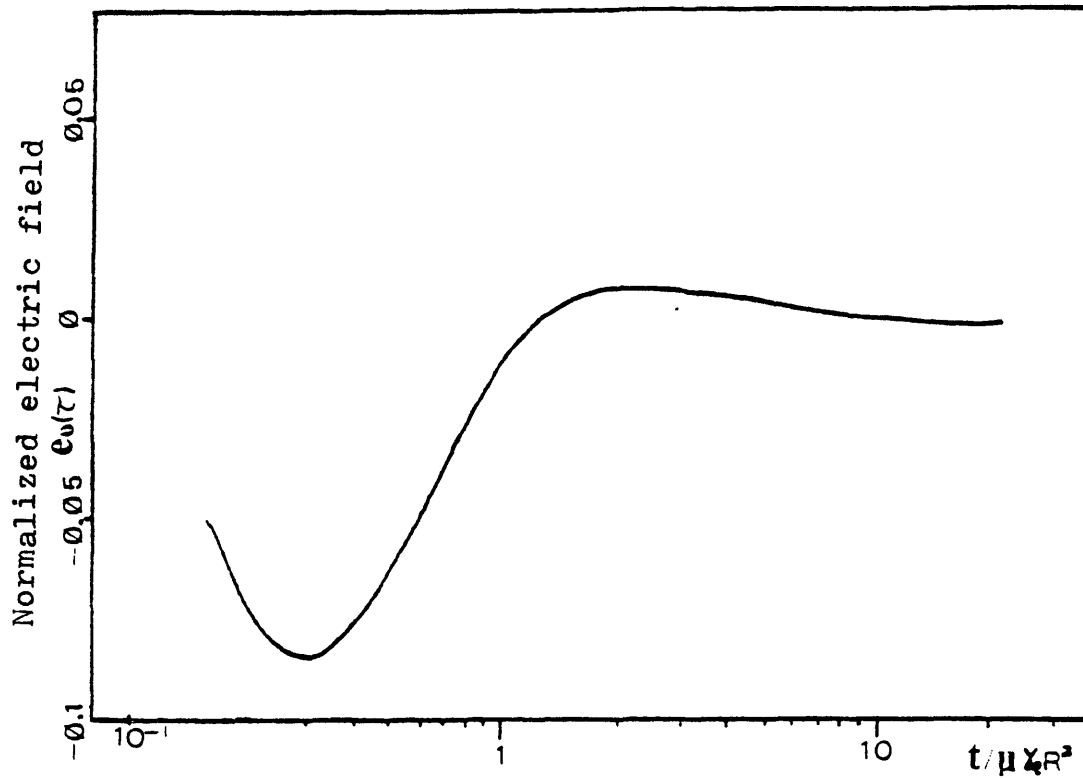


Figure 1-9. Transient response of the null fundamental part of the secondary electric field.

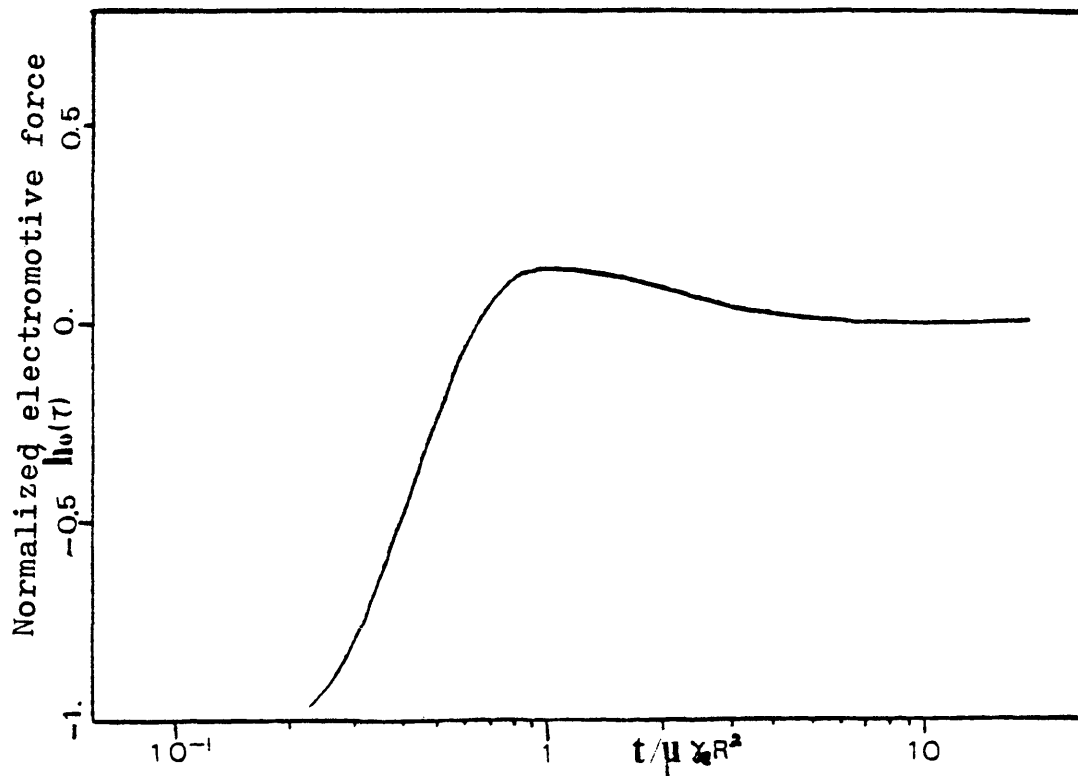


Figure 1-10. transient response of electromotive force. (Fundamental part)

$$L^{-1} \{ k^2 S \ln^2 k^2 S \} = 1/k^2 \left(- \frac{2}{\tau_0^2} \ln (\gamma_0 \tau_0) + \frac{2}{\tau_0^2} \right)$$

$$\text{where } \tau_0 = \frac{t}{\mu \gamma_e a^2} .$$

The transient responses due a step current are

$$e_o (\tau_0) = \frac{u^2 (1-m^2)}{4} \left[\frac{\ln \alpha \beta}{\tau_0^2} - \frac{\ln (\gamma_0 \tau_0)}{\tau_0^2} + \frac{1}{\tau_0^2} \right] \quad (1-49)$$

$$h_o (\tau_0) = - \frac{u (m^2-1)}{4\beta} \frac{1}{\tau_0} \quad (1-50)$$

If $m^2 \gg 1$.

$$\begin{aligned} h_o (\tau_0) &\cong - \frac{u}{4\beta} \frac{\gamma_i}{\gamma_e} \frac{\mu \gamma_e a^2}{t} \\ &= - \frac{U}{4\beta} \frac{\mu \gamma_i a^2}{t} \end{aligned} \quad (1-51)$$

From equation (1-50)

$$h_o' (\tau_0) = \frac{u(m^2-1)}{4\beta \mu \gamma_e a^2} \frac{1}{\tau_0^2} \quad (1-52)$$

Tables (1-3) and (1-4) show the results of the calculation of the numerically integrated values and the asymptotic values.

Through the above investigation, the following facts are found;

Table 1-3. Comparison of the normalized electric field in the time domain computed from exact formula and asymptotic expression.

$t/\mu\gamma_e R^2$	Integrated values	Asymptote
2.253	0.674×10^{-2}	0.776×10^{-2}
4.995	0.318×10^{-2}	0.304×10^{-2}
12.54	0.774×10^{-3}	0.715×10^{-3}
19.88	0.330×10^{-3}	0.327×10^{-3}

Table 1-4. Comparison of the normalized magnetic field in the time domain computed from exact formula and asymptotic expression.

$t/\mu\gamma_e R^2$	Integrated value	Asymptote
2.503	0.515×10^{-1}	0.421×10^{-1}
4.995	0.130×10^{-1}	0.106×10^{-1}
12.54	0.183×10^{-2}	0.168×10^{-2}
19.88	0.707×10^{-3}	0.669×10^{-3}

i) At low frequencies, the magnetic field depends on the conductivities of the cylinder and the surrounding medium.

ii) At the late stage, the magnetic field does not depend on the conductivity of the surrounding medium.

Linear Harmonic Part of the Secondary Field

The secondary fields consist of many harmonics. From equation (1-35), the linear harmonic part of the secondary field can be written as

$$E_{\perp}^S = - \frac{\rho e I_0}{2\pi R^2} \cdot 2 K_e^2 R^2 \sum_{n=1}^{\infty} A_n^{\circ} K_n(\alpha\rho) K_n(\beta\rho) \cos n(\phi - \phi_0) \quad (1-53)$$

or

$$e_{\perp}^S = 2 K_e^2 R^2 \sum_{n=1}^{\infty} A_n^{\circ} K_n(\alpha\rho) K_n(\beta\rho) \cos n(\phi - \phi_0) \quad (1-54)$$

where

$$A_n^{\circ} = - \frac{I_n'(\rho) I_n(m\rho) - m I_n(\rho) I_n'(m\rho)}{K_n'(\rho) I_n(m\rho) - m K_n(\rho) I_n'(m\rho)} \quad (1-55)$$

Unlike the case of the fundamental part of the secondary field, the linear harmonic part of the magnetic field has two components.

According to equation (1-2),

$$H_r = - \frac{1}{i\omega\mu r} \frac{\partial E_z}{\partial \phi}$$

writing

$$H_r = \frac{I_0}{2\pi R} \cdot hr$$

Then

$$hr = - \frac{2\mu}{\beta} \sum_{n=1}^{\infty} n A_n^{\circ} K_n(\alpha\rho) K_n(\beta\rho) \sin n(\phi - \phi_0) \quad (1-56)$$

From equation (1-36)

$$h_{\phi} = u \rho \sum_{n=1}^{\infty} A_n^{\circ} [K_{n-1}(\beta\rho) + K_{n+1}(\beta\rho)] K_n(\alpha\rho) \times \cos n(\phi - \phi_0) \quad (1-57)$$

Frequency Response.

For the case of $|K_e a| \ll 1$, the Bessel function in equation (1-55) can be expressed as

$$I_n(\rho) \cong \frac{\rho^n}{2^n n!} \quad \text{for } n \geq 1$$

$$K_n(\rho) \cong \frac{(n-1)! 2^{n-1}}{\rho^n} \quad \text{for } n \geq 1$$

Correspondingly the function A_n° becomes

$$A_n^{\circ} = - \frac{\rho^{2n}}{2^{2n-1} n! (n-1)!} T_n(m\rho) \quad (1-58)$$

with

$$T_n(m\rho) = \frac{I_{n+1}(m\rho)}{I_{n-1}(m\rho)} \quad (1-59)$$

Substituting the above results into equation (1-53), the linear harmonic part of the secondary field becomes

$$E_1^S = \frac{i\omega\mu I_0}{2\pi} \sum_{n=1}^{\infty} \frac{\rho^{2n}}{2^{2n-2} n! (n-1)!} T_n(m\rho) K_n(\alpha\rho) K_n(\beta\rho) \times \cos n(\phi - \phi_0) \quad (1-60)$$

Considering the field in near zone respect to the source and the cylinder, $|\alpha\rho| < 1$ and $|\beta\rho| < 1$, the first term in equation (1-60) can be written as

$$\frac{i\omega\mu I_0}{2\pi} \cdot T_1(m\rho) \frac{a^2}{r_0 r}$$

This term corresponds to an electric field due to eddy current, closed in a cylinder, when the primary field is uniform in vicinity of the cylinder. At the same time, currents flow in one direction in areas:

$$-\frac{\pi}{2} \leq \phi - \phi_0 \leq \frac{\pi}{2} \quad \text{and} \quad \frac{\pi}{2} \leq \phi - \phi_0 \leq \frac{3\pi}{2}$$

respectively. This is an electric field of the linear dipole. The following terms of equation (1-60) correspond to fields caused by higher order poles.

For the case of very low frequencies as $|m\rho| < 1$, the function $T_n(m\rho)$ becomes

$$T_n(m\rho) = \frac{m^2 \rho^2 (4n+8+m^2 \rho^2)}{4(n+1)(n+2)(4n+m^2 \rho^2)} \quad (1-61)$$

Thus, the fields in this range are

$$E_1^S = \frac{i\omega\mu I_0}{2\pi} m^2 \rho^2 \sum_{n=1}^{\infty} \frac{\cos n(\phi-\phi_0)}{4n(n+1)(n+2)\alpha^n \beta^n} \frac{(m^2 \rho^2 + 4n+8)}{(m^2 \rho^2 + 4n)} \\ + \frac{(-1)^{n+1} \rho^{2n} (\alpha^{2n} + \beta^{2n}) \cos n(\phi-\phi_0)}{2^{2n+2} n(n!)^2 (n+1)\alpha^n \beta^n} \ln \rho^2 \quad (1-62)$$

or

$$e_1^S = u^2 m^2 \rho^4 \sum_{n=1}^{\infty} \frac{\cos n(\phi-\phi_0)}{4n(n+1)(n+2)\alpha^n \beta^n} \frac{(m^2 \rho^2 + 4n+8)}{(m^2 \rho^2 + 4n)} \\ + \frac{(-1)^{n+1} \rho^{2n} (\alpha^{2n} + \beta^{2n}) \cos n(\phi-\phi_0)}{2^{2n+2} n(n!)^2 (n+1)\alpha^n \beta^n} \ln \rho^2 \quad (1-63)$$

In the above two equations, the first term is the dominant one. Thus, at low frequencies

$$E_1^S \cong \frac{i\omega\mu I_0}{2\pi} m^2 \rho^2 \sum_{n=1}^{\infty} \frac{\cos n(\phi-\phi_0)}{4n^2(n+1)\alpha^n \beta^n} \quad (1-64)$$

$$hr = \frac{-u}{4\beta} m^2 \rho^2 \sum_{n=1}^{\infty} \frac{\sin n(\phi-\phi_0)}{(n+1)(n+2)\alpha^n \beta^n} \frac{(4n+8+m^2 \rho^2)}{(4n+m^2 \rho^2)} \\ + \frac{(-1)^{n+1} \rho^{2n} (\alpha^{2n} + \beta^{2n}) \sin n(\phi-\phi_0)}{2^{2n} n(n!)^2 (n+1)\alpha^n \beta^n} \ln \rho^2 \quad (1-65)$$

or

$$h_r \cong \frac{-u}{4\beta} m^2 \rho^2 \sum_{n=1}^{\infty} \frac{\sin n (\phi - \phi_0)}{n(n+1) \alpha^n \beta^n} \quad (1-66)$$

$$h_\phi = u m^2 \rho^2 \sum_{n=1}^{\infty} \left\{ \frac{\cos n (\phi - \phi_0)}{4(n+1)(n+2) \alpha^n \beta^{n+1}} \frac{(m^2 \rho^2 + 4n + 8)}{(m^2 \rho^2 + 4n)} \right. \\ \left. + \frac{(-1)^{n+1} \rho^{2n} (\beta^{2n} - \alpha^{2n}) \cos n (\phi - \phi_0)}{2^{2n+2} (n+1)! (n-1)! \alpha^n \beta^{n+1}} \right\} \ln \rho^2 \quad (1-67)$$

or

$$h_\phi \cong u m^2 \rho^2 \sum_{n=1}^{\infty} \frac{\cos n (\phi - \phi_0)}{4n(n+1) \alpha^n \beta^{n+1}} \quad (1-68)$$

From equations (1-64), (1-66), and (1-68), it is found that (i) the linear harmonic part of the secondary fields do not depend on the conductivity of surrounding medium at low frequencies. (ii) The quadrature component of the magnetic field is proportional to the conductivity of the cylinder.

Taking into account the fact that, at low frequencies, this part of field is created by eddy currents which flow through closed paths inside the cylinder, it is obvious that this part of field mainly contains information about the cylinder.

Transient Responses

The asymptotic expressions of the transient field are obtained in the same way as what was done for the fundamental part of the field.

From equation (1-63), (1-65), and (1-67), the fields at the late stage are,

$$e_1(\tau_0) = \frac{8u^2}{m^2} \sum_{n=1}^{\infty} \frac{\cos n(\phi - \phi_0)}{(n+1)(n+2)\alpha^n \beta^n} e^{-4n/m^2 \tau_0} + u^2 \sum_{n=1}^{\infty} \frac{(\alpha^{2n} + \beta^{2n}) \cos n(\phi - \phi_0)}{2^{2n+2} n! \alpha^n \beta^n} \frac{m^2}{\tau_0^{n+2}} \quad (1-69)$$

$$h_r(\tau_0) = -\frac{u}{4\beta} \sum_{n=1}^{\infty} \left\{ \frac{8}{(n+1)(n+2)} e^{-4n/m^2 \tau_0} + \frac{(\alpha^{2n} + \beta^{2n})}{2^{2n} n!(n+1)} \frac{m^2}{\tau_0^{n+1}} \right\} \frac{\sin n(\phi - \phi_0)}{\alpha^n \beta^n} \quad (1-70)$$

$$h_\phi(\tau_0) = u \sum_{n=1}^{\infty} \left\{ \frac{1}{2(n+1)(n+2)} e^{-4n/m^2 \tau_0} + \frac{(\beta^{2n} - \alpha^{2n})}{2^{2n+2} (n+1)(n-1)!} \frac{m^2}{\tau_0^{n+1}} \right\} \frac{\cos n(\phi - \phi_0)}{\alpha^n \beta^{n+1}} \quad (1-71)$$

The series in the above three equations converge very fast. Thus the transient field at the late stage can be expressed by first one or two terms. Considering the first term of the series and noting that

$$\frac{\tau_0}{m^2} = \frac{t}{\mu \gamma_i a^2}$$

$$\frac{m^2}{\tau_o^2} = \frac{\mu \gamma_e \gamma_i}{t^2} a^4$$

It should be noted that the exponential terms of the fields at the far late stage become negligible compared to the polynomial of inverse power of τ_o . Hence, at the far late stage, the influence of the surrounding medium increases.

Discussion about the Secondary Field

Through the above investigation, the following facts are found.

i) At low frequencies, the fundamental part of the magnetic field is proportional to $i\omega \mu \gamma_i a^2 \ln i\omega \mu \gamma_e a^2$ and the linear harmonic part is proportional to $i\omega \mu \gamma_i a^2$. Thus the linear harmonic part depends only on the conductivity of the cylinder but at the same time, the quadrature component is dominant.

ii) At the late stage, the fundamental part decays as $\mu \gamma_i a^2/t$ and the linear harmonic part decays as

$$Ae^{-t/\mu \gamma_i a^2} + B \frac{\mu^2 \gamma_i \gamma_e a^4}{t}$$

Thus at the late stage, the fundamental part prevails.

iii) Through the numerical way, it is found that the fundamental part of the secondary field is much greater than the linear harmonic part. Fig. (1-11) and (1-12) show the frequency responses of zero harmonic part of the secondary

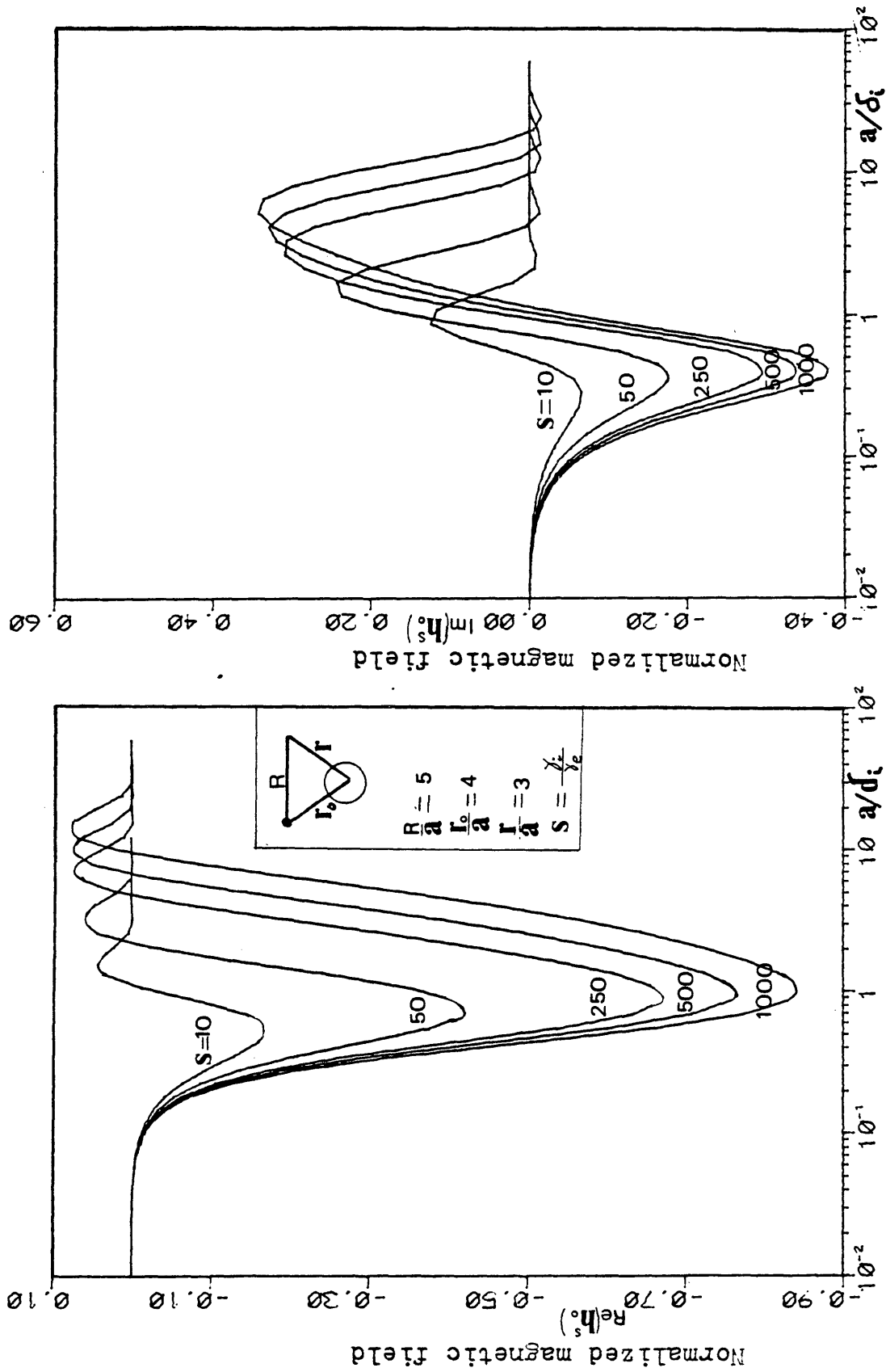


Figure 1-11. Frequency responses of the fundamental part of the magnetic field for several different ratios of conductivities.

Figure 1-12. Frequency responses of the fundamental part of the magnetic field for several different ratios of conductivities.

magnetic fields and figure (1-13) and (1-14) show the same for the total magnetic field.

Influence of the Surrounding medium

To find the range of frequency in which the influence of the surrounding medium is minimum, the ratio of the total magnetic field to the normal magnetic field is calculated. Fig. (1-15) demonstrates the ratio of the inphase component, $h^T/(h_N-1)$. From this figure, it can be seen that the influence of the surrounding medium is minimum at $a/\delta_1 = 0.3$. Comparing Fig. (1-13) and (1-15), it is found that the frequency, which allows one to measure maximum useful signal is different from the frequency which allows one to get the maximum ratio of the useful signal to geological noise.

Fig. (1-16) shows the ratio of quadrature components. Measuring the quadrature component, the influence of the surrounding medium is increased as the frequency increases. By decreasing the frequency, the ratio of the useful signal to the geological noise increases and approaches some constant.

Fig. (1-17) shows the ratio of the total electromotive force to the normal emf in the time domain. Regardless of the conductivity ratio, the location of the maximum ratio remains the same, $t/\mu\gamma_1 a^2 = 6.7$.

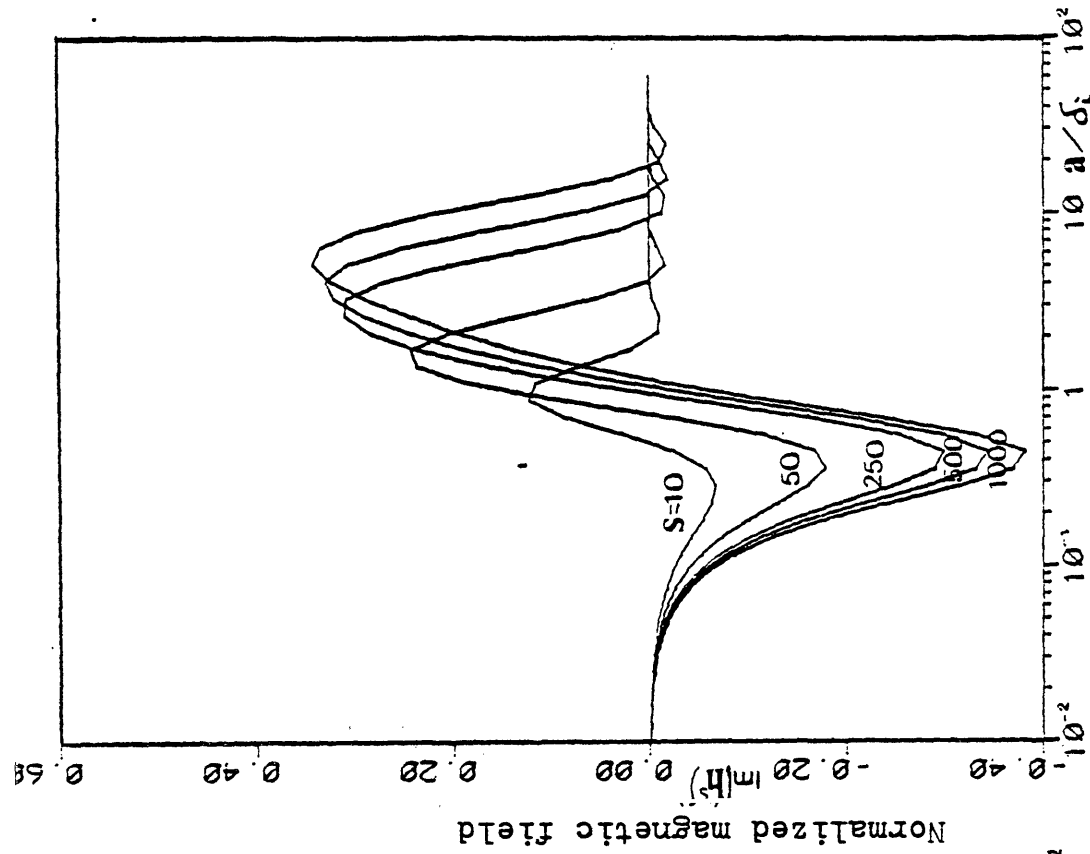


Figure 1-13.

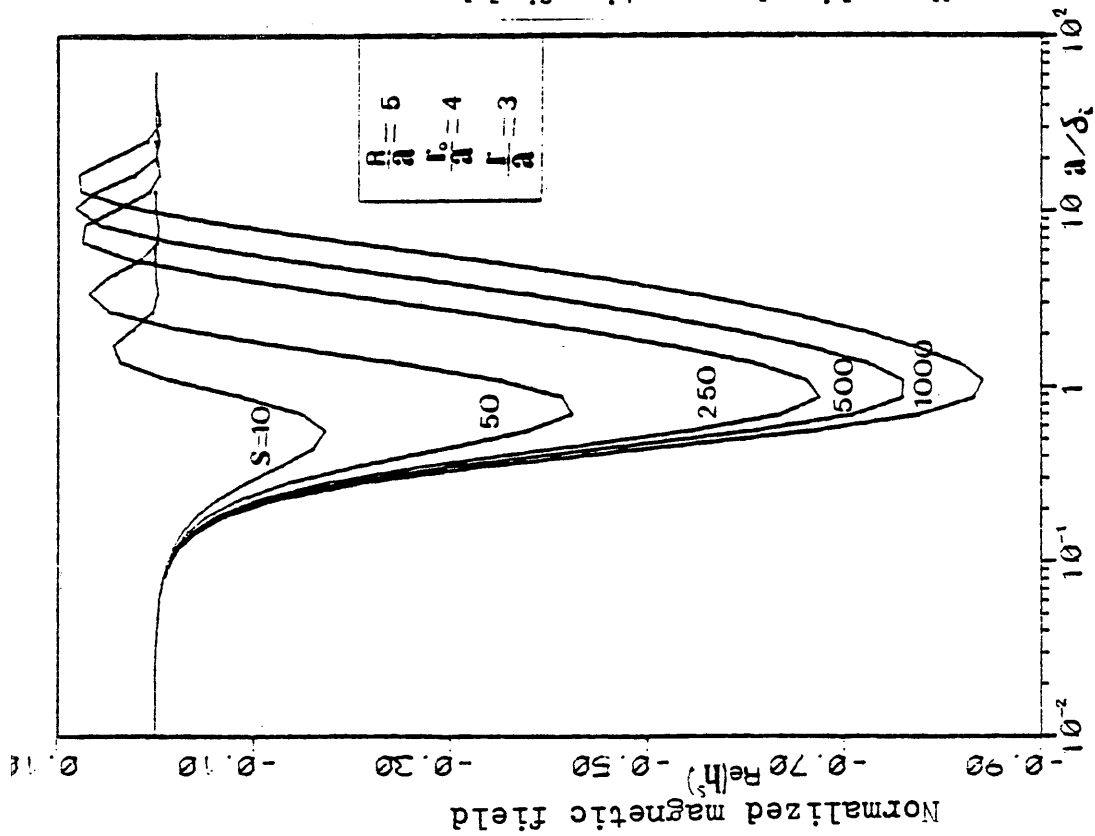


Figure 1-14.

Frequency response of the magnetic field for several different ratios of conductivities.

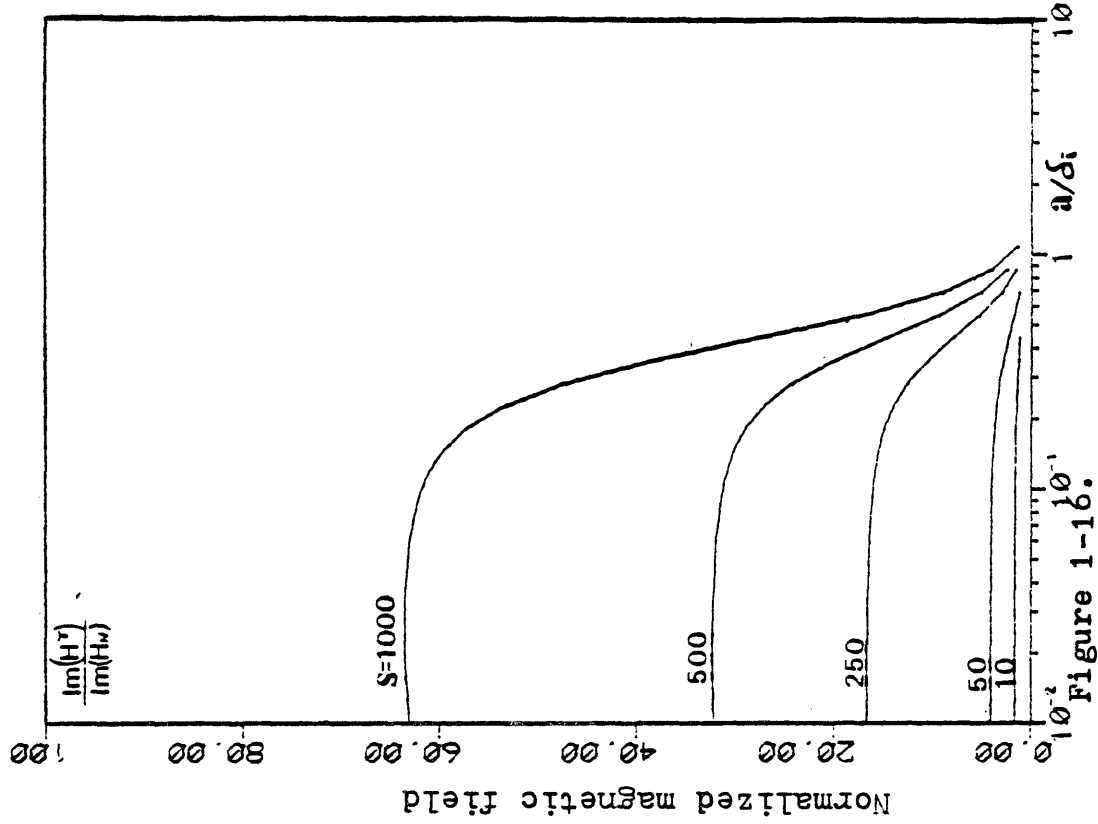


Figure 1-15.

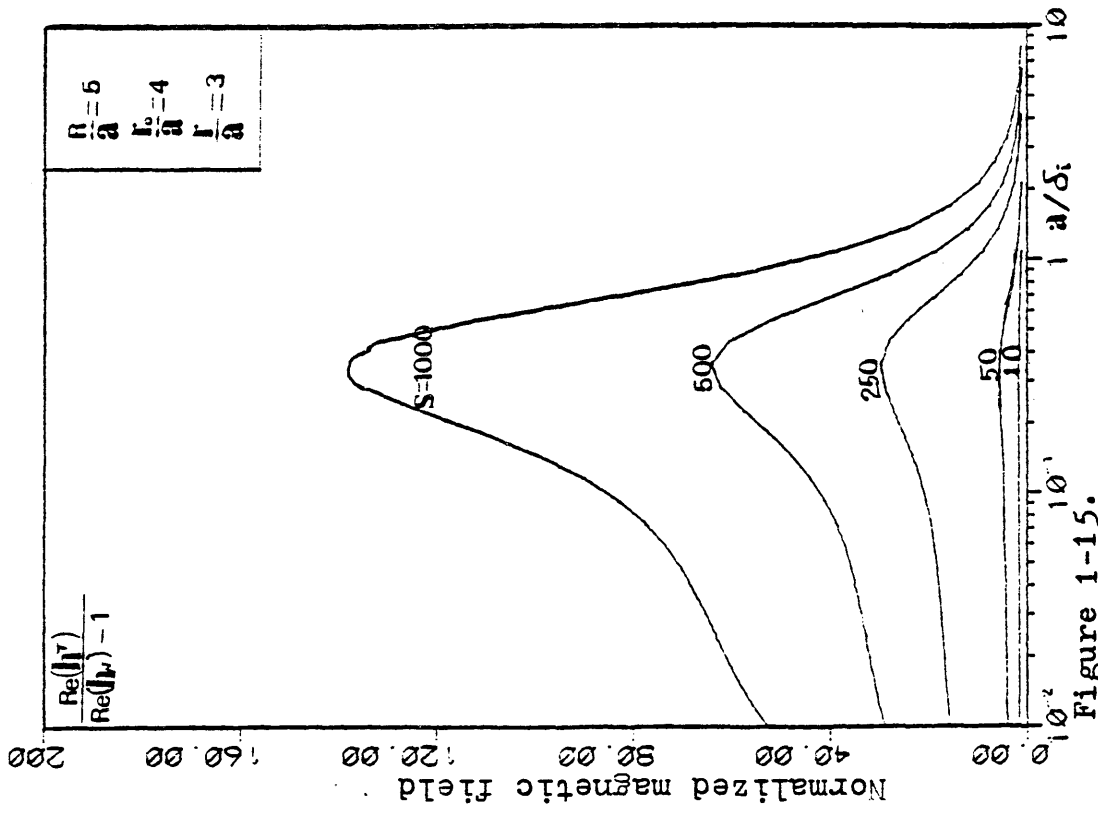


Figure 1-16.

The ratios of the total magnetic field to the normal magnetic field in frequency domain.

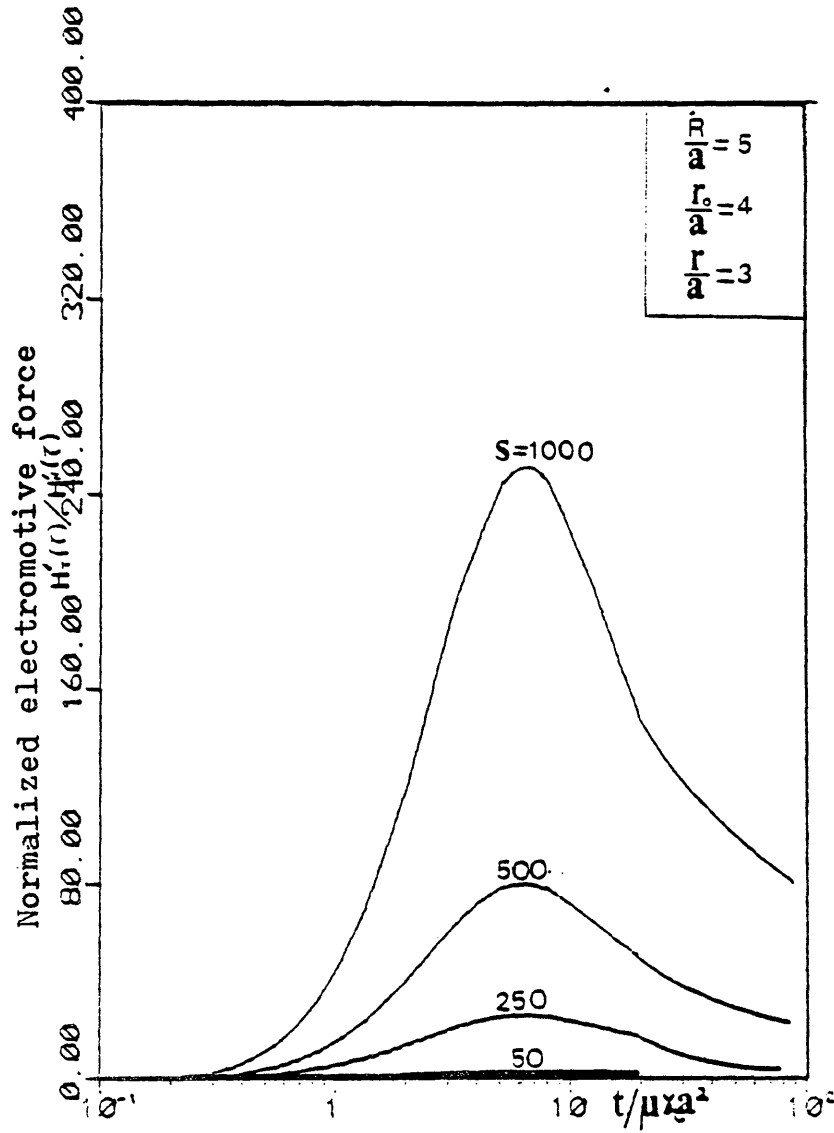


Figure 1-17. The ratios of the total electromotive force to the normal electromotive force in time domain.

In the time domain the normal field and the fundamental part of the secondary magnetic field decay as $1/\tau$ at late stage. The ratio of these two fields at late stage is

$$\frac{H_O^S}{H_N} \approx \frac{m^2 - 1}{\beta U}$$

or

$$\frac{H_O^S}{H_N} \approx \frac{m^2}{\beta U}$$

Taking into account the fact that the fundamental part is the dominant term of the secondary field at the late stage, it can be seen that the ratio of the useful signal to geological noise at the late stage does not depend on the time.

CHAPTER II

THE ELECTROMAGNETIC FIELD OF A CONDUCTING CYLINDER
WHEN THE SOURCE IS A MAGNETIC DIPOLE (SURROUNDING
MEDIUM IS AN INSULATOR)

The secondary field of a conducting cylinder energized by a magnetic dipole is investigated. It is assumed that the surrounding medium is not conductive. The analysis of the electromagnetic field is based on the solution given by Wait(1959).

Derivation of Formulae

The problem is to find the magnetic field inside and outside the cylinder. Since the conductivity of surrounding medium is zero, there is no current in the surrounding medium. Thus from equation(1-2), the magnetic field outside the conductor satisfies the following equation.

$$\text{Curl } \vec{H}_e = 0$$

From the above equation the magnetic field can be expressed by the gradient of a scalar potential

$$\vec{H}_e = - \nabla \Omega \quad (2-1)$$

where H_e denotes the magnetic field outside the conductor. As is known, the field due to a magnetic dipole in free space can be derived from the fictitious field due to a magnetic charge (Fig. 1). Unlike the field outside the conductor, the

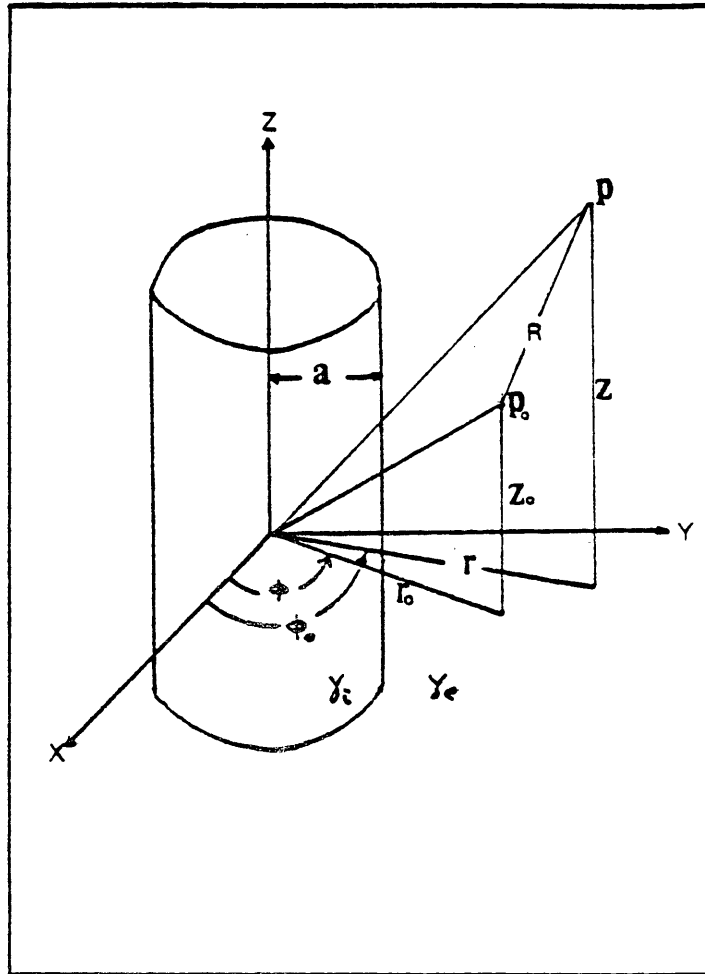


Figure 2-1. The cylindrical body and source P_0 and observer P with the cylindrical coordinate system.

fields inside the conductor are the solution of the wave equation and can be derived from a magnetic vector potential $\vec{\pi}^*$ and an electric vector potential $\vec{\pi}$ with only Z-components . These potentials are introduced as

$$\vec{E}_1 = iw\mu \text{ Curl } \vec{\pi}^* \quad (2-2)$$

$$\vec{H}_2 = \text{Curl } \vec{\pi} \quad (2-3)$$

From equations (1-2) and (2-2), one part of the magnetic field can be expressed using the magnetic type vector potential.

$$\text{Curl } \vec{H}_1 = K^2 \text{ Curl } \vec{\pi}^*$$

where

$$K^2 = iw\mu\gamma$$

or

$$\vec{H}_1 = K^2 \vec{\pi}^* - \text{Grad } U^* \quad (2-4)$$

where U^* is a scalar potential. Substituting equations (2-2) and (2-4) into (1-2)

$$\text{Grad Div } \vec{\pi}^* - \nabla^2 \vec{\pi}^* = K^2 \vec{\pi}^* - \text{Grad Div } U^* \quad (2-5)$$

In order to simplify the above equation, the Lorentz condition is introduced as

$$U^* = - \text{Div } \vec{\pi}^* \quad (2-6)$$

Thus, equation (2-5) becomes

$$\nabla^2 \vec{\pi}^* + K^2 \vec{\pi}^* = 0 \quad (2-7)$$

and \vec{H}_1 can be expressed only in terms of the potential $\vec{\pi}^*$ as

$$\vec{H}_1 = K^2 \vec{\pi}^* + \text{Grad Div } \vec{\pi}^* \quad (2-8)$$

The part of the electric field, which is a function only of the electric type vector potential, can be obtained as follows:

From equations (1-2) and (2-3)

$$\text{Curl } \vec{E}_{(2)} = i\omega\mu \text{ curl } \vec{\pi}$$

or

$$\vec{E}_{(2)} = i\omega\mu \vec{\pi} - \text{Grad } U \quad (2-9)$$

Substituting (2-3) and (2-9) into (1-2)

$$\text{Grad Div } \vec{\pi} - \nabla^2 \vec{\pi} = K^2 \vec{\pi} - \gamma \text{ Grad } U$$

Using Lorentz condition, the above equation becomes

$$\nabla^2 \vec{\pi} + K^2 \vec{\pi} = 0 \quad (2-10)$$

with

$$U = -1/\gamma \text{ Div } \vec{\pi} \quad (2-11)$$

Thus the one part of the electric field is

$$\vec{E}_2 = i\omega\mu \vec{\pi} + \text{Grad } (1/\gamma \text{ Div } \vec{\pi})$$

Using the above equations, the electric and the magnetic field inside the conductor can be written as

$$\begin{aligned} \vec{E}_e &= \vec{E}_{(1)} + \vec{E}_2 \\ &= i\omega\mu (\text{Curl } \vec{\pi}^* + \vec{\pi}) + 1/\gamma \text{ Grad Div } \vec{\pi} \end{aligned} \quad (2-12)$$

and

$$\begin{aligned} \vec{H}_i &= \vec{H}_{(1)} + \vec{H}_2 \\ &= \text{Curl } \vec{\pi} + K^2 \vec{\pi}^* + \text{Grad Div } \vec{\pi}^* \end{aligned} \quad (2-13)$$

The next step is to apply boundary conditions to derive the proper expressions for the field. To simplify the process of obtaining solutions, the field due to the magnetic charge is considered. As is shown in Fig. (2-1), the magnetic charge m is located at point P_0 . In this system the primary component of the scalar potential, Ω^P , is

$$\Omega^P = \frac{m}{4\pi R} \quad (2-14)$$

where R is the distance between source and observation point. Equation (2-14) is expressed in a cylindrical coordinate system to apply boundary conditions.

Using a formula (Watson, 1945)

$$1/R = 1/\pi \int_{-\infty}^{\infty} K_0(\lambda \hat{r}) e^{-i\lambda(z-z_0)} d\lambda \quad (2-15)$$

where $R = [\hat{r}^2 + (z-z_0)^2]^{1/2}$

with $\hat{r} = [r_0^2 + r^2 - 2rr_0 \cos(\phi - \phi_0)]^{1/2}$

and addition theorem

$$K_0(\lambda \hat{r}) = \sum_{n=0}^{\infty} \sigma_n K_n(\lambda r_0) I_n(\lambda r) \cos n(\phi - \phi_0)$$

where $\sigma_0 = 1$

$\sigma_n = 2$ for $n \geq 1$.

The equation (2-14) can be written as

$$\Omega^P = \frac{m}{4\pi^2} \sum_{n=-\infty}^{\infty} \sigma_n \int_{-\infty}^{\infty} K_n(\lambda r_0) [I_n(\lambda r) e^{-i\lambda(z-z_0)} e^{-in(\phi-\phi_0)}] d\lambda \quad (2-16)$$

for $r_0 > r$

or

$$\Omega^P = \frac{m}{2\pi^2} \sum_{n=0}^{\infty} \sigma_n \int_0^{\infty} K_n(\lambda r_0) I_n(\lambda r) \cos \lambda(z-z_0) \cos n(\phi-\phi_0) d\lambda \quad (2-17)$$

For the convenience of the algebraic operation, the following operator is introduced (Wait, 1959).

$$\Omega^P = \Gamma I_n(\lambda r) \quad (2-18)$$

In equation (2-1), the scalar potential can be considered as the sum of primary and secondary components.

$$\Omega = \Omega^P + \Omega^S$$

It is natural to find the secondary field as a similar form as the primary. The expression in equation (2-18) suggests the secondary potential outside the cylinder as

$$\Omega^S = \Gamma A_n(\lambda) K_n(\lambda r) \quad (2-19)$$

where $A_n(\lambda)$ is an unknown coefficient. Thus the expression of scalar potential Ω becomes

$$\Omega = \Gamma [I_n(\lambda r) + A_n K_n(\lambda r)] \quad (2-20)$$

The next step is to find the field inside the conductor. Assuming the vector potentials have only a Z component, the wave equation (2-7) becomes

$$\nabla^2 \pi_Z^* + K^2 \pi_Z^* = 0.$$

In cylindrical coordinate system, the above equation is

$$\frac{1}{r} \frac{\partial}{\partial r} \left(r \frac{\partial \pi_Z^*}{\partial r} \right) + \frac{1}{r^2} \frac{\partial^2 \pi_Z^*}{\partial \phi^2} + \frac{\partial^2 \pi_Z^*}{\partial z^2} + K^2 \pi_Z^* = 0$$

Considering the fact that the potential outside the cylinder is periodic in the Z-direction, the proper solution of the above differential equation is a linear combination of $I_n(ur)$, $K_n(ur)$, $e^{-in(\phi-\phi_0)}$ and $e^{-ix(Z-Z_0)}$ with $U^2 = \lambda^2 - K^2$. However, since the potential should have a finite value at the origin ($r=0$), the potential inside the cylinder can be written

$$\pi_Z^* = \Gamma a_n(\lambda) I_n(ur) \quad (2-21)$$

By analogy, the electric type vector potential π_Z has the form

$$\pi_Z = \Gamma b_n(\lambda) I_n(ur) \quad (2-22)$$

The unknown coefficients $A_n(\lambda)$, $a_n(\lambda)$, and $b_n(\lambda)$ are determined by boundary conditions. These conditions are the continuity of the tangential components of electric and magnetic field on the surface of the conductor. However, in this case, only the magnetic field is considered. Thus, instead of the continuity of E_ϕ the continuity of the normal flux of magnetic field is used as one of the boundary conditions.

These conditions are

$$i) H_\phi^e = H_\phi^i \text{ at } r = a.$$

or

$$\left. \frac{1}{r} \frac{\partial \Omega}{\partial \phi} \right|_{r=a} = \left[- \frac{\partial \pi_Z}{\partial r} + \frac{1}{r} \frac{\partial^2 \pi_Z^*}{\partial \phi \partial Z} \right]_{r=a}$$

Using equations (2-20), (2-21), and (2-22), the above equation becomes

$$\begin{aligned} & - \Gamma \frac{in}{a} [I_n(\lambda a) + A_n K_n(\lambda a)] \\ & = \Gamma \left[-U b_n I'_n(ua) - \frac{\lambda n}{a} a_n I_n(ua) \right] \end{aligned} \quad (2-23)$$

Taking into account the orthogonality of the function $e^{-in(\phi - \phi_0)}$ in the operator Γ , equation (2-23) can be written as

$$\frac{in}{a} [I_n(\lambda a) + A_n K_n(\lambda a)] = u b_n I'_n(ua) + \frac{\lambda n}{a} a_n I_n(ua) \quad (2-24)$$

$$\text{ii) } H_z^e = H_z^i$$

$$i\lambda [I_n(\lambda a) + A_n K_n(\lambda a)] = -u^2 a_n(\lambda) I_n(ua) \quad (2-25)$$

$$\text{iii) } H_r^e = H_r^i$$

$$\begin{aligned} & \lambda [I_n'(\lambda a) + A_n K_n'(\lambda a)] \\ &= i\lambda u a_n(\lambda) I_n'(ua) - \frac{in}{a} b_n(\lambda) I_n(ua) \end{aligned} \quad (2-26)$$

From the above three equations A_n is found to be

$$A_n(\lambda) = - \frac{\tilde{I}_n(\lambda a) - \tilde{I}_n(ua) + \frac{n^2 K^2}{a^4 \lambda^2 u^4} \frac{1}{\tilde{I}_n(ua)} I_n(\lambda a)}{\tilde{K}_n(\lambda a) - \tilde{I}_n(ua) + \frac{n^2 K^2}{a^4 \lambda^2 u^4} \frac{1}{\tilde{I}_n(ua)} \frac{I_n(\lambda a)}{K_n(\lambda a)}} \quad (2-27)$$

where

$$\begin{aligned} \tilde{I}_n(\lambda a) &= \frac{I_n'(\lambda a)}{\lambda a I_n(\lambda a)} \\ \tilde{K}_n(\lambda a) &= \frac{K_n'(\lambda a)}{\lambda a K_n(\lambda a)} \end{aligned}$$

Substitute

$$\lambda a = m, \quad ua = m_1, \quad K^2 a^2 = ip^2$$

then

$$A_n = \frac{\tilde{I}_n(m) - \tilde{I}_n(m_1) + \frac{in^2 p}{m^2 m_1^4} \frac{1}{\tilde{I}_n(m_1)} I_n(m)}{\tilde{K}_n(m) - \tilde{I}_n(m_1) + \frac{in^2 p}{m^2 m_1^4} \frac{1}{\tilde{I}_n(m_1)} \frac{I_n(m)}{K_n(m)}} \quad (2-28)$$

Thus the secondary magnetic field due to a magnetic charge is

$$\vec{H}^S = - \nabla \Omega^S$$

or

$$H_\phi = 1/r \int \sin A_n K_n (\lambda r)$$

$$H_r = -\Gamma \lambda A_n K_n' (\lambda r)$$

$$H_z = \Gamma i \lambda A_n K_n (\lambda r).$$

Electromagnetic Field Due to a Magnetic Dipole

Magnetic fields of a magnetic dipole can be calculated by taking the gradient of the field of the magnetic charge.

Axial Magnetic Dipole

In the case of a Z-directed magnetic dipole at P_0 (Fig. 2-1), the potential at P is

$$\Omega_0 = dl \frac{\partial \Omega}{\partial Z_0}$$

The magnetic field due to this dipole is

$$\vec{H}_{DZ} = - \text{Grad} \left(dl \frac{\partial \Omega}{\partial Z_0} \right)$$

and the radial component of the secondary magnetic field

become
$$H_{DZ}^r = - \nabla_r \left(dl \frac{\partial \Omega^S}{\partial Z_0} \right).$$

Defining

$$H_{DZ}^r \triangleq \frac{mdl}{4\pi r^3} \cdot h_r ,$$

it now readily follows that

$$h_r = - \frac{2u^3}{\pi} \sum_{n=0}^{\infty} \sigma_n \int_0^{\infty} m^2 A_n K_n'(\beta m) K_n(\alpha m) \sin \hat{z} m \, dm \cdot \cos n (\phi - \phi_0) . \quad (2-29)$$

By analogy, the corresponding ϕ - and r -components are

$$h_\phi = \frac{4u^3}{\pi\beta} \sum_{n=1}^{\infty} \sigma_n \int_0^{\infty} A_n K_n(\beta m) K_n(\alpha m) \sin \hat{z} m \, dm \sin n (\phi - \phi_0) \quad (2-30)$$

$$h_z = - \frac{2u^3}{\pi} \sum_{n=0}^{\infty} \sigma_n \int_0^{\infty} m^2 A_n K_n(\alpha m) K_n(\beta m) \cos \hat{z} m \, dm \cos n (\phi - \phi_0) \quad (2-31)$$

where $\hat{z} = (z - z_0)/a$

According to the above three equations, it can be found that the ϕ - and r -components of the secondary magnetic field do not exist on the plane $z = z_0$.

Transverse Magnetic Dipole

The secondary magnetic field due to the y -directed magnetic dipole is immediately obtained as

$$\vec{H}_{Dy} = - \text{Grad} \left(dl \frac{\partial \Omega^S}{\partial y_0} \right)$$

Noting that

$$\frac{\partial}{\partial y} = \sin \phi \frac{\partial}{\partial r} + \cos \phi \frac{\partial}{r \partial \phi}$$

it follows that

$$h_r = \frac{2u^3}{\pi} \sum_{n=0}^{\infty} \sigma_n \int_0^{\infty} m A_n K_n'(\beta m) [m \sin \phi_0 K_n'(\alpha m) \cos n(\phi - \phi_0) + \frac{n}{\alpha} \cos \phi_0 K_n(\alpha m) \sin n(\phi - \phi_0)] \cos \hat{z} m \, dm \quad (2-32)$$

$$h_\phi = \frac{4u^3}{\beta\pi} \sum_{n=1}^{\infty} A_n \int_0^{\infty} K_n(\beta m) [-mn \sin \phi_0 \sin n(\phi - \phi_0) \cdot K_n'(\alpha m) + \frac{n^2}{\alpha} \cos \phi_0 \cos n(\phi - \phi_0) K_n(\alpha m)] \, dm \cos \hat{z} m \, dm \quad (2-33)$$

$$h_z = \frac{2u^3}{\pi} \sum_{n=0}^{\infty} \sigma_n A_n \int_0^{\infty} -m K_n(\beta m) [m \sin \phi_0 K_n'(\alpha m) \cos n(\phi - \phi_0) + \frac{n}{\alpha} K_n(\alpha m) \cos \phi_0 \sin n(\phi - \phi_0)] \sin \hat{z} m \, dm \quad (2-34)$$

In this case the Z component of the field does not exist on the plane $z=z_0$. Using r- and ϕ -component, the vertical component of the secondary magnetic field on the plane $z=z_0$ is calculated as

$$h = (h_r \sin \theta + h_\phi \cos \theta) \quad (2-35)$$

where $\theta = \cos^{-1} \left(\frac{\beta^2 + u^2 - \alpha^2}{2\beta u} \right)$.

Vertical Magnetic Dipole

The secondary magnetic field of a conducting cylinder due to a vertical magnetic dipole is obtained as

$$\vec{H}_{DX} = - \text{Grad} \left(dl \frac{\partial \Omega^S}{\partial X_0} \right).$$

Taking into account the fact that

$$\frac{\partial}{\partial X} = \cos \phi \frac{\partial}{\partial r} + \sin \phi \frac{\partial}{r \partial \phi}.$$

Three components of the corresponding field are

$$h_r = \frac{2u^3}{\pi} \sum_{n=0}^{\infty} \sigma_n \int_0^{\infty} m A_n K_n'(\beta m) [m \cos \phi_0 K_n'(\alpha m) \cos n(\phi - \phi_0) + \frac{n}{\alpha} \sin \phi_0 K_n(\alpha m) \sin n(\phi - \phi_0)] \cos \hat{Z} m \, dm \quad (2-36)$$

$$h_\phi = \frac{4u^3}{\beta\pi} \sum_{n=1}^{\infty} \int_0^{\infty} A_n K_n(\beta m) [-nm \cos \phi_0 \sin n(\phi - \phi_0) K_n'(\alpha m) + \frac{n}{\alpha} \sin \phi_0 \cos n(\phi - \phi_0) K_n(\alpha m)] \cos \hat{Z} m \, dm \quad (2-37)$$

$$h_z = \frac{2u^3}{\pi} \sum_{n=0}^{\infty} \sigma_n \int_0^{\infty} -m K_n(\beta m) [m \cos \phi_0 K_n'(\alpha m) \cos n(\phi - \phi_0) + \frac{n}{\alpha} K_n(\alpha m) \sin \phi_0 \sin n(\phi - \phi_0)] \sin \hat{Z} m \, dm \quad (3-38)$$

Unlike the case of the infinite line source, the field due to a magnetic dipole source is expressed as integral form. This fact makes it difficult to figure out the behavior of the field. However, considering the field expressions, the following facts can be recognized.

i) The frequency and the conductivity dependence in the integrand is only in function A_n . In other words, the behavior of the frequency response is the same as that of function A_n .

ii) If $r_0/a \gg 1$, the secondary magnetic field is mainly defined by small value of m . In other words, in this case the primary field in the vicinity of the cylinder can be considered as a uniform field.

iii) If $r/a \gg 1$, the secondary magnetic field is also defined by small values of m . This statement can be explained as follows: Increasing the value of m , the eddy currents in the cylinder increase in oscillation in the Z-direction so that this current is the same as the one due to the higher order electric pole. The magnetic field due to the higher order pole decay very fast with respect to distance r .

iv) In case of small values of m , with increasing n , due to the factor $I_n(m)/K_n(m)$, the integrand decreases rapidly. This follows from the following approximation

$$\frac{I_n(m)}{K_n(m)} \cong \frac{m^{2n}}{n!(n-1)!2^{2n-1}} \quad \text{for } |m| < 1$$

Analysis of Function $A_n(m)$

$A_n(m)$ in equation (2-28) is a function of spatial frequency, m , wave number, and n . The behavior of this function is discussed with respect to these variables.

Small Value of m

Writing the function A_n as

$$A_n = \tilde{A}_n \frac{I_n(m)}{K_n(m)}$$

then

$$\tilde{A}_n = - \frac{\tilde{I}_n(m) - \tilde{I}_n(m_1) + \frac{in^2 p}{m^2 m_1^4} \frac{1}{\tilde{I}_n(m_1)}}{\tilde{K}_n(m) - \tilde{K}_n(m_1) + \frac{in^2 p}{m^2 m_1^4} \frac{1}{\tilde{I}_n(m_1)}} \quad (2-39)$$

For small values of m , $|m| < 1$.

$$I_n(m) \cong \frac{m^n}{2^n n!} \quad n \geq 1$$

$$K_n(m) \cong \frac{(n-1)! 2^{n-1}}{m^n} \quad n \geq 1$$

From the above expressions

$$\tilde{I}_n(m) \cong \frac{n}{m^2}$$

$$\tilde{K}_n(m) = -\frac{n}{m^2}$$

Substituting these relations into equation (2-39), \tilde{A}_n becomes

$$\tilde{A}_n = \frac{\frac{n}{m^2} - \frac{I_n'(m_1)}{m_1 I_n(m_1)} + \frac{in^2 p}{m^2 m_1^4} \frac{m_1 I_n(m_1)}{I_n'(m_1)}}{\frac{n}{m^2} + \frac{I_n'(m_1)}{m_1 I_n(m_1)} - \frac{in^2 p}{m^2 m_1^4} \frac{m_1 I_n(m_1)}{I_n'(m_1)}} \quad (2-40)$$

In case of $m^2 \ll K^2 a^2$, $m_1^2 \approx -ip$

and

$$\frac{in^2 p}{m^2 m_1^4} \frac{m_1 I_n(m_1)}{I_n'(m_1)} \approx - \frac{n^2}{m^2 m_1} \frac{I_n(m_1)}{I_n'(m_1)}$$

The numerator of equation (2-40) is

$$\begin{aligned} & \frac{n}{m^2} - \frac{I_n'(m_1)}{m_1 I_n(m_1)} - \frac{n^2}{m^2 m_1} \frac{I_n(m_1)}{I_n'(m_1)} \\ & \approx \frac{n[m_1 I_n'(m_1) - n I_n(m_1)]}{m^2 m_1 I_n'(m_1)} \end{aligned}$$

Noting the identity

$$I_n'(m_1) = \frac{n}{m_1} I_n(m_1) + I_{n+1}(m_1)$$

The numerator of equation (2-40) becomes

$$\frac{n I_{n+1}(m_1)}{m^2 I_n'(m_1)}$$

With the same approximation, the denominator of equation(2-40) is

$$\frac{n[m_1 I_n' (m_1) + n I_n (m_1)]}{m^2 m_1 I_n' (m_1)} = \frac{n[2n I_n (m_1) + m_1 I_{n+1} (m_1)]}{m^2 m_1 I_n' (m_1)} .$$

Using the relation

$$I_n (m_1) = m_1 \frac{I_{n-1} (m_1) - I_{n+1} (m_1)}{2n}$$

then the denominator is

$$\frac{n I_{n-1} (m_1)}{m^2 I_n' (m_1)} .$$

Thus, at small values of m the function \tilde{A}_n is

$$\tilde{A}_n = \frac{I_{n+1} (m_1)}{I_{n-1} (m_1)} \quad (2-41)$$

or with further approximation as

$$m_1 = \sqrt{m^2 - k^2 a^2} \cong iKa$$

Then

$$\tilde{A}_n = \frac{I_{n+1} (iKa)}{I_{n-1} (iKa)} = - \frac{I_{n+1} (Ka)}{I_{n-1} (Ka)} \quad (2-42)$$

This result is the same as function T_n in equation (1-59). It means, through the above-mentioned approximation, the field due to a magnetic dipole becomes very similar to the field due to an infinite line source.

Low Frequency Approximation

At the low frequencies, $|Ka| < 1$, equation(2-42) becomes as follows

$$\begin{aligned} \tilde{A}_1 &\cong - \frac{I_2(K_a)}{I_0(K_a)} \\ &\cong - \frac{K^2 a^2}{8} \left(1 - \frac{1}{6} K^2 a^2\right) \end{aligned} \quad (2-43)$$

$$\tilde{A}_n \cong - \frac{K^2 a^2}{4n(n+1)} \left(1 - \frac{K^2 a^2}{2n(n+2)}\right) \quad (2-44)$$

Investigating the above two expressions, it is found that the quadrature component of the magnetic field is proportional to $\omega\mu\gamma a^2$ and the inphase component is proportional to $(\omega\mu\gamma a^2)^2$ at low frequencies.

Frequency Responses of the Magnetic Field

Frequency responses corresponding to axial and transverse magnetic dipoles are investigated numerically.

Axial Magnetic Dipole

Using equation (2-31), the z-component of the secondary magnetic field was calculated for several different geometries. From numerical calculation, it is found that the integrand converges very fast with respect to n. Fig. (2-2) and (2-3) show the ratio of the secondary to the primary magnetic field.

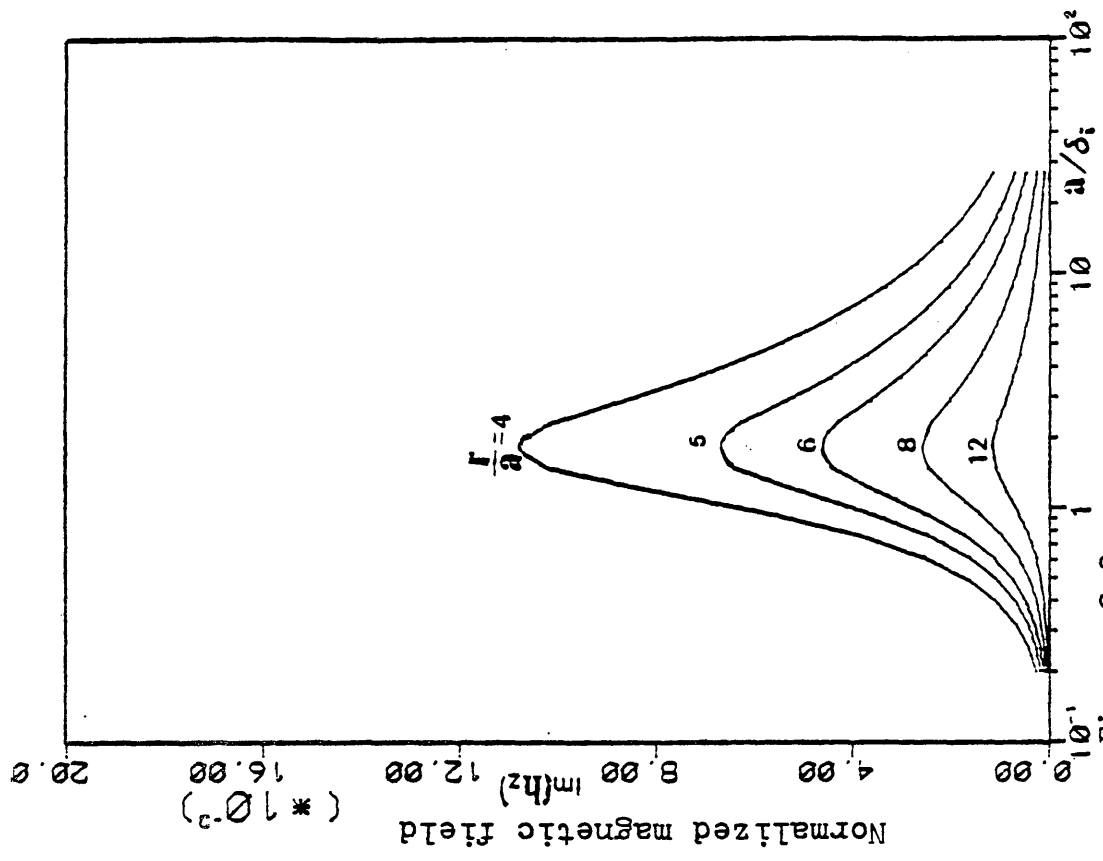


Figure 2-3.

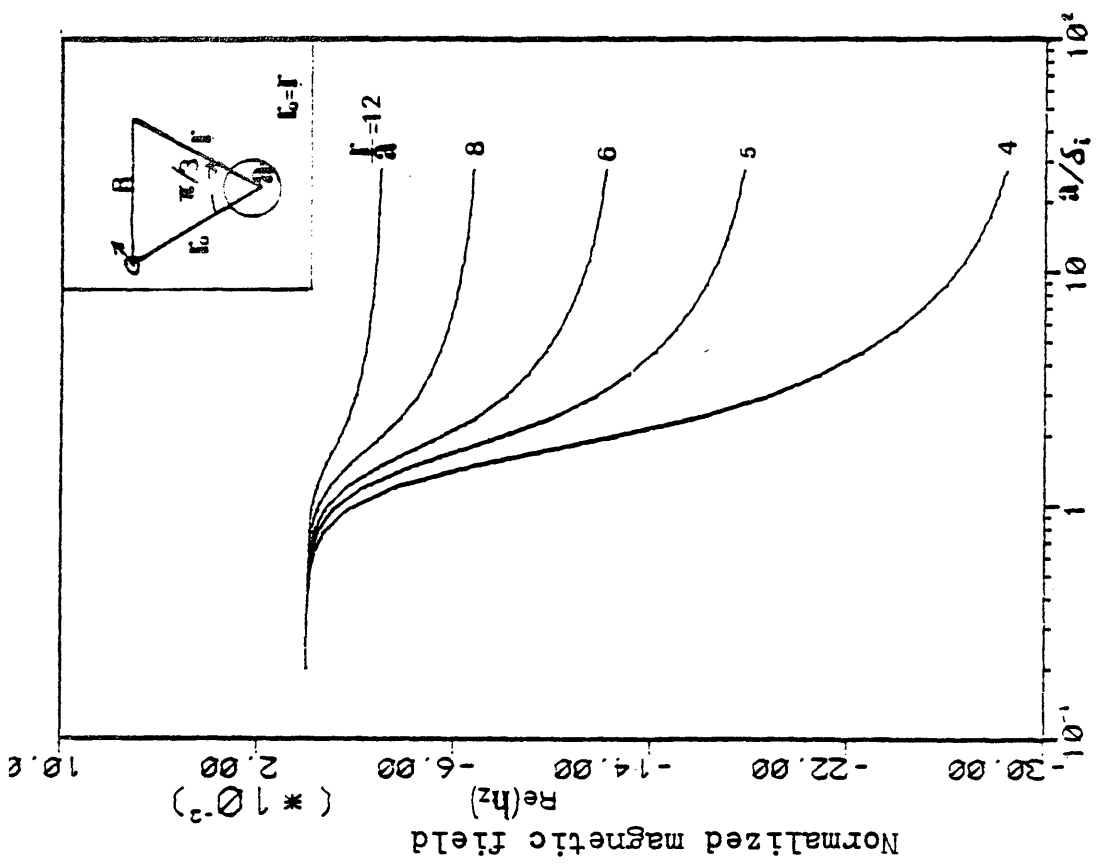


Figure 2-2.

Frequency response of the magnetic field for several different geometries of the system (source is a transverse magnetic dipole)

Increasing the distance from the conductor, this ratio monotonically decreases. The magnitude of the inphase components increases as frequency increases. The quadrature component of the field has a maximum value at the point around $a/\delta_i = 1.9$. Increasing the distance from the conductor, the magnitude decreases but the maximum ratios appear at the same frequency.

At low frequencies, the secondary magnetic field can be expressed as

$$R_e [H^S] = a_1 (w\mu\gamma a^2)^2 + a_2 (w\mu\gamma a^2)^4 + \dots \quad (2-45)$$

$$I_m [H^S] = b_1 (w\mu\gamma a^2) + b_2 (w\mu\gamma a^2)^3 + \dots \quad (2-46)$$

Considering the field with respect to conductivity, theoretically, the inphase component is more sensitive than the quadrature component but usually the inphase component of the secondary field is relatively small compared to the primary field. In other words, to differentiate the secondary field, very accurate measurements are needed. In equation(2-46), the first term is the dominant term. This term can be eliminated by the following operation.

$$\Delta H = H (w_1) - \frac{w_1}{w_2} H (w_2) \quad (2-47)$$

It readily follows

$$I_m \{ \Delta H \} \cong b_2 w_1 (w_1^2 - w_2^2) (\mu\gamma a^2)^3 \quad (2-48)$$

Through the above operation, the quadrature component of the field becomes proportional to γ^3 at low frequencies. By measuring at two different frequencies the resolving capability is increased. Figure (2-4) shows the computed results for this operation.

Transverse Magnetic Dipole

Using equation (2-35) the vertical component of the secondary magnetic field is calculated. As can be seen from equations (2-31), (2-32), and (2-33), the behavior of the fields with respect to frequency is the same. Frequency response of the magnetic field is shown in Fig. (2-5) and (2-6). Comparing with the figures (2-2) and (2-3), it can be noted that the frequency responses due to two different magnetic dipoles are the same except for the difference of the magnitude. The vertical component of the magnetic field due to a transverse magnetic dipole is larger than the horizontal component of the magnetic field due to an axial magnetic dipole. Fig. (2-7) shows the difference of magnetic field at two different frequencies. This corresponds to Fig. (2-4) in the previous section.

Discussion About the Magnetic Fields in Frequency Domain

The secondary magnetic fields, due to different excitation, are considered. It was known that the secondary magnetic field for a conducting cylinder due to the uniform primary magnetic

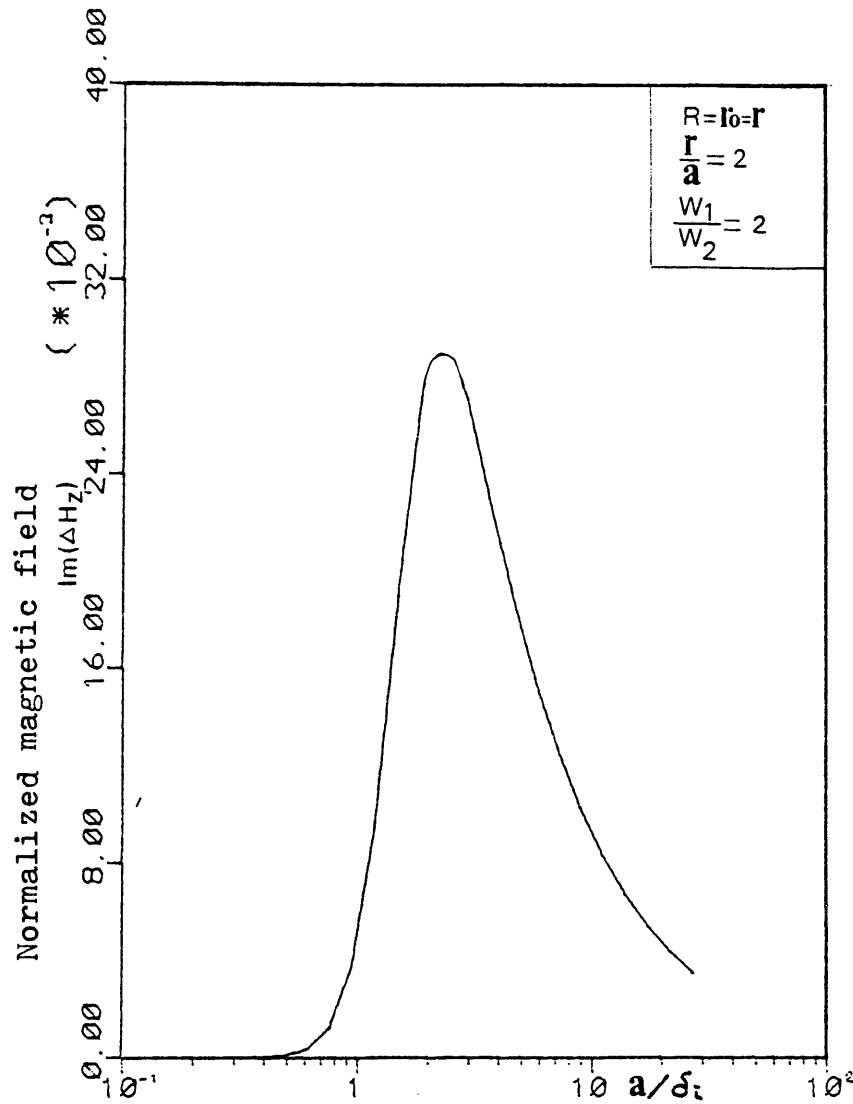


Figure 2-4. Frequency response of the quadrature component of magnetic field with the leading term of the low frequency asymptote removed.
 (Source is an axial magnetic dipole)

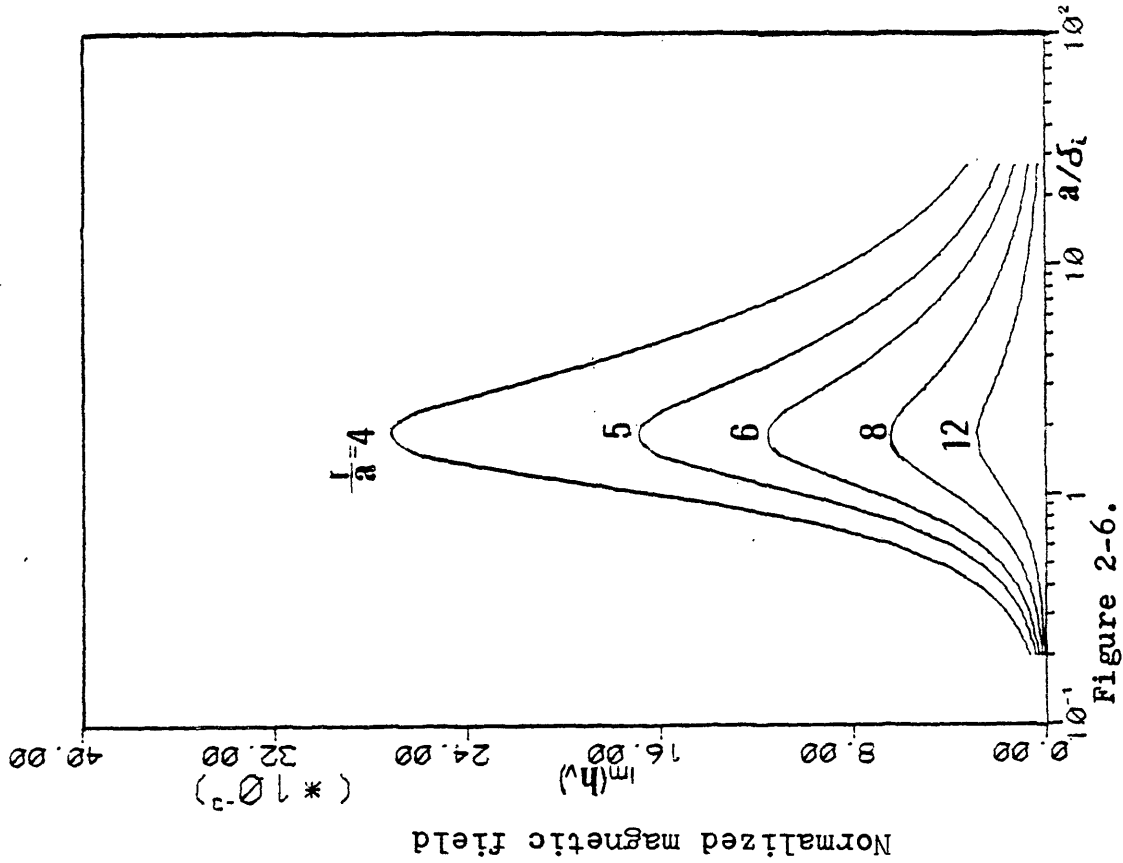


Figure 2-6.

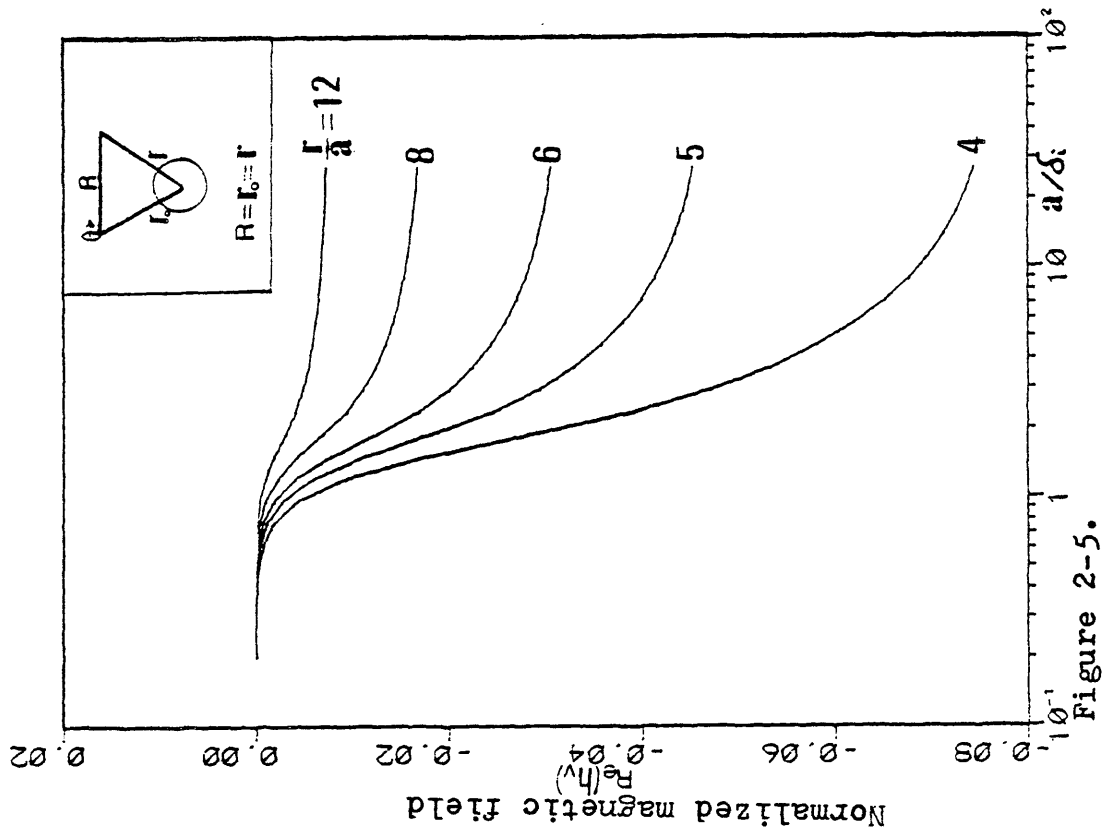


Figure 2-5.

Frequency response of the magnetic field for several different geometry of the system (source is a transverse magnetic dipole)

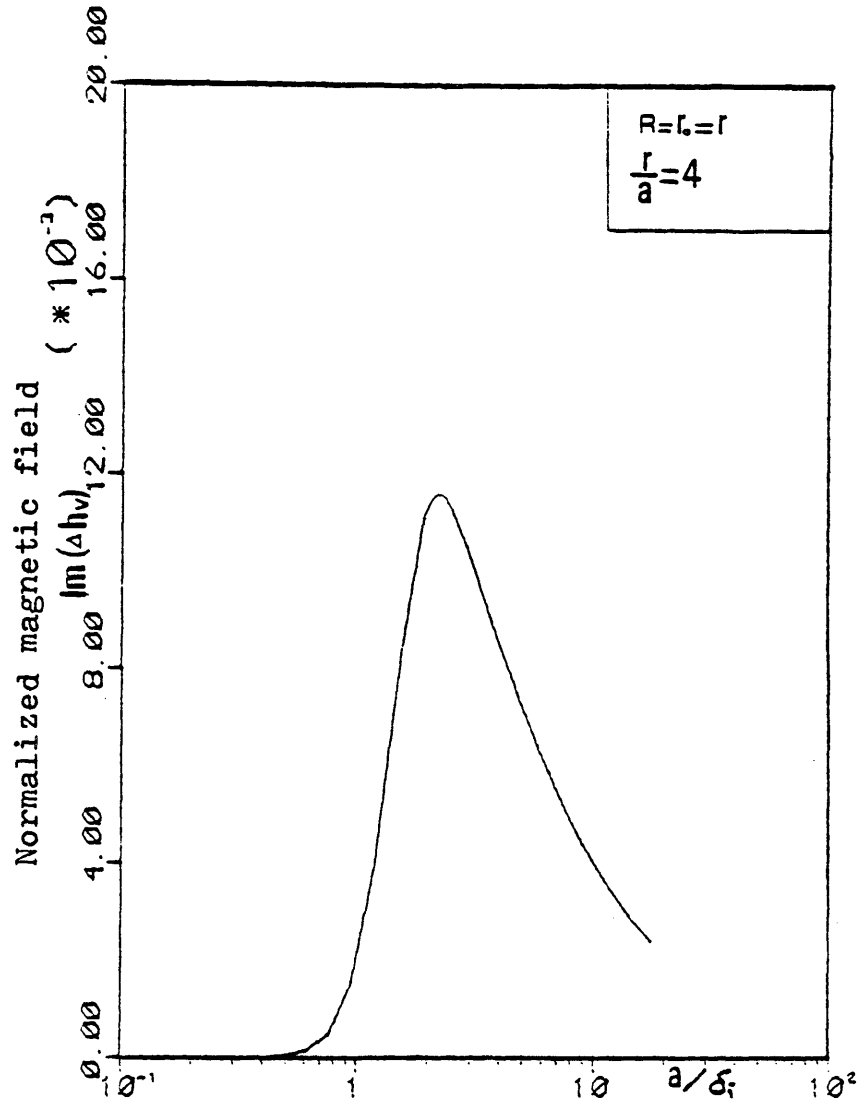


Figure 2-7. Frequency response of the quadrature component of the magnetic field with the leading term of the low frequency asymptote removed
 (Source is a transverse magnetic dipole)

field has the some form as (Fig. 2-8)

$$H_r = H_o \left(\frac{a}{y}\right)^2 \frac{I_2 (Ka)}{I_o (Ka)} \cos \theta_2 \quad (2-43)$$

$$H_\phi = H_o \left(\frac{a}{y}\right)^2 \frac{I_2 (Ka)}{I_o (Ka)} \sin \theta_2 \quad (2-50)$$

where y is the distance between the center of the cylinder and the observation point.

H_o is the primary magnetic field. Thus, at low frequencies quencies, this secondary field behaves as (see equation 2-43)

$$H \cong G [iw\mu\gamma a^2 - 1/6 (w\mu\gamma a^2)^2]$$

where G is a geometric factor.

The secondary magnetic field due to a magnetic dipole is investigated numerically. From the numerical results, it is found that the asymptotic behavior of the secondary magnetic field, regardless of the different excitations, is

$$H \cong G [iw\mu\gamma a^2 - 1/6.2 (w\mu\gamma a^2)^2]$$

For the case of $r/a \geq 4$ and $r_o/a \geq 4$.

Comparing the above two expressions, the following fact can be recognized:

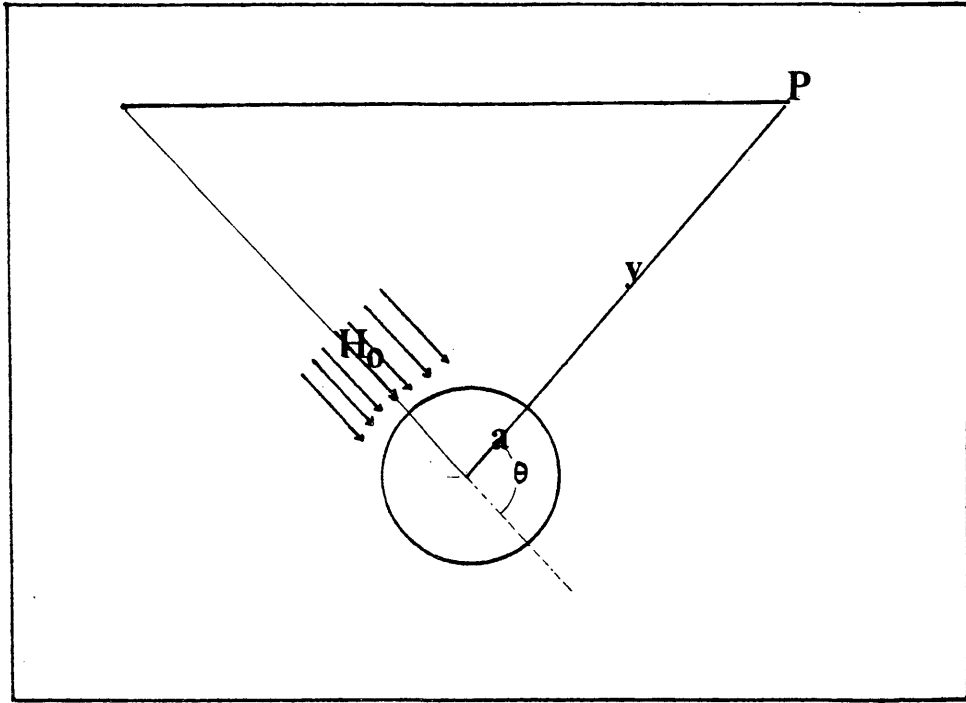


Figure 2-8. Configuration of the observer P and cylinder when the primary field, in the vicinity of the cylinder, is uniform

If the source and the observation point are located relatively far from the cylinder, the secondary magnetic field has similar behavior to the one due to the uniform primary field. To examine this, the vertical component of secondary magnetic field due to a transverse magnetic dipole is considered. Suppose the primary magnetic field is uniform in the vicinity of the cylinder and the magnitude of this field is the same as the primary field due to the magnetic dipole at the center of the cylinder.

Then the secondary magnetic field can be calculated using equations (2-49) and (2-50). For the case of the geometry shown in Fig. (2-5),

$$H_r^S = H_0 (a/r)^2 \frac{I_2(Ka)}{I_0(Ka)} \cos 221^\circ$$

$$H_\phi^S = H_0 (a/r)^2 \frac{I_2(Ka)}{I_0(Ka)} \sin 221^\circ$$

Thus the vertical component of the field becomes

$$H_v^S = -1.081 H_0 (a/r)^2 \frac{I_2(Ka)}{I_0(Ka)}$$

According to the above expression, the value of H_v^S/H_0 at high frequencies is $H_v^S/H_0 \cong - (a/r)^2$ (2-51)

From Fig. (2-5) it can be seen that the inphase components of the field approximately approach the value of $-a^2/r^2$ at the high frequencies.

Transient Response of the Magnetic Field

The secondary magnetic field is calculated in time domain through Fourier transform. For the case of the source is a step-off current, the transient field is calculated as

$$f(t) = \frac{2}{\pi} \int_0^{\infty} \frac{I_m[F(w)]}{w} \cos wt \, dw \quad (2-52)$$

Applying the above operation to equation (2-31), the Z-component of the magnetic field becomes

$$h_z(t) = \frac{2}{\pi} \int_0^{\infty} \frac{\text{Im}[h_z(w)]}{w} \cos wt \, dw \quad (2-53)$$

Through transformation of integral variables as

$$x = \mu\gamma wa^2 \quad \text{and} \quad \tau = t/\mu\gamma a^2 \quad (2-54)$$

it follows that

$$h_z(\tau) = \frac{2}{\pi} \int_0^{\infty} \frac{\text{Im}[h_z(x)]}{x} \cos \tau x \, dx \quad (2-55)$$

Fig. (2-9) shows transient response of magnetic field due to an axial magnetic dipole. By analogy, using equation (2-35) the transient response for the case of a transverse magnetic dipole is calculated and this result is presented in Fig. (2-10). As is shown in the above two figures, at the early stage the magnetic field approaches the value of the inphase component at the

high frequency. As the time increases the field monotonically decays, The magnetic fields due to two different excitations have similar behavior in the time domain. As in the frequency domain, the only difference is the magnitude.

The Asymptotic Behavior of the Magnetic Field at the Late Stage

The behavior of magnetic field at the late stage is investigated. It was known that the transient field at the late stage can be expressed exponentially if the low frequency part of the spectrum is described as the sum of integer powers of w (Kaufman, 1978). There is a relation between low frequency part of the spectrum and the late stage of the transient field. If the low frequency part of the spectrum is

$$D(w) = i C_1 (\gamma \mu w a^2) - C_2 (\gamma \mu w a^2)^2 + \dots$$

then the transient field at the late stage is

$$D(t) \cong A e^{-q_1 \frac{t}{\gamma \mu a^2}}$$

with

$$q_1 = \frac{C_1}{C_2} \quad \text{for } q_1 \frac{t}{\gamma \mu a^2} \geq 1.$$

Through numerical calculation, regardless of the change of geometry ($r/a \geq 4$, $r_0/a \geq 4$), it is found that the value for q_1 remains around 6.2 in frequency domain. This value q_1 agrees with the coefficient of the exponent at the late stage. For the case of uniform primary magnetic field, this coefficient is 6 (see equation (2-43)).

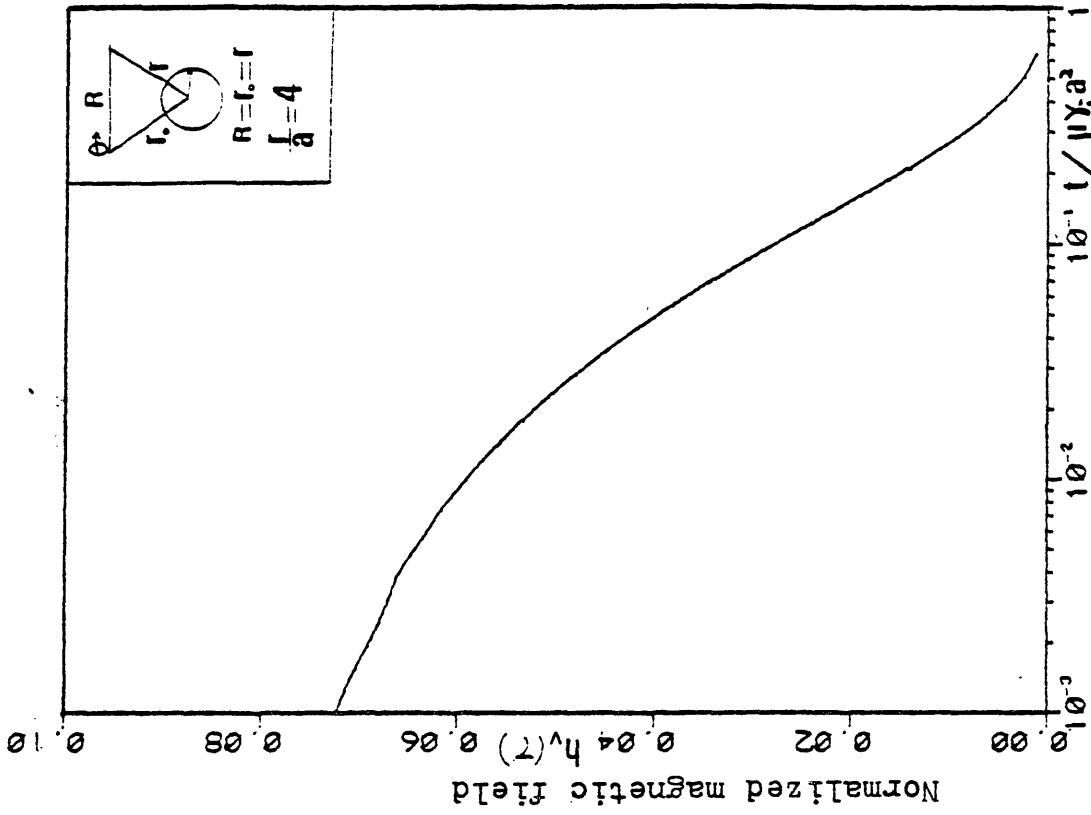


Figure 2-10. Transient response of the magnetic field (source is a transverse magnetic dipole)

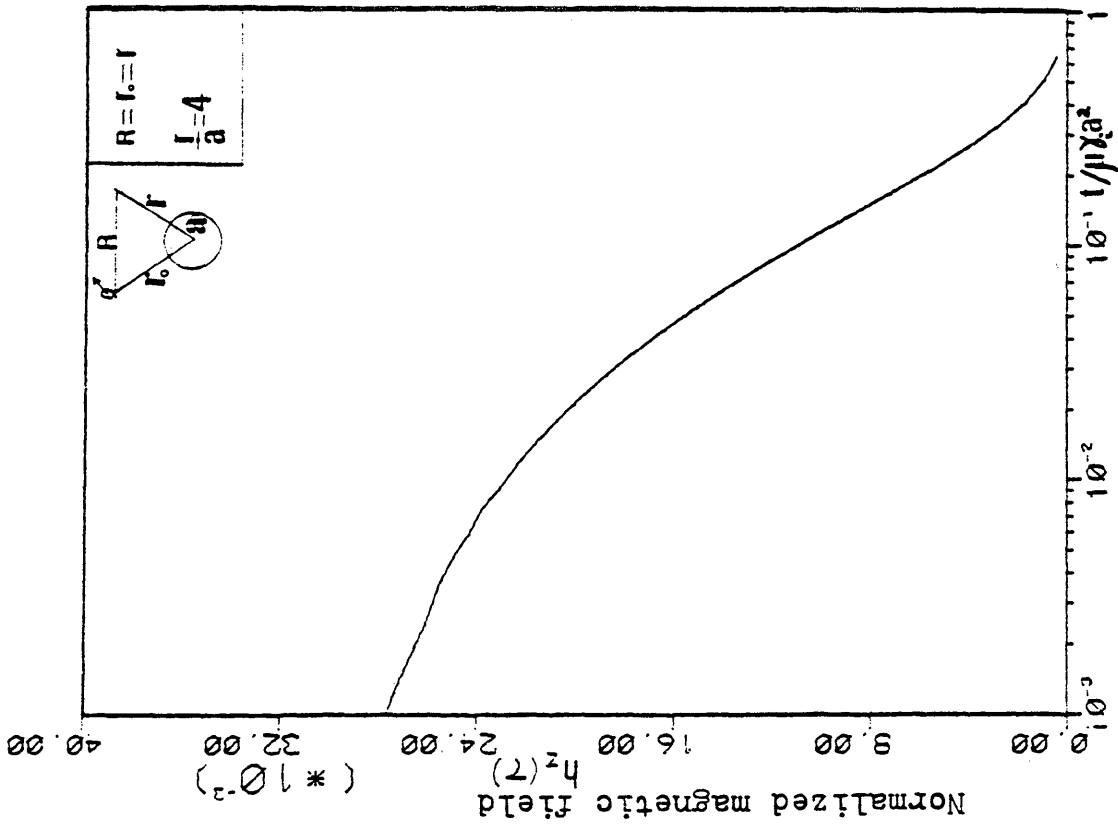


Figure 2-9. Transient response of the magnetic field (source is an axial magnetic dipole)

Thus it should be pointed out that the frequency response of the magnetic field due to a magnetic dipole is very similar to that of a uniform primary field if the distance from the cylinder is a few times greater than radius of cylinder ($r/a \geq 4$, $r_0/a \geq 4$). Transient responses of the magnetic field due to an axial magnetic dipole and a transverse magnetic dipole are shown in Fig. (2-9) and (2-10), respectively. From the above figures, it is found that the field decays as $e^{-6.2 \frac{t}{\mu\gamma a^2}}$ for the range of $t/\mu\gamma a^2 \geq 1.2$.

The Horizontal Profiling

To figure out the shape of curves corresponding to horizontal profiling, the magnetic fields are calculated at several different locations on the horizontal plane with fixed separation of transmitter and receiver. The profiling is investigated at two different frequencies. Figures (2-11, 12, 13, 14) show these results in case of an axial magnetic dipole. As can be seen from the above figures, the inphase component has minimum value and the quadrature component shows maximum value over the conductor.

The corresponding horizontal profiling for the case of a transverse magnetic dipole are presented in figures (2-15, 16, 17, 18). In this case, the characteristics of the curves are similar to the previous case. However, in this case

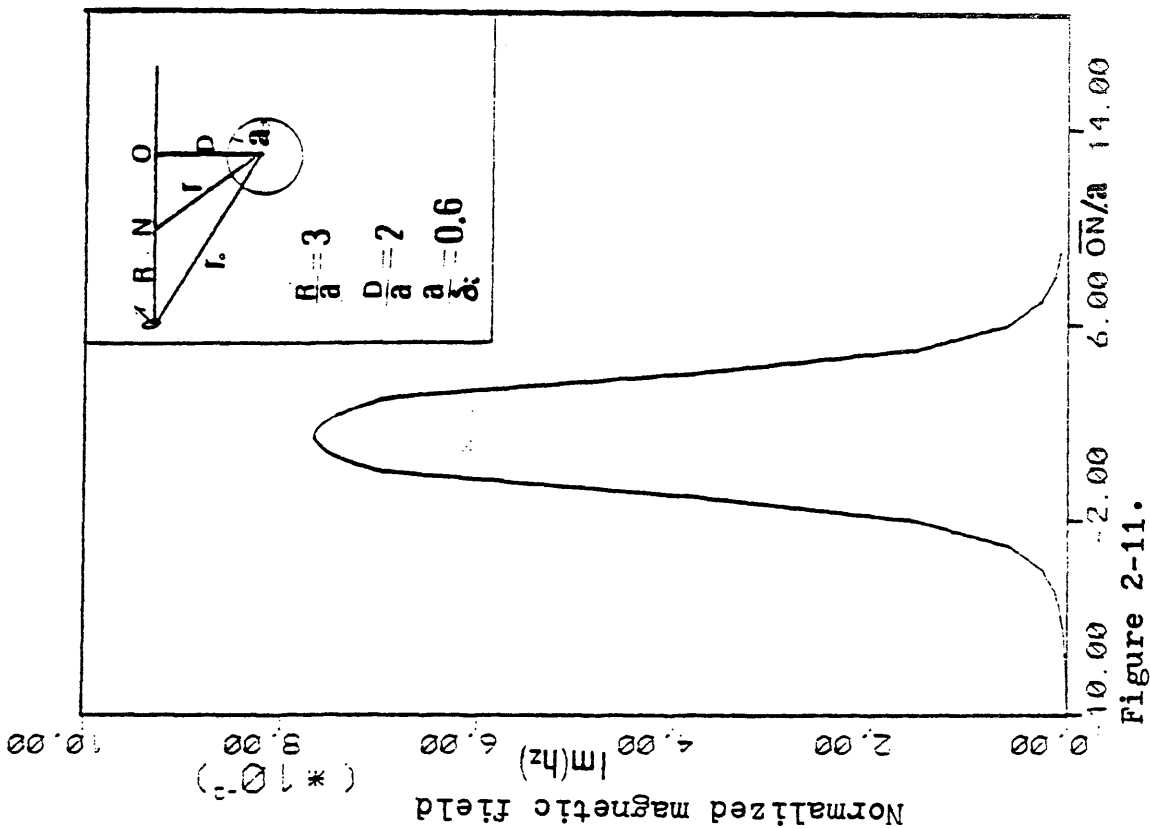


Figure 2-11.

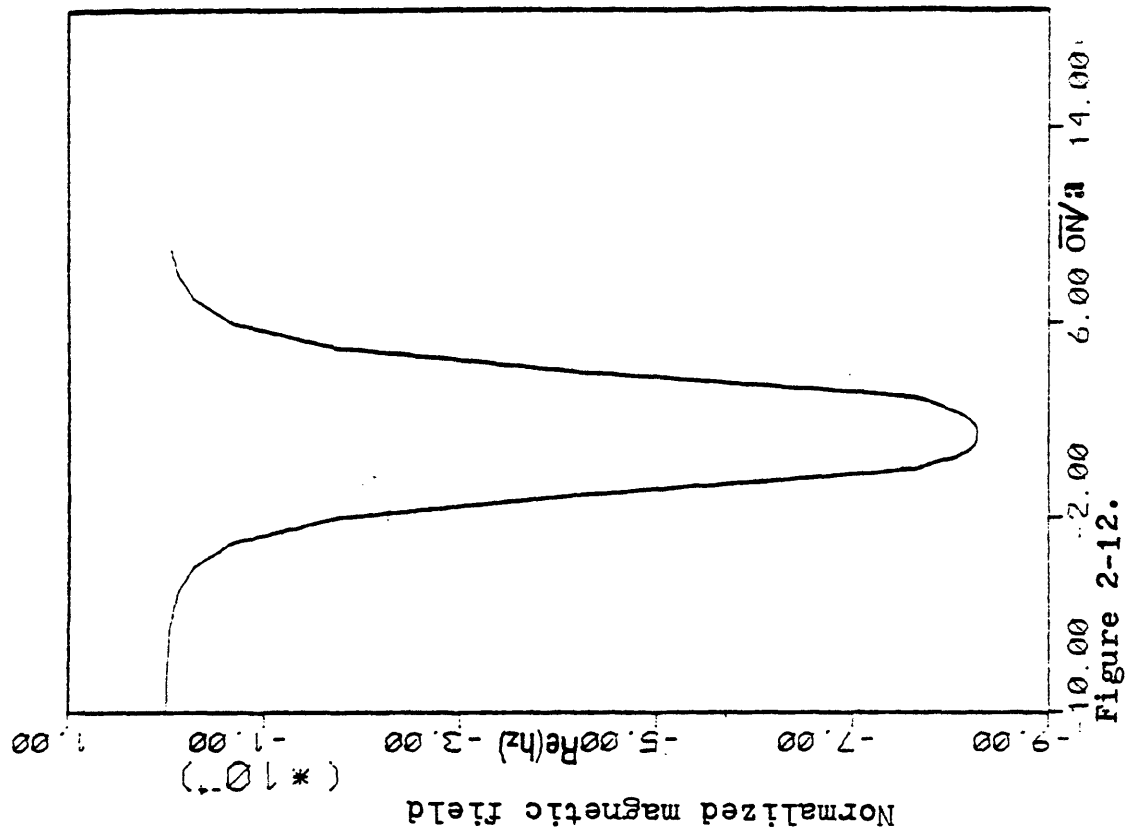


Figure 2-12.

Horizontal profiling with fixed frequency, $a/\delta = 0.6$, and separation (transmitter is an axial magnetic dipole)

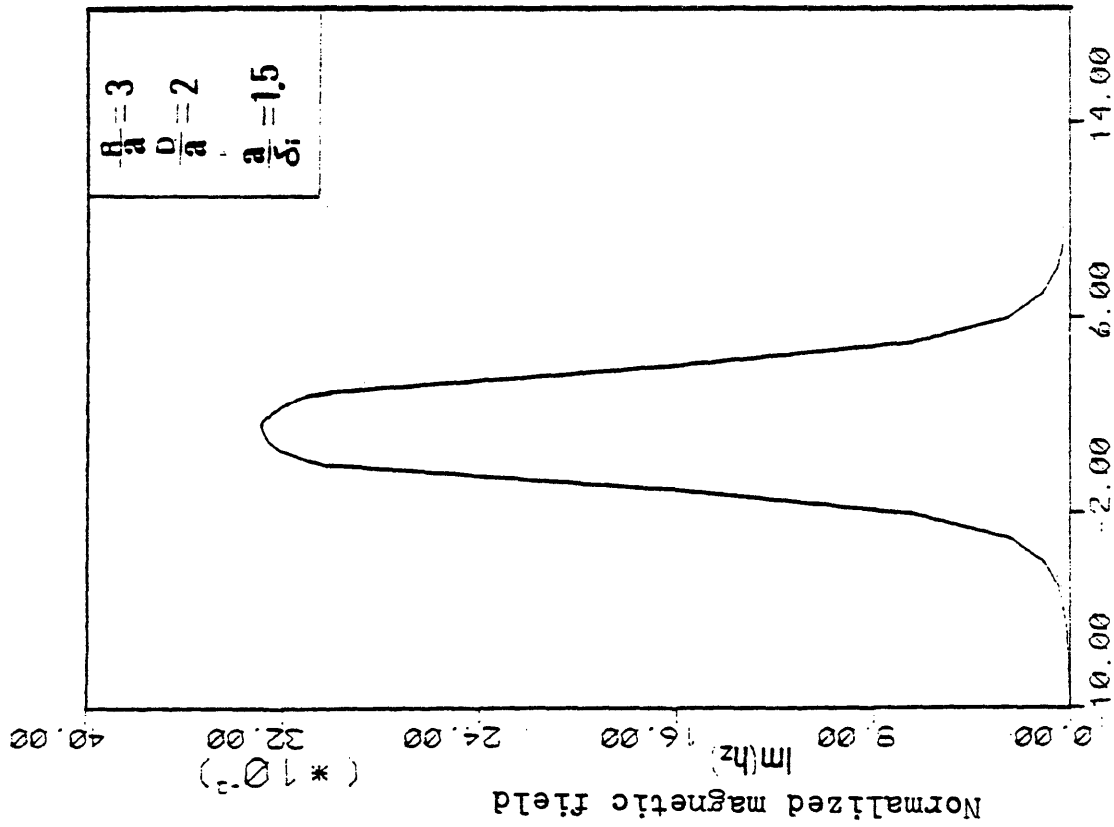


Figure 2-13.

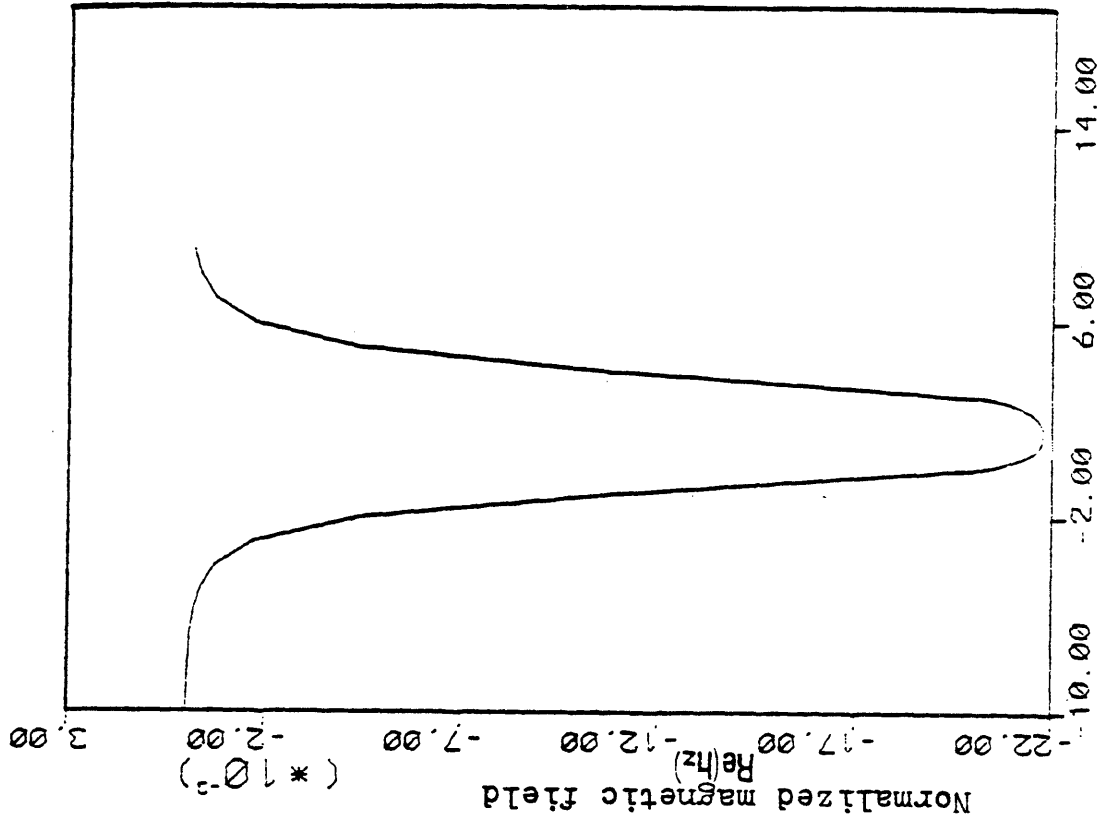


Figure 2-14.

Horizontal profiling with fixed frequency, $a/\delta_i = 1.5$, and separation (transmitter is an axial magnetic dipole)

the curves form a narrow peak above the conductor.

Figures (2-19) and (2-20) show the same profiling results for a transverse magnetic dipole source with the assumption that the primary field in the vicinity of the cylinder is uniform. In this case the magnitude of primary field is assumed to be the same value of the primary field at the center of cylinder due to this magnetic dipole. These figures show the vertical component of the magnetic field. As can be seen from the figures, if the ratio of separation to the depth is small ($L/D \leq 0.25$), the curves are symmetrical to the axis of the cylinder. If this ratio increases, the shapes of the curves are distorted from symmetry. Fig. (2-21) and (2-22) show the profiling results for measurements of horizontal component of the magnetic field.

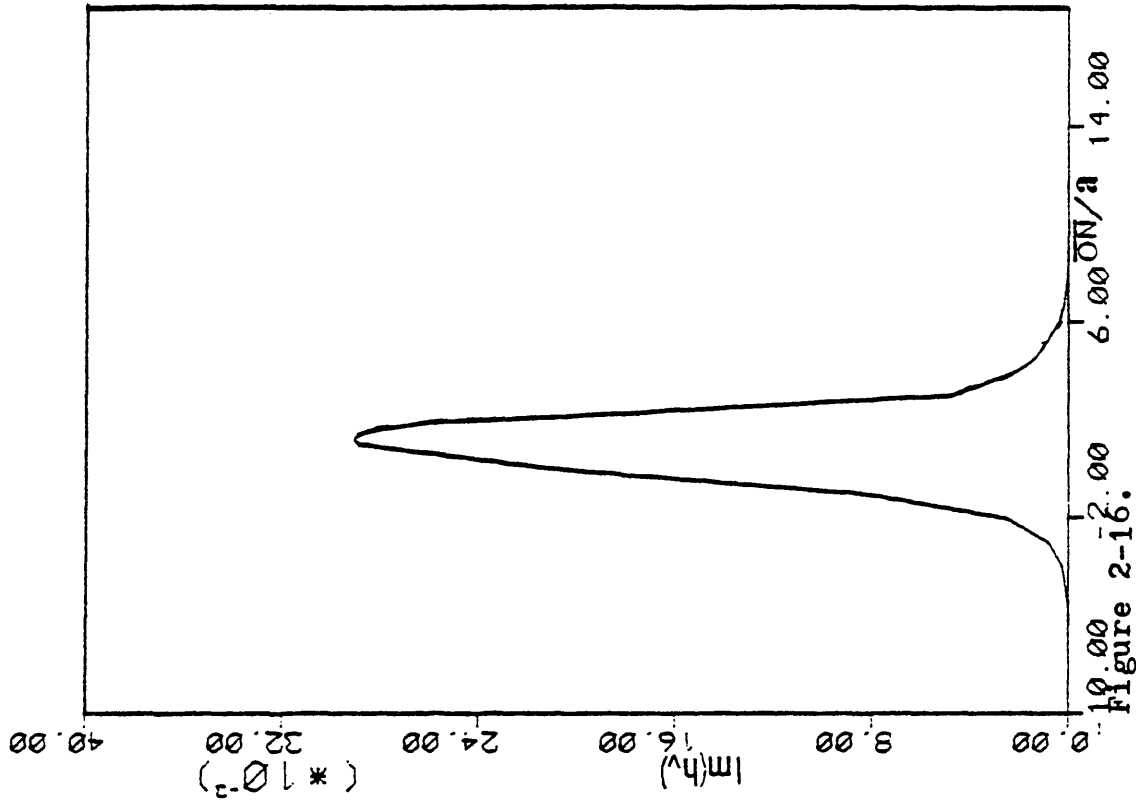


Figure 2-16.

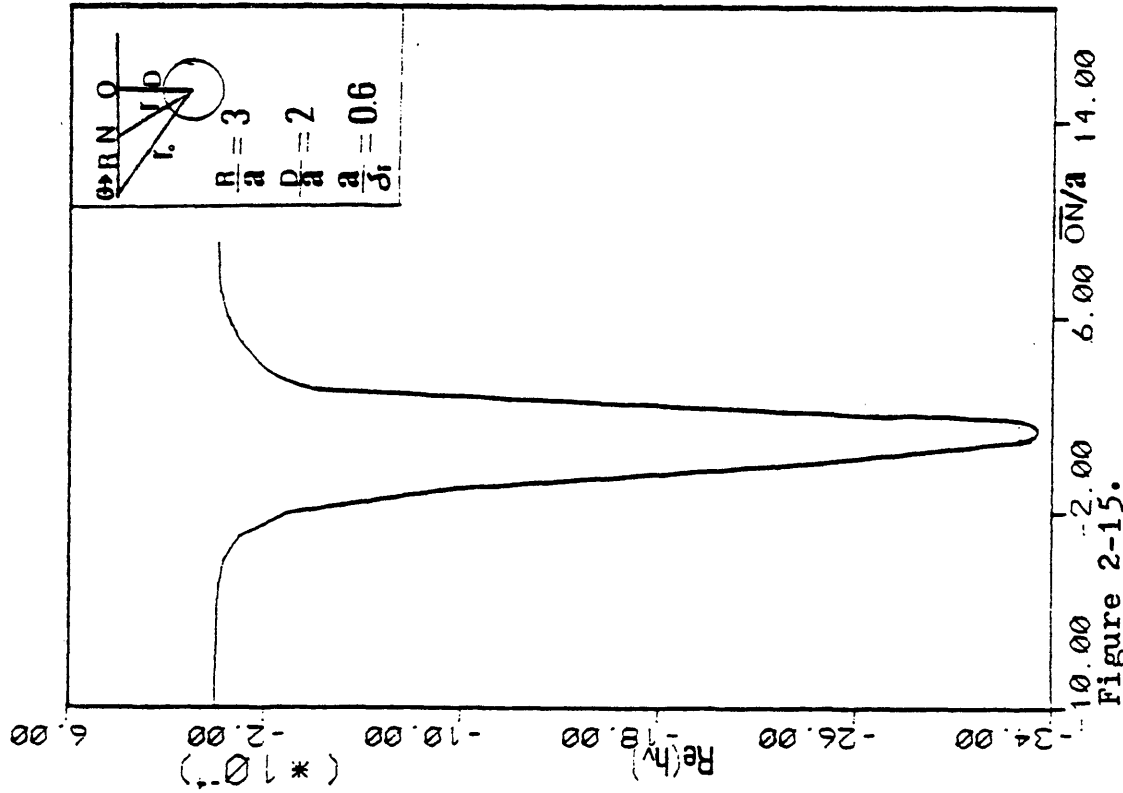


Figure 2-15.

Horizontal profiling with fixed frequency, $a/\delta_1 = 0.6$, and separation (Transmitter is a transverse magnetic dipole)

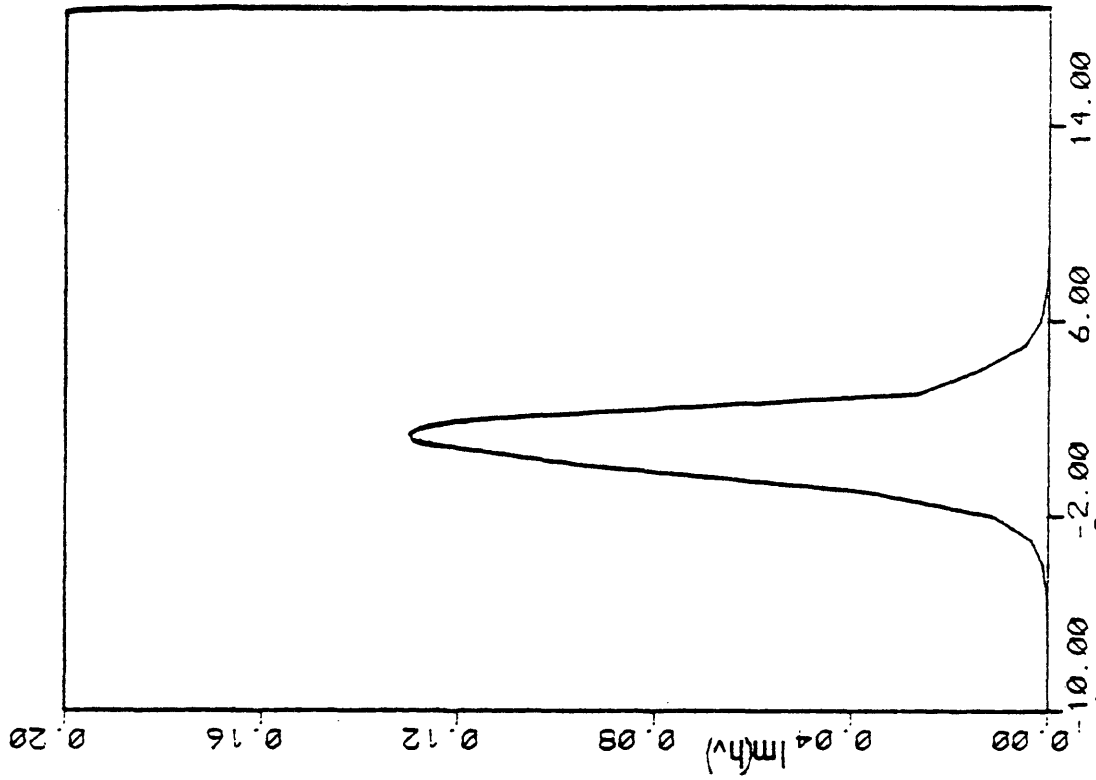


Figure 2-17.

Horizontal profiling with fixed frequency, $a/\delta = 1.8$, and separation (Transmitter is a transverse magnetic dipole)

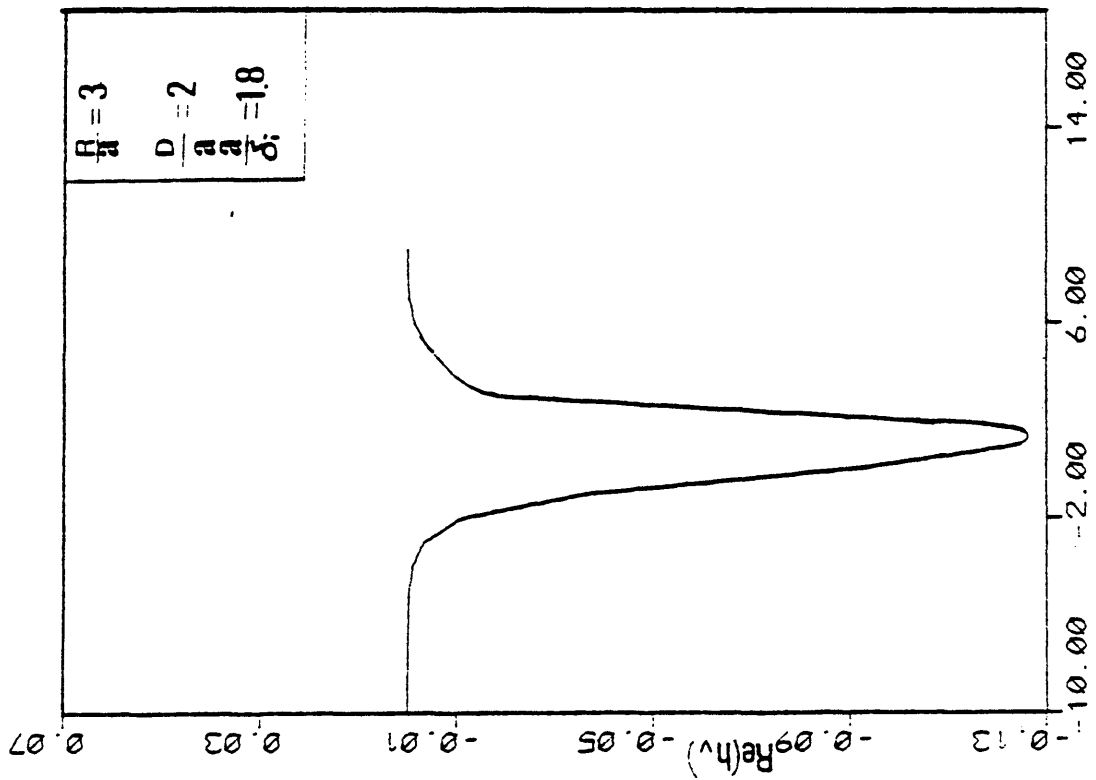


Figure 2-18.

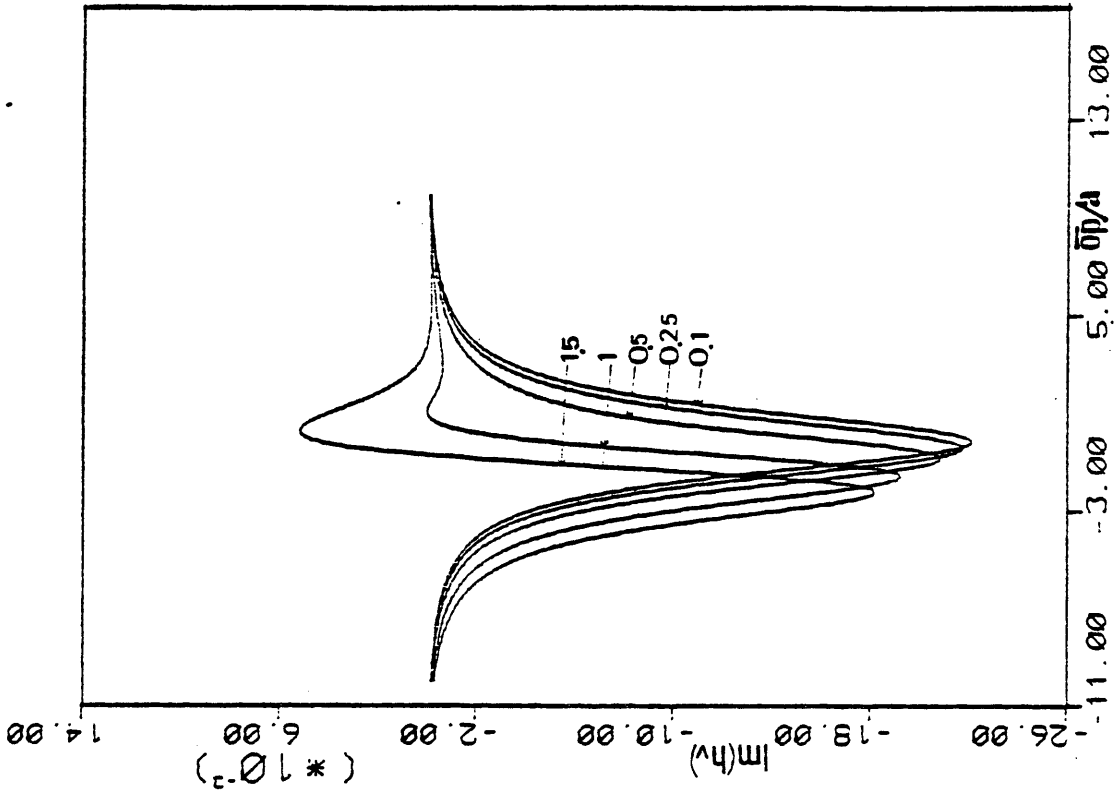


Figure 2-19.

Horizontal profiling with fixed frequency, $a/\delta_f = 0.6$, and separation (transmitter is a transverse magnetic dipole. The vertical component of the magnetic field was calculated, assuming primary field is uniform in the vicinity of the cylinder.)

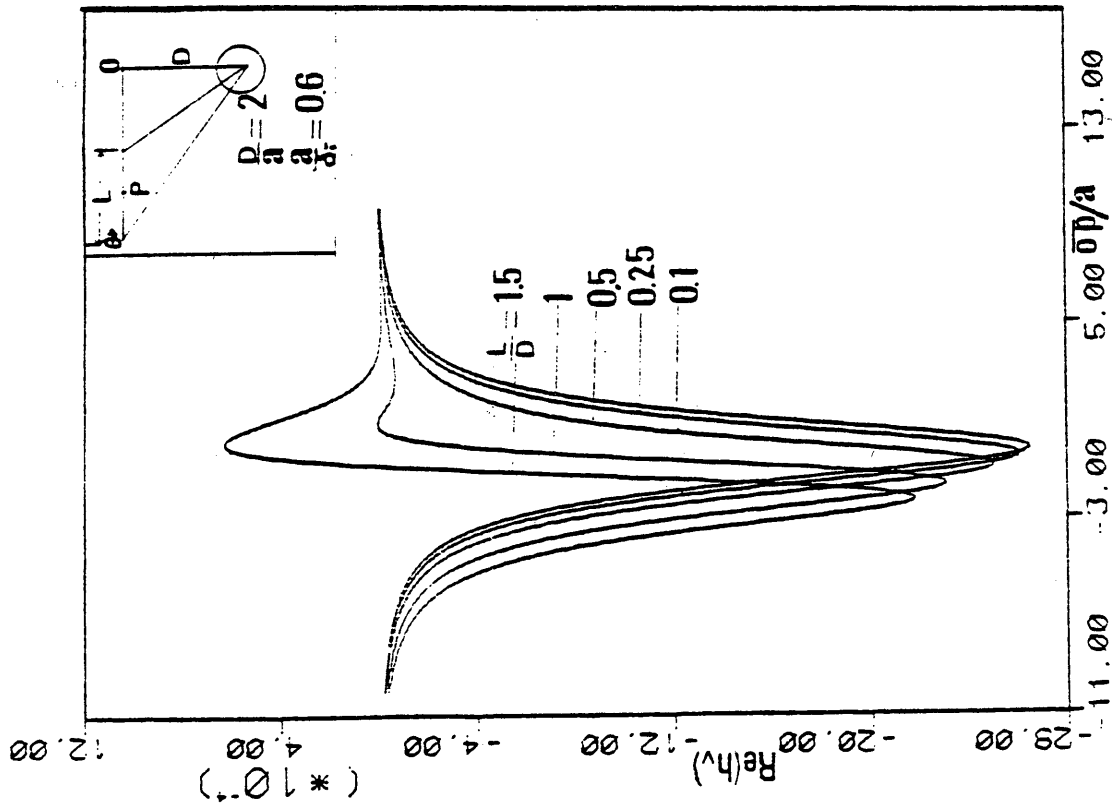


Figure 2-20.

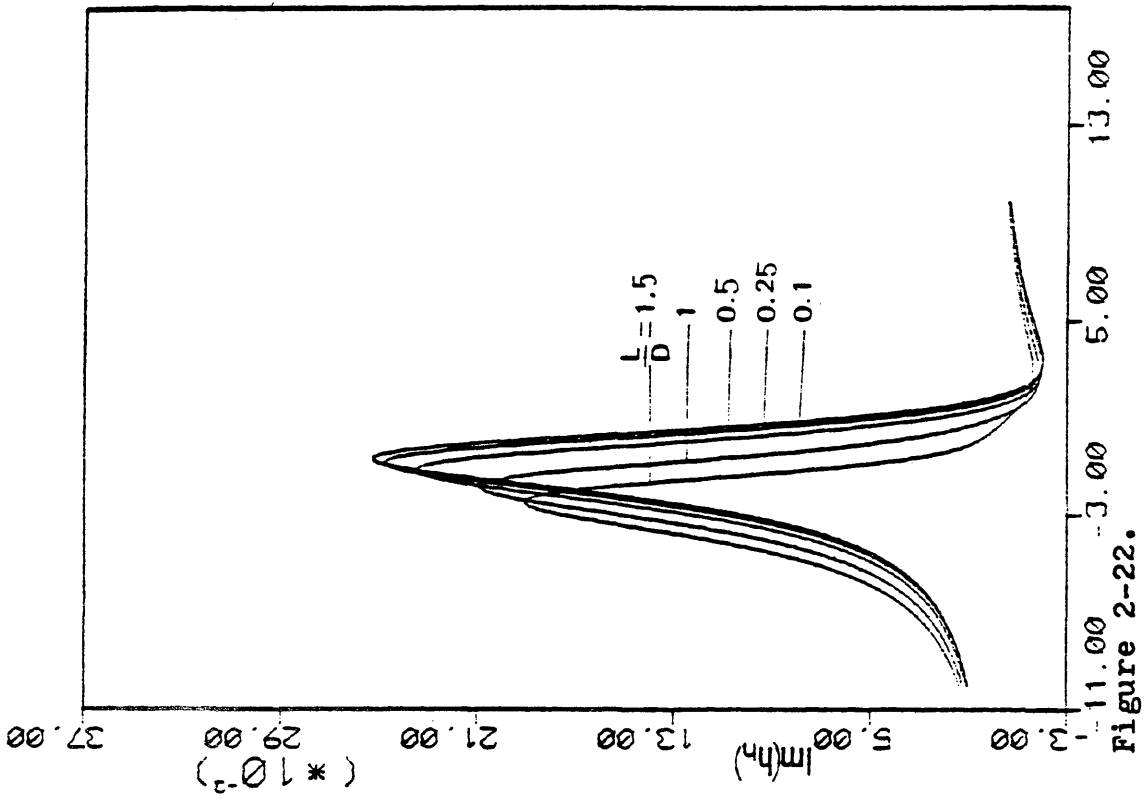


Figure 2-21.

Horizontal profiling with fixed frequency, $a/\delta_i = 0.6$, and separation (Transmitter is a tranverse magnetic dipole. The horizontal component of the magnetic field was calculated, assuming the primary field is uniform in the vicinity of the cylinder)

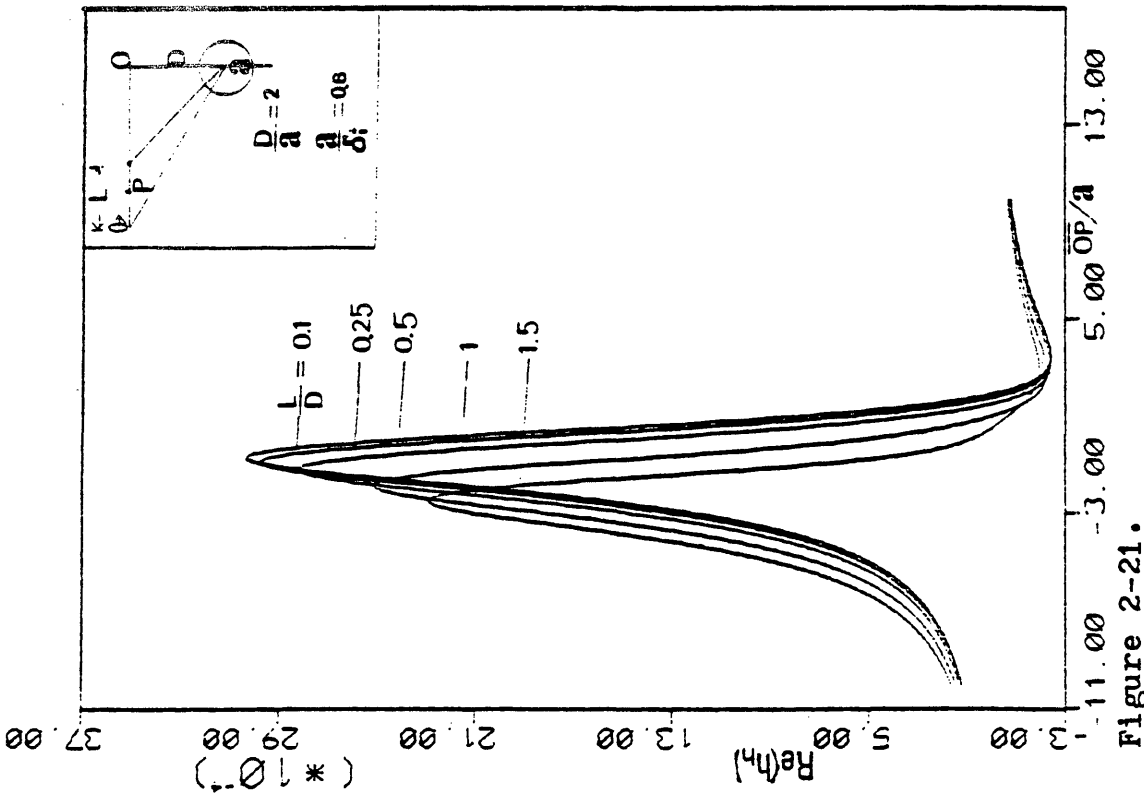


Figure 2-22.

CHAPTER III

INFLUENCE OF SURROUNDING MEDIUM ON THE FREQUENCY AND THE
TRANSIENT RESPONSES IN THE PRESENCE OF A CONDUCTING CYLINDER

(The Axial Magnetic Dipole)

Derivation of field equations

Unlike the previous chapter, in this case, due to the presence of the conducting surrounding medium, in other words, the currents in the surrounding medium, the magnetic field outside the cylinder can't be expressed as a gradient of a scalar potential. Now two kinds of vector potentials are used for deriving fields inside and outside the cylinder. To find the proper form of the vector potentials for this problem, primary component of the vector potential is considered. The normal field of the magnetic dipole can be expressed by only one vector potential

$$\pi_o^* = \frac{M e^{iKR}}{4 \pi R} \quad (3-1)$$

To facilitate applying boundary condition, the above equation is presented as an integral

$$\pi_o^* = \frac{M}{2 \pi^2} \int_0^{\infty} k_o (\lambda e^{\hat{r}}) \cos \lambda (z - z_o) d\lambda$$

$$\text{with } \lambda_e = \sqrt{\lambda^2 - k_e^2}$$

k_e ; wave number of surrounding medium

Using the addition theorem,

$$\pi_o^* = \frac{M}{2\pi^2} \sum_{\eta=0}^{\infty} \int_0^{\infty} \sigma_{\eta} k_{\eta} (\lambda_e r_o) I_{\eta}(\lambda_e r) \cos \lambda (z - z_o) \cdot \cos \eta (\phi - \phi_o) \quad (3-2)$$

for $r_o > r$

or

$$\pi_o^* = \frac{M}{4\pi^2} \sum_{\eta=-\infty}^{\infty} \int_{-\infty}^{\infty} k_{\eta} (\lambda_e r_o) I_{\eta}(\lambda_e r) e^{-i\lambda(z-z_o)} d\lambda e^{-i\eta(\phi-\phi_o)} \quad (3-3)$$

For the convenience in algebraic operations the operator Γ is used

$$\pi_o^* = \Gamma I_{\eta}(\lambda_e r) \quad (3-4)$$

Considering the Π^* and Π are the solution of the wave equation and the field should decrease as the distance increases from the cylinder the secondary potential outside the conductor has the form

$$\pi_s^* = \Gamma A_n K_n(\lambda_e r) \quad (3-5)$$

Thus the potential outside the conductor are ,

$$\pi_e^* = \Gamma \{ I_n(\lambda_e r) + A_n K_n(\lambda_e r) \} \quad (3-6)$$

$$\pi_e = \Gamma C_n K_n(\lambda_e r) \quad (3-7)$$

and inside the conductor

$$\pi_i^* = \Gamma B_n I_n(\lambda_i r) \quad (3-8)$$

$$\pi_i = \Gamma D_n I_n(\lambda_i r) \quad (3-9)$$

Boundary Conditions

The problem is to determine the unknown coefficients, A_n and C_n . The first case is that of a magnetic dipole oriented parallel to the axis of the conducting cylinder.

Boundary conditions for this system are the continuity of the tangential components of the electric and the magnetic field on the surface of the cylinder.

Substituting equations (3-6, 7, 8, 9) into equations (2-12, 13) and applying boundary conditions $E_\phi^i = E_\phi^e$ at

$r = a$

it becomes

$$\begin{aligned} & \frac{1}{k_i} \left\{ \frac{-\lambda \eta}{a} I_n(\lambda_i a) D_n - k_i^2 \lambda_i I_n'(\lambda_i a) B_n \right\} \\ &= \frac{1}{\gamma_e} \left\{ \frac{-\lambda \eta}{a} k_n(\lambda_e a) C_n - k_e^2 \lambda_e [I_n'(\lambda_e a) + A_n k_n'(\lambda_e a)] \right\} \end{aligned}$$

Through transformation of variable as

$$\lambda a = m, \quad \lambda_i a = m_1, \quad \lambda_e a = m_2$$

$$\text{and } S = \frac{\gamma_i}{\gamma_e}$$

the above equation becomes

$$\begin{aligned} & -k_i^2 m_2 k_n'(m_2) A_n + k_i^2 m_1 I_n'(m_1) B_n - S \lambda \eta k_n(m_2) C_n \\ & + \lambda \eta I_n(m_1) D_n = k_i^2 m_2 I_n'(m_2) \end{aligned} \quad (3-10)$$

From the condition

$$\begin{aligned} E_z^i &= E_z^e \quad \text{at } r = a \\ D_n &= S \left(\frac{m_2}{m_1} \right)^2 \frac{k_n(m_2)}{I_n(m_1)} C_n \end{aligned} \quad (3-11)$$

From the condition

$$\begin{aligned} H_\phi^i &= H_\phi^e \quad \text{at } r = a \\ \lambda \eta k_n(m_2) A_n - \lambda \eta I_n(m_1) B_n + m_2 k_n'(m_2) C_n \\ - m_1 I_n'(m_1) D_n &= -\lambda \eta I_n(m_2) \end{aligned} \quad (3-12)$$

Finally $H_z^i = H_z^e$ at $r = a$

$$\text{or } B_n = \left(\frac{m_2}{m_1}\right)^2 \frac{I_n(m_2) + K_n(m_2) A_n}{I_n(m_1)} \quad (3-13)$$

From the above four equations A_n and C_n are determined as

$$A_n = \frac{k_i^2 a^2 q_3 + S m^2 n^2 q_2}{k_i^2 a^2 q_1 - S m^2 n^2 q_2} \frac{I_n(m_2)}{K_n(m_2)} \quad (3-14)$$

$$C_n = \frac{k_i^2 a n m (q_5 - q_4)}{k_i^2 a^2 q_1 - S m^2 n^2 q_2} \frac{I_n(m_2)}{K_n(m_2)} \quad (3-15)$$

where

$$q_1 = \left\{ -\frac{m_2 K_n'(m_2)}{K_n(m_2)} + \left(\frac{m_2}{m_1}\right)^2 \frac{m_1 I_n'(m_1)}{I_n(m_1)} \right\} \left\{ -\frac{m_2 K_n'(m_2)}{K_n(m_2)} + S \left(\frac{m_2}{m_1}\right)^2 \frac{m_1 I_n'(m_1)}{I_n(m_1)} \right\} \quad (3-16)$$

$$q_2 = 1 - \left(\frac{m_2}{m_1}\right)^2 \quad (3-17)$$

$$q_3 = \left\{ \frac{m_2 I_n'(m_2)}{I_n(m_2)} - \left(\frac{m_2}{m_1}\right)^2 \frac{m_1 I_n'(m_1)}{I_n(m_1)} \right\} \left\{ -\frac{m_2 K_n'(m_2)}{K_n(m_2)} + S \left(\frac{m_2}{m_1}\right)^2 \frac{m_1 I_n'(m_1)}{I_n(m_1)} \right\} \quad (3-19)$$

$$q_4 = \left(1 - \frac{m_2^2}{m_1^2}\right) \left\{ -\frac{m_2 K_n'(m_2)}{K_n(m_2)} + \left(\frac{m_2}{m_1}\right)^2 \frac{m_1 I_n'(m_1)}{I_n(m_1)} \right\}$$

$$q_5 = \left(1 - \frac{m_2^2}{m_1^2}\right) \left\{ \frac{m_2 I_n'(m_2)}{I_n(m_2)} - \left(\frac{m_2}{m_1}\right)^2 \frac{m_1 I_n'(m_1)}{I_n(m_1)} \right\} \quad (3-20)$$

Normal field

The normal field, which is due to the currents in the source and in the uniform medium, is derivable from the primary component of the magnetic type vector potential Π_0^* .

$$\vec{E}_N = i\omega\mu C\mu\Gamma \Pi_0^*$$

$$\vec{H}_N = (k^2 + \text{Grad. Div.}) \Pi_0^*$$

Using equation (3-1), the z-component of the magnetic field

$$\text{is } H_N^z = i\omega\mu\gamma \frac{M e^{ikR}}{4\pi R} + \frac{M}{4\pi} \frac{\partial^2}{\partial z^2} \left(\frac{e^{ikR}}{R} \right)$$

$$\text{or } H_N^z = \frac{M}{4\pi R^3} e^{ikR} (k^2 R^2 + ikR - 1) \quad (3-21)$$

By analogy the r-component of the magnetic field is

$$H_N^r = \frac{M}{4\pi} \frac{z\Gamma}{R^5} e^{ikR} (3 - 3ikR - k^2 R^2) \quad (3-22)$$

The above expressions are expressed in cylindrical coordinate and R is the distance of source to observation point.

Secondary magnetic field

Substituting equations (3-5) and (3-6) into equation (2-13), the secondary magnetic fields are derived as

$$H_r^S = -\frac{M}{2\pi^2} \left\{ \sum_{n=0}^{\infty} \sigma_n \int_0^{\infty} \lambda e^{-\lambda z} A_n k_n'(\lambda e^{\Gamma}) k_n(\lambda e^{\Gamma_0}) \sin \lambda (z - z_0) d\lambda \right. \\ \cdot \cos n(\phi - \phi_0) + \frac{z}{r} \sum_{n=1}^{\infty} \int_0^{\infty} n C_n k_n(\lambda e^{\Gamma}) k_n(\lambda e^{\Gamma_0}) \\ \left. \cdot \cos \lambda (z - z_0) d\lambda \cdot \sin n(\phi - \phi_0) \right\}$$

Writing
$$H_r^s = \frac{M}{4\pi R^3} \cdot h_r$$

and
$$C_n = \frac{k^2 a^2}{a} \tilde{C}_n,$$

the above equation becomes

$$h_r = -\frac{2U^3}{\pi} \sum_{n=0}^{\infty} \sigma_n \int_0^{\infty} m m_2 A_n k_n'(\beta m_2) k_n(\alpha m_2) \sin \hat{z} m \, dm$$

$$\cdot \cos n(\phi - \phi_0) - \frac{4U^3}{\pi \beta} \sum_{n=1}^{\infty} \int_0^{\infty} n(m^2 - m_i^2) \tilde{C}_n k_n(\beta m_2)$$

$$\cdot k_n(\alpha m_2) \cdot \cos \hat{z} m \, dm \cdot \sin n(\phi - \phi_0) \quad (3-23)$$

where

$$\tilde{C}_n = \frac{n m (g_5 - g_4)}{(m^2 - m_i^2) g_1 - S n^2 m^2 g_2^2} \cdot \frac{I_n(m_2)}{k_n(m_2)} \quad (3-24)$$

$$R = u a, \quad r_0 = \alpha a, \quad r = \beta a, \quad z - z_0 = \hat{z} a$$

$$m_2 = \lambda_e a, \quad m = \lambda a$$

Measuring the field on the plane $z = z_0$, the first term of equation (3-23) disappears.

Similarly,

$$h_\phi = \frac{4U^3}{\pi} \sum_{n=1}^{\infty} \int_0^{\infty} \left\{ \frac{n m}{\beta} A_n k_n(\beta m_2) k_n(\alpha m_2) \sin \hat{z} m \, dm \right.$$

$$\cdot \sin n(\phi - \phi_0) - m_2 (m^2 - m_i^2) \tilde{C}_n k_n'(\beta m_2)$$

$$\left. \cdot k_n(\alpha m_2) \cos \hat{z} m \, dm \cdot \cos n(\phi - \phi_0) \right\} \quad (3-25)$$

$$h_z = -\frac{2U^3}{\pi} \sum_{n=0}^{\infty} \sigma_n \int_0^{\infty} m_2^2 A_n k_n(\lambda_e r_0) k_n(\lambda_e r) \cos \hat{z} m \, dm$$

$$\cdot \cos n(\phi - \phi_0) \quad (3-26)$$

Secondary electric field

Substituting equations (3-5) and (3-6) into equation (2-12) and writing

$$\vec{E}^s = \frac{i\omega\mu M}{2\pi R^2} \vec{e}$$

$$e_\phi = -\frac{U^2}{\pi} \sum_{n=0}^{\infty} \sigma_n \int_0^{\infty} \left\{ A_n m_2 k_n'(\beta m_2) k_n(\alpha m_2) \cos \hat{z}m \cos n(\phi - \phi_0) \right. \\ \left. - \frac{S}{\beta} n m \tilde{C}_n k_n(\beta m_2) k_n(\alpha m_2) \sin \hat{z}m \sin n(\phi - \phi_0) \right\} dm \quad (3-27)$$

$$e_r = -\frac{U^2}{\pi} \sum_{n=0}^{\infty} \sigma_n \int_0^{\infty} \left\{ \frac{m}{\beta} A_n k_n(\beta m_2) k_n(\alpha m_2) \cos \hat{z}m \sin n(\phi - \phi_0) \right. \\ \left. + S n m_2 \tilde{C}_n k_n'(\beta m_2) k_n(\alpha m_2) \sin \hat{z}m \cos n(\phi - \phi_0) \right\} dm \quad (3-28)$$

$$e_z = -\frac{2U^2}{\pi} S \sum_{n=1}^{\infty} \int_0^{\infty} m_2^2 \tilde{C}_n k_n'(\beta m_2) k_n(\alpha m_2) \cos \hat{z}m dm \cos n(\phi - \phi_0) \quad (3-29)$$

EXAMINATION OF THE RESULTS

The field expressions are very complicated, but these formulae can be examined for some limiting cases. Here the field expressions are compared with those for free space by decreasing the ratio of the conductivity of the surrounding medium to that of the cylinder.

cylinder.

Magnetic field

For the case of very large value of S , the variable

m_2 approaches m and the function A_n in equation (3-14) becomes the same as the one in equation (2-38). From the following fact:

$$\lim_{S \rightarrow \infty} q_1 \cong m^4 \{ -\tilde{K}_n(m) + \tilde{I}_n(m_1) \} S \tilde{I}_n(m)$$

$$\lim_{S \rightarrow \infty} q_3 \cong m^4 \{ \tilde{I}_n(m) - \tilde{I}_n(m_1) \} S \tilde{I}_n(m)$$

it follows

$$\lim_{S \rightarrow \infty} A_n = - \frac{\tilde{I}_n(m) - \tilde{I}_n(m_1) + \frac{\eta^2 k_i^2 a^2}{m_i^4 m^2} \frac{1}{\tilde{I}_n(m_1)}}{\tilde{K}_n(m) - \tilde{I}_n(m_1) + \frac{\eta^2 k_i^2 a^2}{m_i^4 m^2} \frac{1}{\tilde{I}_n(m_1)}} \cdot \frac{I_n(m)}{K_n(m)} \quad (2-30)$$

where $\tilde{I}_n(m)$ and $\tilde{K}_n(m)$ are defined in equation (2-27).

Thus for the case of very large value of S the magnetic field in equation (3-26) approaches the expression in free space. Unlike free space, in the conducting medium there are ϕ and r components of the secondary magnetic field on the plane $z = z_0$. These components, as can be seen in equations (3-24) and (3-25), come from the electric type vector potential. This part of field is caused by the induced electric charges on the surface of cylinder. (see the next paragraph) These charges are induced by the intersection of the primary electric field and the conductor surface.

These charges create galvanic part of the electric field. If the conductivity of the surrounding medium is zero, the current due to charges can't flow out of the surrounding medium and have a closed path inside the cylinder, in other words, it forms a solenoid. As is known these currents can't create a magnetic field outside. Through numerical evaluation it is found that the ϕ - and r -component of the magnetic field decrease as the ratio of the conductivities increases (see Figure (3-6), (3-7)). Now function C_n in equation (3-15) is examined through investigating the electric field.

Electric Field

The electric field due to an axial magnetic dipole is compared with the secondary electric field of uniform transverse primary electro static field. If the source is located far from the conductor the primary field in the vicinity of the conductor can be considered approximately uniform field. With above mentioned assumption, for the case of very low frequencies the field can be considered as electrostatic field, in other words, the vortex part of electric field is negligible. The secondary electric field of a conducting cylinder due to uniform transverse electrostatic field is

$$E_{\phi}^s = \frac{a^2}{r^2} \cdot E_0 \cdot \left(\frac{\gamma_i - \gamma_e}{\gamma_i + \gamma_e} \right) \cdot \sin \theta \quad (3-31)$$

The secondary electric field is calculated by using equation (3-27) for certain geometry with different ratio of conductivities. Table (3-1) shows the calculation results of inphase component of electric field for the case of $\alpha = 40$, $\beta = 2$, $u = 39.04$ and $z = 0.5$. From table (3-1) it can be recognized that the field, at the very low frequencies, is proportional to $(\gamma_i - \gamma_e) / (\gamma_e + \gamma_i)$. As is shown in this table the inphase component, at the low frequencies, approaches some constant. The quadrature component of the field is much less than inphase component. The above mentioned behavior is investigated by considering the electric field in free space.

For this case the function C_n in (3-15) becomes

$$\lim_{s \rightarrow \infty} C_n = i\omega\mu\gamma_e \frac{1}{a} \hat{C}_n$$

with
$$\hat{C}_n = \frac{\frac{\eta m}{m_i^2} \{ 2 \tilde{I}_n(m_i) - \tilde{K}_n(m) - \tilde{I}_n(m) \}}{m^2 \{ -\tilde{K}_n(m) + \tilde{I}_n(m) \} \tilde{I}_n(m_i) - \frac{\eta^2}{m_i^2} (m^2 - m_i^2)} \cdot \frac{I_n(m)}{K_n(m)} \quad (3-32)$$

and the electric field in equation (3-27) turned out to be

$$E_{\phi} = -\frac{u^2}{\pi} \sum_{n=0}^{\infty} \hat{C}_n \int_0^{\infty} \{ A_n m K_n'(\beta m) K_n(\alpha m) \cos \frac{z}{2} m \cos n(\phi - \phi_0) - \frac{1}{\beta} \hat{C}_n \eta m K_n(\beta m) K_n(\alpha m) \sin \frac{z}{2} m \sin n(\phi - \phi_0) \} dm \quad (3-33)$$

Table 3-1. The inphase component of the normalized electric field with $\alpha=40$, $\beta=2$, $u=39,04$ and $\hat{z}=0.5$

$R/\delta_i \backslash S$	10	5	3
0.01	0.186×10^{-2}	0.158×10^{-2}	0.114×10^{-2}
0.02	0.187×10^{-2}	0.152×10^{-2}	0.115×10^{-2}
0.04	0.189×10^{-2}	0.163×10^{-2}	0.135×10^{-2}
0.08	0.234×10^{-2}	0.249×10^{-2}	0.225×10^{-2}

Table 3-2 The normalized electric field when a source is located very far from the cylinder. ($\alpha=40$, $\beta=2$, $\hat{z}=0.2$ and $\phi - \phi_s = \pi/3$)

R/δ_i	Inphase component	Quadrature component
0.01	0.165799×10^{-2}	0.233732×10^{-6}
0.02	0.165799×10^{-2}	0.935147×10^{-6}
0.04	0.165797×10^{-2}	0.374054×10^{-5}
0.08	0.165763×10^{-2}	0.149522×10^{-4}

In the above equation, at very low frequencies it can be seen the following facts:

1. Real part of A_n is proportional to $(\gamma\omega\mu a^2)^2$.
2. Imaginary part of A_n is proportional to $\gamma\omega\mu a^2$.
3. Function \hat{C}_n becomes only function of m and it approaches real value.
4. Inphase component of electric field is mainly defined by function \hat{C}_n , in other words, this component comes from electric type vector potential.
5. Quadrature component of electric field is mainly defined by magnetic type vector potential, in other words, it is proportional to $\gamma\omega\mu a^2$.
6. Inphase component prevail at low frequency

Table (3-2) shows some calculation results of equation (3-33) for the case of $r_o = 40a$, $r = 2a$, $\phi - \phi_o = \pi/3$, $\hat{Z} = 0.2$.

Through all the above discussions it can be understood that the field derived from the magnetic type vector potential is mainly induction part of the field and the one from the electric type vector potential can be considered as the galvanic part of the field.

Analysis of the magnetic field in frequency domain

Using equations (3-23), (3-25) and (3-26) secondary magnetic fields are numerically calculated.

Z component of magnetic field

Through numerical evaluation it is found that the field, at the low frequencies, has similar behavior to the field in free space. The inphase component is proportional to $(\gamma\mu\omega a^2)^2$ and the quadrature component is proportional to $\gamma\mu\omega a^2$. Figure (3-1) and (3-2) show the frequency responses for several different ratio of the conductivities. From these figures it can be recognized the following fact. At given conductivity of the surrounding medium, increasing the conductivity of the cylinder the magnitude of the secondary field is increased for the range of frequency $a/\delta_e < 1$. Regardless of the different ratio of conductivities, inphase component of the field has minimum value at $a/\delta_e \cong 0.7$ and by increasing the frequency above this range the field start to oscillate with decreasing magnitude. At the low frequencies the maximum value of the quadrature component is shifted to higher frequencies as the conductivity of the cylinder increases. To find the optimum range of frequency which allow one to get maximum ratio of useful signal to geological noise, the ratio of the secondary field to the

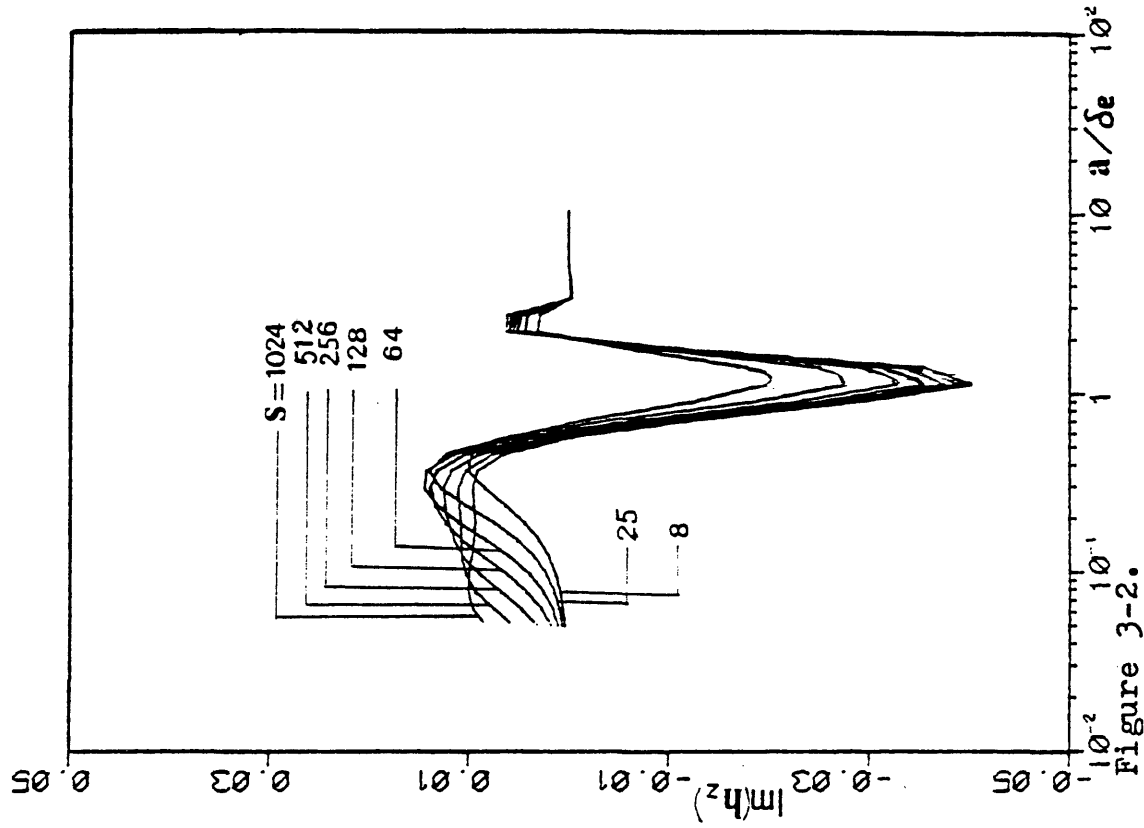


Figure 3-2.

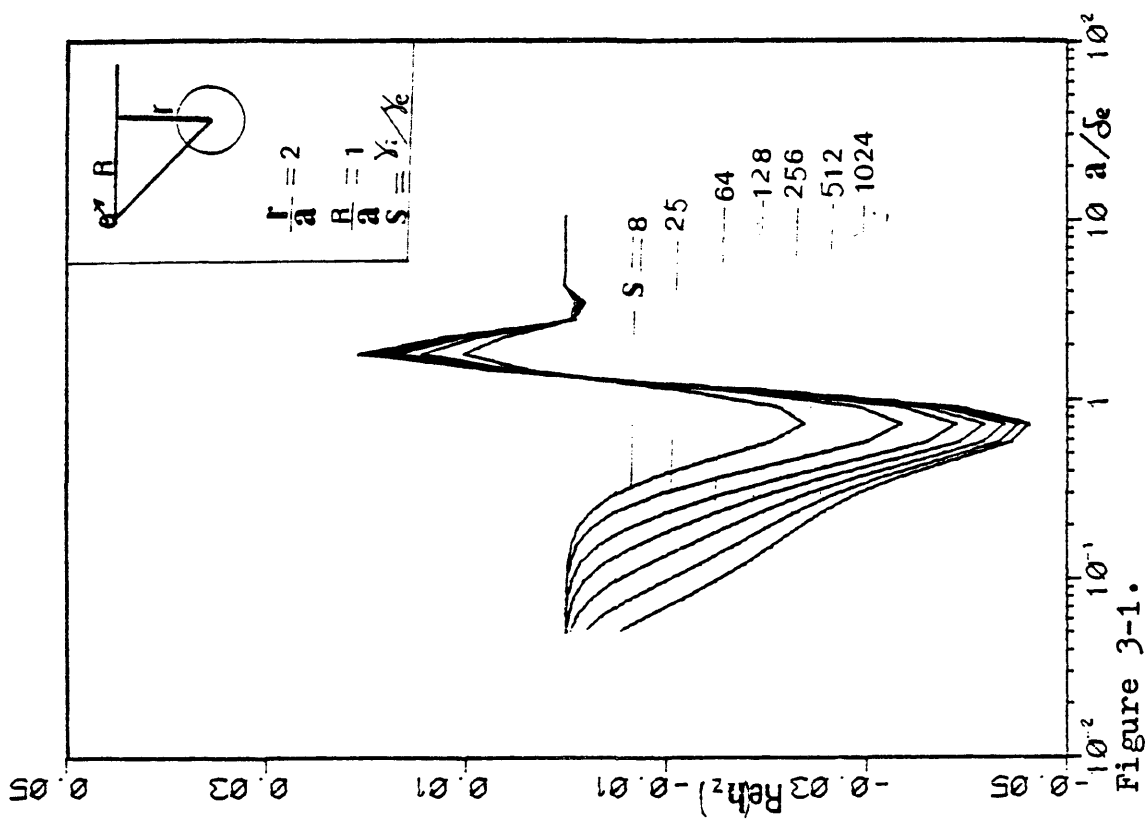


Figure 3-1.

Frequency response of the magnetic field in the presence of a conducting cylinder in uniform space (transmitter is an axial magnetic dipole)

normal field is calculated. Figure (3-3) shows the ratio of the quadrature components. As can be seen from this figure these ratio approaches some constant. This fact can be explained by considering the behavior of the normal and the secondary field. At the low frequencies the quadrature components of the normal and the secondary field are proportional to frequency. Thus the ratio of this component should approaches some constant as the frequency decreases. From this figure it is found that the ratio practically doesn't change for the range of $a/\delta_i < 1$, in other words, decreasing the frequency below $a/\delta_i = 1$, the depth of investigation doesn't increase. It just brings the result of decreasing the signal.

Figure (3-4) shows the ratio of the inphase component of the secondary field to that of the normal field. Inphase component of the normal field contains primary field so it was removed before taking ratio. From this figure it is found that the maximum ratio of the useful signal to geological noise can be obtained at $a/\delta_i = 1.2$. Thus measuring the inphase component the resolving capability of the method will be reduced by decreasing or increasing the frequency from $a/\delta_i = 1.2$. From these two figures it should be pointed out that measuring inphase component has higher resolving capability than measuring quadrature

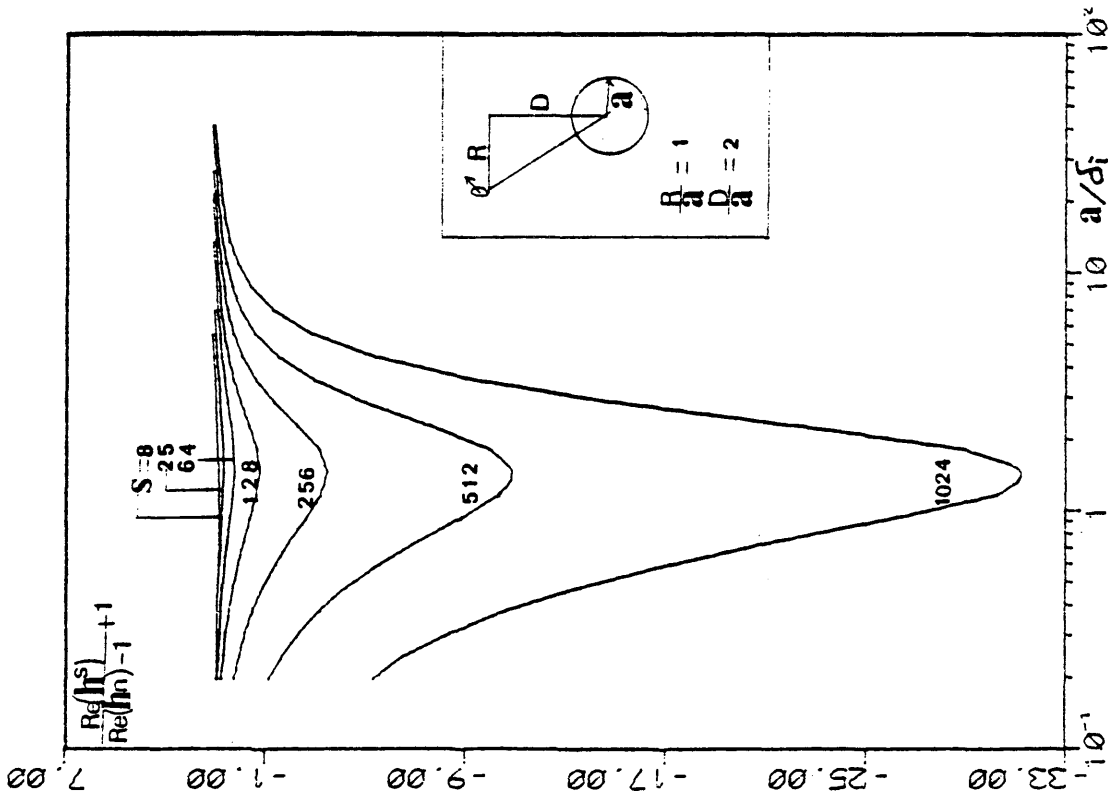


Figure 3-3.

Ratio of the total to normal magnetic field in the frequency domain (transmitter is an axial magnetic dipole)

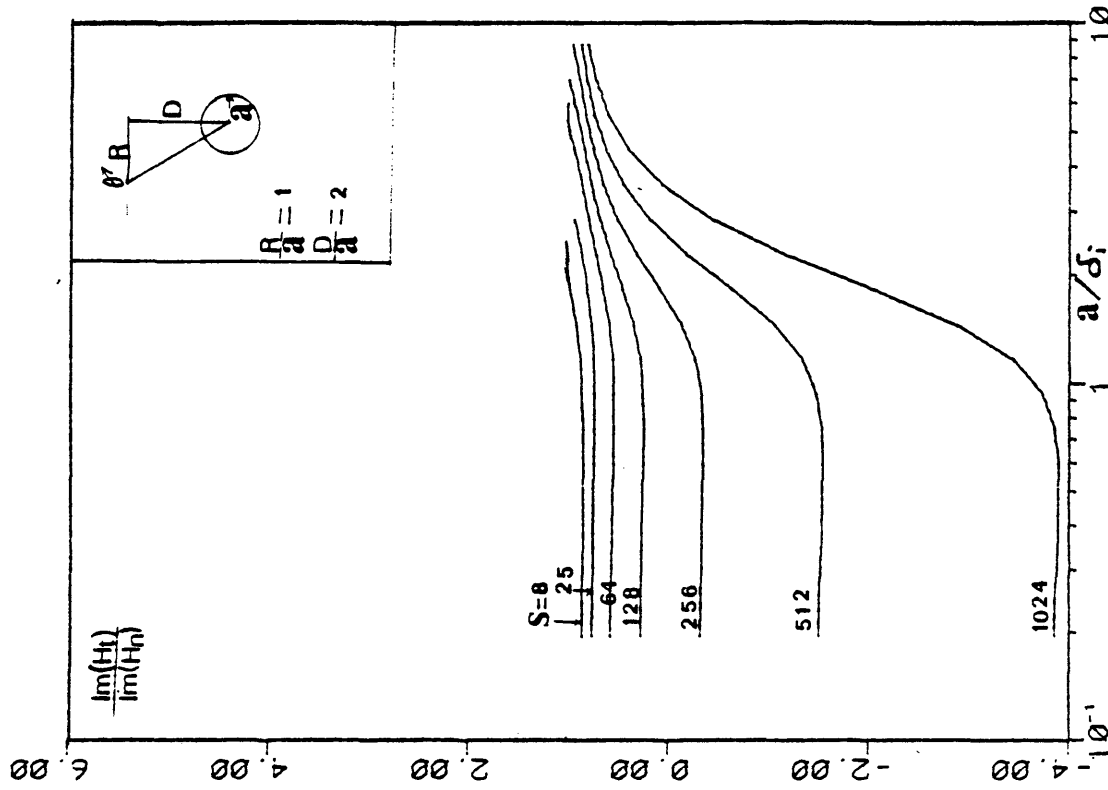


Figure 3-4.

component of the magnetic field. However sometimes inphase component of secondary field is much less than that of normal field so it may be very difficult to differentiate this part, in other words, it needs very accurate instruments.

To figure out the feasibility of increasing depth of investigation by measuring the quadrature component at two different frequencies, the operation, which is described in equation (2-47), is applied to the quadrature component of the secondary and the normal field. The ratio of the difference of the fields is presented in Figure (3-5). Regardless of the different contrasts of the conductivities the maximum ratio of the useful signal to geological noise is arrived at $a/\delta_i = 1.2$. This frequency is same as the optimum frequency of measuring inphase component. Comparing this figure to Figure (3-3) it can be noticed that this method possesses much higher resolving capability than the method of measuring the inphase component.

From all this discussion, the optimum frequency, regardless of the different methods, is about $a/\delta_i = 1$.

Vertical components of secondary magnetic field.

Vertical components of the magnetic field is calculated by using equations (3-23) and (3-25). According to these

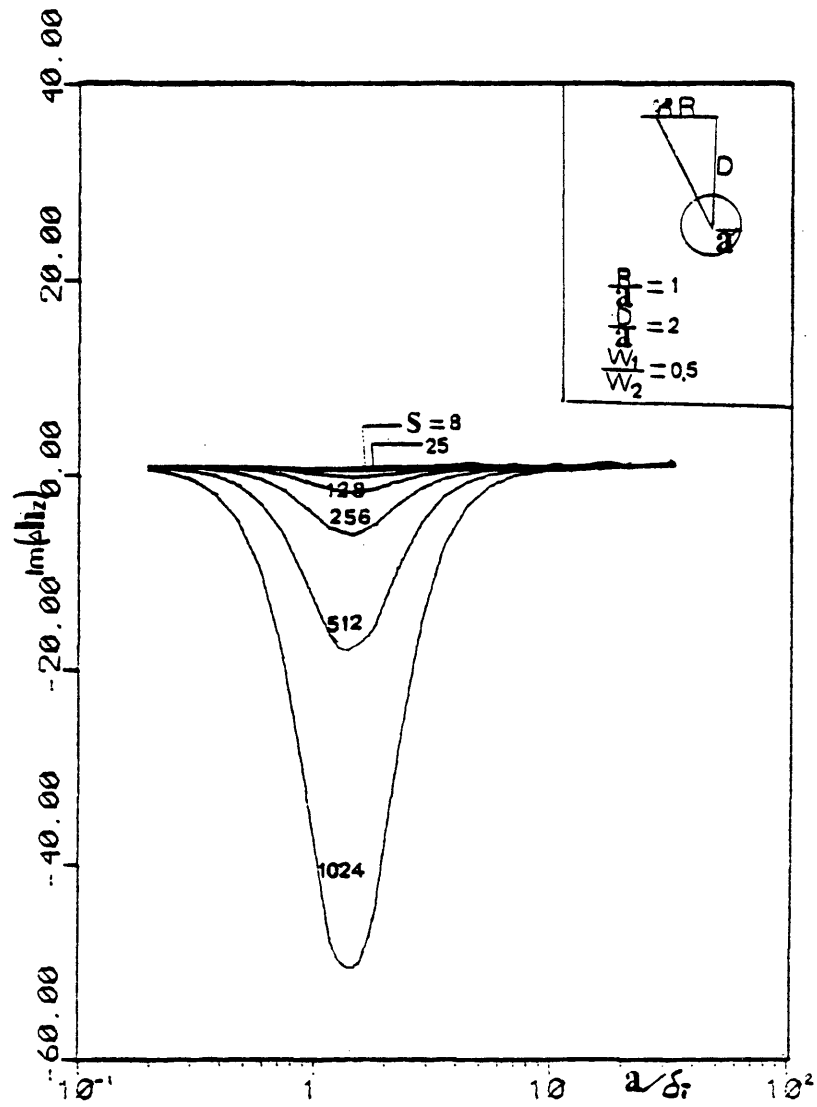


Figure 3-5.

Frequency response of the quadrature component of the magnetic field with the leading term of the low frequency asymptote removed (Source is an axial magnetic dipole)

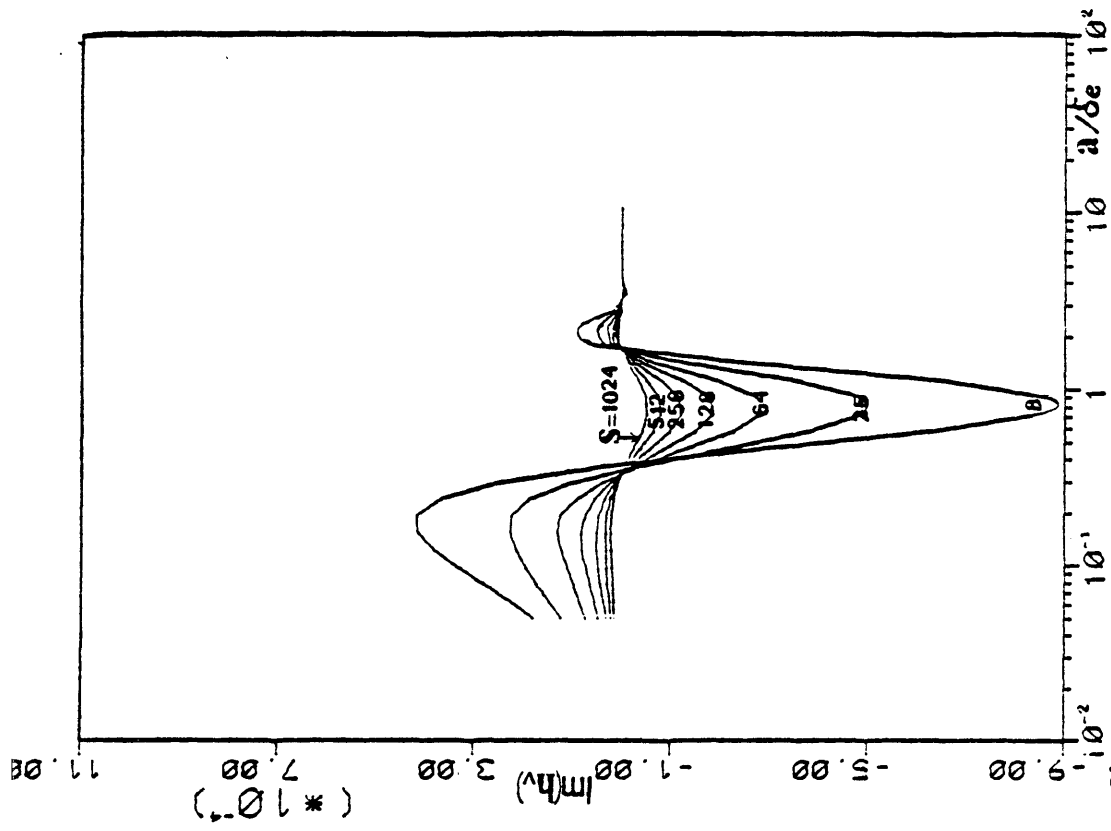


figure 3-7.

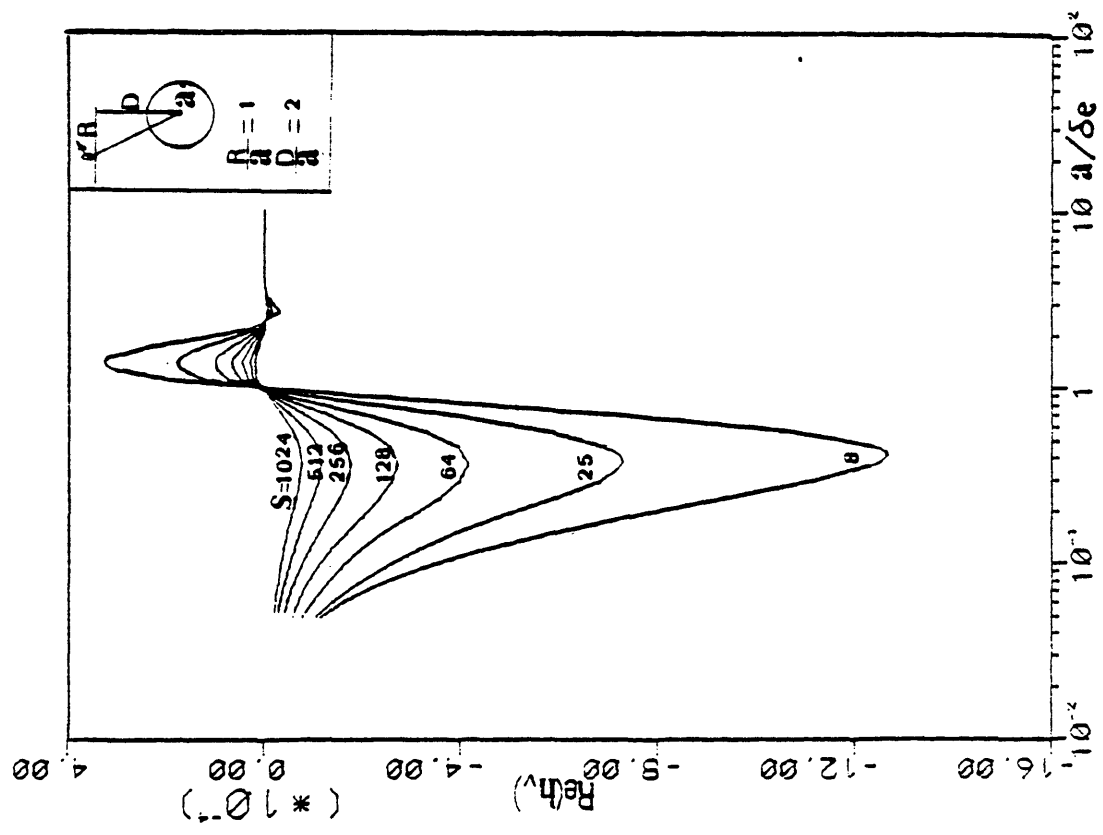


Figure 3-6.

Frequency response of the vertical component of magnetic field(Source is an axial magnetic dipole)

equations, on the plane $z=z_0$, this component of the field is defined by only electric type vector potential. Figure (3-6) and (3-7) show the frequency response of vertical component of magnetic field. From these figures it is found that this component of the field decreased as the conductivity of surrounding medium decreases. This fact can be recognized from equation (3-32). In this equation the function C_n reduced to zero as the conductivity of surrounding medium decreases.

Transient Response of the Magnetic Field

The secondary magnetic field is calculated numerically. Figure (3-8) show the z-component of secondary magnetic field for a given geometry with several different ratios of the conductivities.

At the early stage, due to the skin effect, currents are concentrated mainly near the source and the field does not feel the existence of the conducting body. As the time increases, the currents diffuse farther from the source and the field starts to feel the conducting body. Thus the secondary field increases until a certain time. However, at the late stage the currents decay as time increases. Correspondingly, the magnetic field decays at late stage. Thus, the maximum value of the field is located at the intermediate stage. As can be seen from Figure (3-8), increasing the

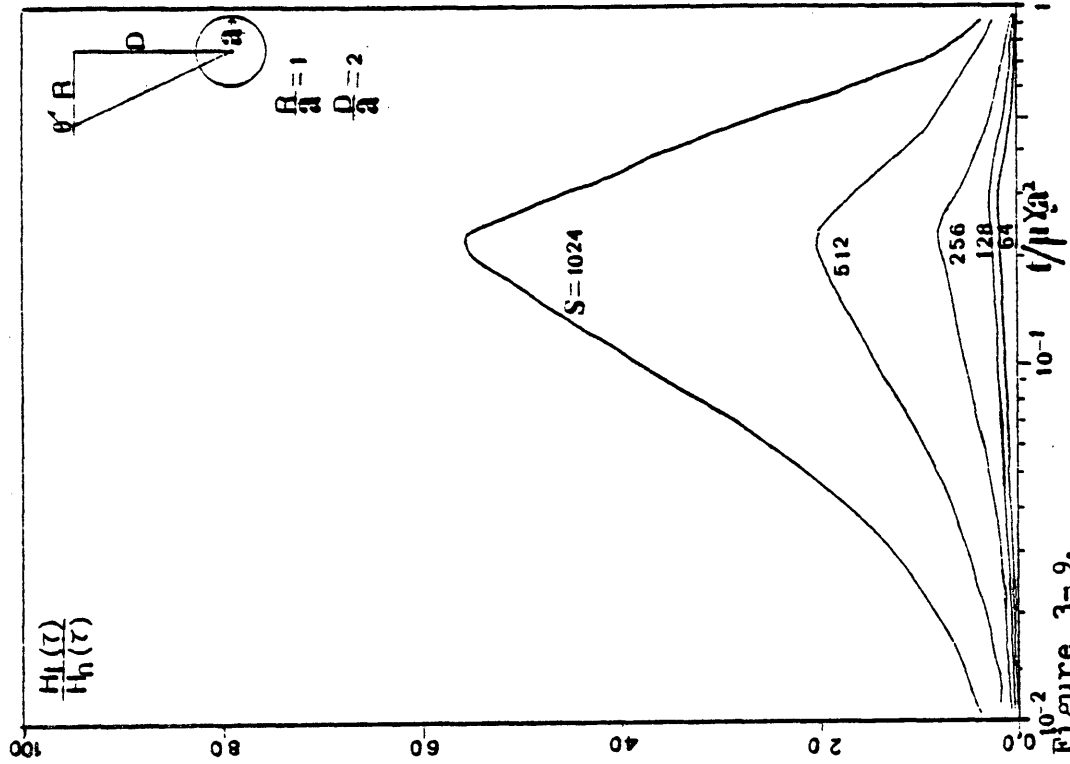


Figure 3-9.

Ratio of the total to normal magnetic field in time domain (Source is an axial magnetic dipole)

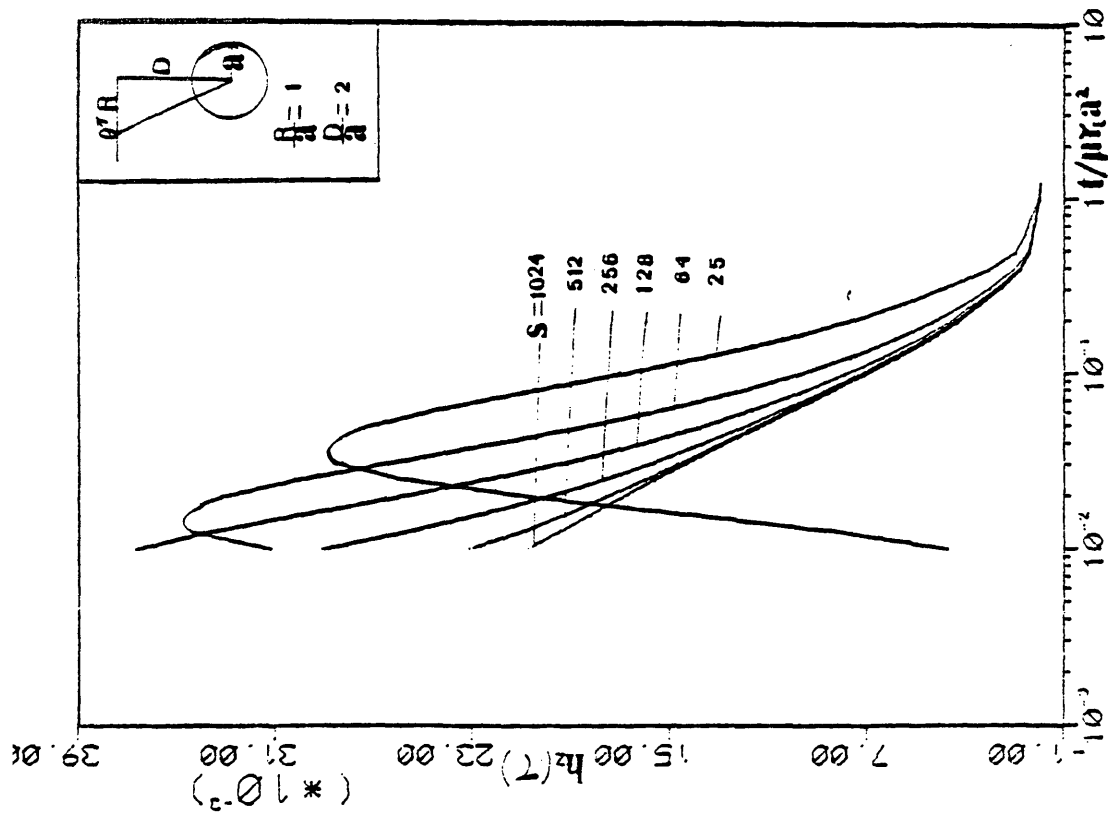


Figure 3-8.

Transient response of the magnetic field (Source is an axial magnetic dipole)

conductivity of surrounding medium it takes longer time to reach maximum point, in other words, in the high resistive medium currents penetrate faster than the low resistive one.

At the late stage the currents in the medium and in the body decay in different ways, and the currents in the body decay faster than the one in the surrounding medium. Thus at far late stage main contribution of the field comes from the currents in the medium. According to the above discussion it can be expected that the maximum ratio of the useful signal to geological noise is in the intermediate range of time. To find this optimum range of time the ratio of the secondary field to the normal field is calculated. Figure (3-9) shows this result. As is shown in this figure, regardless of the different contrasts of the conductivities, the maximum points are located at the same time, $t/\mu\gamma_1 a^2 = 0,25$.

If the geological noise is less than 10% of total signal, practically the influence of surrounding medium can be neglected. From this figure it can be recognized that the following fact.

If the ratio of conductivities is higher than 500, the influence of the geological noise is negligible within relatively wide range of time.

CONCLUSION

Electromagnetic fields of a conducting cylinder have been investigated for the case of an infinitely long linear current source and a magnetic dipole source. The behavior of the fields has been studied through numerical evaluation of the exact formula and the asymptotic expressions for some limiting cases.

The secondary magnetic fields, due to a line source, can be considered as the sum of the fundamental part and the linear harmonic part. The fundamental part of the field is caused by a linear current in the cylinder and it has some relation to the conductivity of the surrounding medium. Since the linear harmonic part of the secondary field is caused by the eddy current in the cylinder, in a certain range of frequency or time, this part of the field doesn't depend on the conductivity of the medium. Numerically it is found that the fundamental part dominates the secondary field.

Regardless of the orientation of the source the secondary field, due to a magnetic dipole, of a conducting cylinder in free space possesses similar behavior. At the low frequencies the inphase component is proportional to $(\gamma\mu\omega a)^2$ and the quadrature component is proportional to $\gamma\mu\omega a$. If a transmitter and a receiver are located far ($r/a \geq 4$), $r/a \geq 4$) from the cylinder, the secondary magnetic field has

a behavior similar to the secondary magnetic field in which the primary field, in the vicinity of the cylinder, is uniform. At the late state the secondary fields decay exponentially. The coefficient of the exponent is defined by the ratio of the constant of the proportionality of the inphase to that of the quadrature component at the low frequencies.

Comparing the normal and the secondary field, it is found that the influence of the surrounding medium manifests itself as different ways in the frequency and the time domains. The characteristics of the influence can be summarized as:

- i) The influence on measuring the quadrature component increases as the frequency increases and decreases to some constant as the frequency decreases. At the low frequency $a/\delta_i < 0.2$ for an infinitely long linear current source or $a/\delta_i < 1$ for an axial magnetic dipole source, the influence of the medium remains the same.
- ii) For measuring the inphase component of the magnetic field, the influence is minimum at $a/\delta_i = 0.3$ for a line source or $a/\delta_i = 1.2$ for an axial magnetic dipole source.
- iii) In the time domain, the influence of the medium is minimum at $t/\mu \gamma_i a^2 = 7$ for a line source or $t/\mu \gamma_i a^2 = 0.2$ for a magnetic dipole source. Thus it should

be recognized that at the far late stage the influence of the surrounding medium increases.

From the results of the numerical evaluation, it is found that the method in the time domain possesses a higher resolving capability than the one in the frequency domain. In the frequency domain, measuring the inphase component has a higher resolving capability than measuring the quadrature component. If we measure the quadrature component at two different frequencies, the resolving capability of the method is increased very much and it can be comparable to that of the method in the time domain.

APPENDICESA-1 Fourier transforms

In this thesis Fourier transform is carried out by applying finite Fourier sine and cosine transform

To calculate the integral

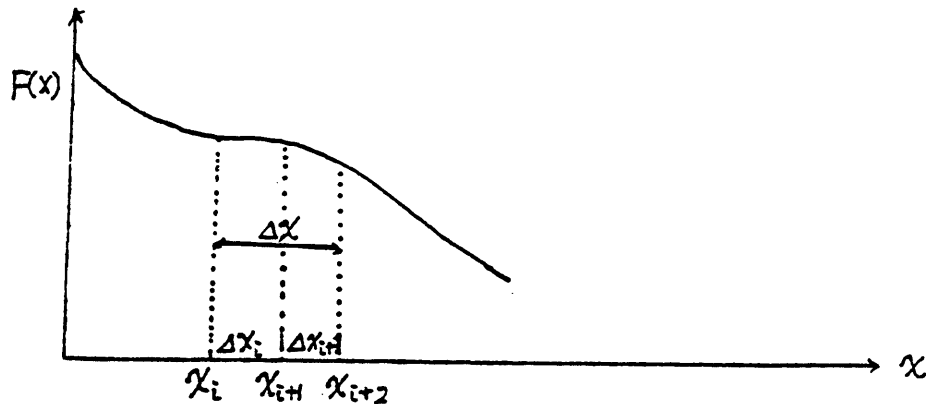
$$I(k) = \int_a^b f(t) \cos kt \, dt$$

in Filon's method (Davis, et al, 1975), the interval a, b , is divided into $2N$ subinterval of equal length h .

$$h = (b-a)/2N$$

Over each double subinterval, $f(t)$ is approximated by a parabola obtained by interpolation to $f(t)$ at the mesh point. For parabola $f(t)$, the Fourier integral can be computed explicitly by integration by parts.

In this thesis, different length of interval is used. Considering the contribution of each interval integration to the final one and the time of computation, it is better to increase the length of interval to the direction of decreasing the magnitude of integrand. The integration is carried out to the direction of decaying magnitude of integrand.



Using three values $F(x_i)$, $F(x_{i+1})$ and $F(x_{i+2})$ $F(x)$ can be approximated as

$$F(x) = a_x^2 + b_x + c$$

where

$$a = \frac{F(x_i)\Delta x_{i+1} - F(x_{i+1})\Delta x + F(x_{i+2})\Delta x_i}{\Delta x \Delta x_i \Delta x_{i+1}}$$

$$b = \frac{F(x_i)(x_{i+1}^2 - x_{i+2}^2) + F(x_{i+1})(x_{i+2}^2 - x_i^2) + F(x_{i+2})(x_{i+1}^2 - x_i^2)}{\Delta x \Delta x_i \Delta x_{i+1}}$$

$$c = \frac{F(x_i)\Delta x_{i+1}x_{i+1}x_{i+2} + F(x_{i+1})\Delta x x_i x_{i+2} + F(x_{i+2})\Delta x_i x_i x_{i+1}}{\Delta x \Delta x_i \Delta x_{i+1}}$$

in the interval $[x_i, x_{i+2}]$

Thus the Fourier integral within the above interval

becomes

$$\int_{x_i}^{x_{i+2}} (ax^2 + bx + c) \cos kx \, dx$$

$$= \left[\frac{2ax+b}{k^2} \cos kx + \frac{ak^2x^2 - 2a + bK^2x + ck^2}{k^3} \sin kx \right]_{x_i}^{x_{i+2}}$$

The length of interval is chosen as

$$\frac{\Delta x_{i+1}}{\Delta x_i} = 2^{1/N}$$

In case of relatively slow change of integrand, $N = 4$ is used. If the integrand has some different sign of gradient within the range of integration $N = 8$ or 16 is used.

A-2 Calculation of Bessel function

The Bessel functions are numerically calculated. For the case of small argument series expressions are used.

(Janke and Emde, 1960).

$$I_m(z) = \left(\frac{z}{2}\right)^m \sum_{k=0}^{\infty} \frac{\left(\frac{z}{2}\right)^{2k}}{k! \Gamma(m+k+1)}$$

$$\text{for } |z| \leq 12 \quad \text{or} \quad |z| \leq 11$$

$$\begin{aligned} K_m(z) &= (-1)^{m+1} I_m(z) \ln(\gamma z/2) \\ &+ \frac{(-1)^m}{2} \sum_{k=0}^{\infty} \frac{\left(\frac{z}{2}\right)^{m+2k}}{k! (m+k)!} \left(\sum_{l=1}^k \frac{1}{l} + \sum_{l=1}^{m+k} \frac{1}{l} \right) \\ &+ \frac{1}{2} \sum_{k=1}^{\infty} \frac{(-1)^k (\gamma - k - 1)!}{k!} \left(\frac{z}{2}\right)^{2k-\gamma} \end{aligned}$$

where $\gamma = 1.781072$ (Euler's constant) The above formula

is used for $|z| < 4$

and

$$-\frac{\pi}{2} \leq \arg(z) \leq \frac{\pi}{2}$$

In case of big argument asymptotic expressions are used

$$I_n(z) = \frac{e^z}{\sqrt{2\pi z}} \left\{ 1 + \sum_{l=1}^{\infty} \frac{(2l-2n-1)!! (2l+2n-1)!!}{(8z)^l l!} \right\}$$

for $|z| > 2$ and $|z| > n$

$$K_n(z) = \sqrt{\frac{\pi}{2z}} e^{-z} \left\{ 1 + \sum_{l=1}^{\infty} (-1)^l \frac{(2l-2n-1)!! (2l+2n-1)!!}{(8z)^l l!} \right\}$$

for $|z| > 4$

where $(2m)!! = 2^m m!$

$(2m+1)!! = (2m+1)! / 2^m m!$

A-4. List of symbols

<u>Symbols</u>	<u>Quantity</u>	<u>M.K.S. unit</u>
E	Electric field intensity	Volt/meter
H	Magnetic field intensity	Ampere/meter
μ	Magnetic permeability	Henry/meter
γ	Conductivity	Mhos/meter
I_0	Source current	Ampere
j	current density	Ampere/m ²
M	Magnetic dipole moment	Ampere-m ²
δ	Skin depth	Meter
K	Wave number	
τ	Normalized time	
ρ	Resistivity	Ohms meter
e_0	Normalized electric field of the fundamental part	
e_1	Normalized electric field of harmonics part	
h_0	Normalized magnetic field of fundamental part	
h_1	Normalized magnetic field of harmonics part	
$I_n(r), K_n(r)$	Modified Bessel functions	
R	Distance between source and observation point.	
r_0	Distance between source and the cylinder.	

SymbolsQuantity

r	Distance between the cylinder and observation point.
a	Radius of the cylinder.
u	R/a
α	r_0/a
β	r/a

REFERENCES

- Davis, P.J., Rabinowitz, P., 1975, Methods of numerical integration, Academic Press.
- Erdelyi, A., Magnus, W., et al, 1954, Tables of integral transform, McGraw-Hill, New York.
- Fuller, B.D., 1971, Quasi-static time domain electromagnetic response of a homogeneous conducting infinite cylinder: Geophysics, v. 36, no. 1, p. 9-24.
- Janke, Emde L., 1960, Tables of higher function, McGraw-Hill, New York.
- Kaufman, A.A., 1961, The influence of the surrounding environment on results of inductive prospecting ore deposit in the wave zone: Trans. IGG SOAI SSR.
- _____, 1965, Theory of the induction logging: Nanka Siberian Division, Acad. Sci., USSR.
- _____, 1977, The theoretical basis of transient sounding in the near zone (English translation).
- _____, 1978, Frequency and transient responses of electromagnetic fields created by currents in confined conductor: Geophysics, V. 43, p. 1002-1010.
- Keller, G.V., Frischknecht, F.C., 1966, Electrical methods in geophysical prospecting, Oxford, Pergamon Press.
- Nabighian, M.N., 1970, Quasi-static transient response of a conducting permeable sphere in a dipolar field: Geophysics, v. 35, pp. 303-309.
- _____, 1971, Quasi-static transient response of conducting permeable two-layer sphere in a dipolar field: Geophysics, v. 36, pp. 25-37.
- Negi, J.G., 1962, Inhomogeneous cylindrical orebody in presence of a time varying magnetic field: Geophysics, v. 27, pp. 386-392.
- Parasnis, D.S., 1966, Mining Geophysics.
- Schelkunoff, S.A., 1943, Electromagnetic waves, D. Van Nostrand, New York.

- Smythe, W. R., 1950, Static and dynamic electricity, McGraw-Hill, New York
- Vanyan, L. L., 1967, Electromagnetic depth sounding: New York, Consultants Bureau.
- Verma, S. K., 1972, Transient electromagnetic response of a conducting sphere excited by different typed os input pulses: Geophysical prospecting, v. 20, pp. 752-770.
- Wait, J. R., 1951, A conducting sphere in a time varying magnetic field: Geophysics, v. 16, p. 666.
- Wait, J. R., 1953, The cylindrical ore body in the presence of a cable carrying an oscillating current: Geophysics, v. 17, pp. 378-386.
- Wait, J. R., 1960, Some solutions for electromagnetic problems involving spheroidal, spherical, and cylindrical bodies: J. Research Nat'l. Bur. Stards., B. 64, pp. 15-32.
- Wait, J. R., 1969, Electromagnetic induction in a solid conducting sphere enclosed by a thin spherical conducting shell: Geophysics, v. 34, pp. 753-759.
- Ward, S. H., 1959, Unique determination of conductivity, susceptibility, size and depth in multi-frequency electromagnetic exploration: Geophysics, v. 26, pp. 531-546.
- Ward, S. H., 1967, Mining geophysics, v. 2, The society of exploration geophysicists.
- Watson, G. N., 1945, Theory of Bessel functions, Cambridge Univ. Press, England.
- Wesley, J. P., 1958, Response of dyke to oscillating dipole: Geophysics, v. 23, pp. 128-133.